Tenascin-X: Expression, biochemical properties and functional aspects

David Egging Tenascin-X: Expression, biochemical properties and functional aspects

Thesis University Medical Center of the Radboud University, Nijmegen, The Netherlands

Print Printpartners Ipskamp, Enschede

ISBN/EAN 978-90-9022092-5

Layout David Egging

Tenascin-X: Expression, biochemical properties and functional aspects

Een wetenschappelijke proeve op het gebied van de

Medische wetenschappen

Proefschrift

ter verkrijging van de graad van doctor

aan de Radboud Universiteit Nijmegen

op gezag van de rector magnificus prof. mr. S.C.J.J. Kortmann,

volgens besluit van het College van Decanen

in het openbaar te verdedigen op maandag 24 september 2007

om 13.30 uur precies

door

David Franciscus Egging

geboren op 21 oktober 1979

te Arnhem

Promotor: Prof. dr. J. Schalkwijk

Manuscriptcommissie:

Prof. dr. B.G.M. van Engelen

Prof. dr. M. Koch (Universiteit van Keulen)

Dr. A.H.M.S.M van Kuppevelt

TABLE OF CONTENTS

CHAPTER 1

GENERAL INTRODUCTION

Parts of this chapter have been previously published:
Bristow J, Carey W, Egging D, Schalkwijk J. Tenascin-X, collagen, elastin, and the Ehlers-Danlos syndrome. Am J Med Genet C Semin Med Genet. 2005 Nov 15;139(1):24-30. Reprinted with permission.

GENERAL INTRODUCTION

THE EXTRACELLULAR MATRIX

The development of an extracellular matrix (ECM) has played a pivotal role in the evolution of multicellular organisms. It imparts strength, resilience and structure to tissues and provides a framework for cells. There are essentially four types or major macromolecules in the ECM; collagens, elastin (a major component of the elastic fibers), glycoproteins and proteoglycans. Collagen fibrils provide strength to the ECM while elastic fibers define the stretch and recoil properties of a tissue. The composition and structure of the ECM is highly dependant on the function of the tissue. While the cells determine the ECM around them, the cells themselves are influenced by components of the ECM or changes therein. This gives rise to a highly complex tissue specific aggregate of macromolecules essential for structure and development of animals.

COLLAGENS

Collagens are abundantly expressed in the ECM. They provide strength and structure to skin, ligaments, blood vessels, cartilage, bone and most other connective tissues. Collagens are characterised by triple helical domains, which are composed of three polypeptide chains (α-chains). The polypeptide chains can be identical (homotrimers) or genetically distinct (heterotrimers). The collageneous triple helix is made possible by a specific repeating sequence of glycine-X-Y were in most instances X and Y are proline and hydroxyproline. The formed triple helix is a semi-rigid domain; therefore collagens are flexible, rod like molecules. Thus far 28 different collagen types have been identified. Based on the triple helix size, physical, physiological and chemical properties collagens can be divided into several groups.

Fibrillar collagens (type I, II, III, V, XI, XXIV and XXVII) [1-4] are the largest group of collagens and form long unbranched fibrils of stacked collagen (triple helical) molecules. Fibril composition and aggregation is dependant on the type of collagen. Collagen types II, XI and XXVII are predominantly expressed in cartilage, while types I, III, V and XXIV are expressed in most other tissues. Fibrillar collagens self-assemble into correctly stacked fibrils of 67nm axial periodicity (D) in vitro [5-8]. However, the organisation of the fibrils into higher-order structures is only present in vivo. The molecular details of fibril assembly are not yet completely understood, although it appears highly regulated in the fibroblasts. Briefly, procollagen is cotranslationally translocated into the lumen of the endoplasmatic reticulum (ER) were a number of enzymes and chaperones assist in the trimerization and folding. The C-terminal propetide of procollagen ensures association of three appropriate procollagens. The collagen triple helix self assembles in the C-to-N-terminal direction. A large number of post-translational modifications occur in the ER. Hydroxylation of proline and lysine residues is an important step in the process as hydroxyproline stabilizes the triple helix and hydroxylysine is important in intra- and inter molecular crosslinks between fibrils through the actions of lysyl oxidase. Removal of the C- and N-terminal propetides occurs after transport of procollagen across the Golgi stacks. By removing the C-terminal propeptide collagen molecules are triggered to self-assemble into fibrils. Golgi-to-plasma membrane carriers transport one or more collagen fibrils to the plasma membrane where they are deposited into the ECM. Collagen fibril growth takes place by end-to-end fusion of collagen fibrils to other collagen fibrils or at the base of the fibril by addition of individual collagen molecules. The fibrils subsequently form collagen fibril bundles that are organised into higher-order structures [1;8-10].

Non-fibrillar collagens can be divided into several subgroups based on their structure and (bio)chemical properties, however, the exact function of these collagens is not always known. FACIT (fibril-associated collagens with interrupted triple helices, types IX, XII, XIV, XVI, XIX) mostly function as linkers between collagen fibrils and other ECM molecules. Collagens type XX and XXI may be associated with collagen fibrils and type XXII with microfibrils. The short chain collagens (type VI VIII X) are microfibril forming collagens. They also contain a putative cell binding sequence; RGD (arginine-glycine-aspartic acid) [1;11-15]. Collagen XXVI consists of two collagenous domains interrupted by three non-collagenous domains. It is expressed in testis and ovary, although its function is not yet fully understood [16].

Basement membrane collagens type IV and VII are collagenous components of the basement membrane. Their function is to anchor the basement membrane to underlying structures. Collagens type XV and XVIII are collagens with multiple interrupted triple helical domains that are associated with basement membrane zones, possibly providing structure and integrity to the basement membrane. Cleaved products form antiangiogenic fragments restin (from type XV) and endostatin (from type XVIII). The function of the newly discovered collagen type XXVIII is not known, although it possibly has a role in nerve fibre basement membrane assembly [1;17;18].

Type XIII, XVII, XXIII and XXV are transmembrane collagens. They are an integral part of the plasma membrane. Collagen type XVII is a component of hemidesmosomes, while collagen type XIII is expressed ubiquitously. Collagen XXIII was identified in tumor cells and thought to be involved in cell-cell interactions. A cleaved form of collagen type XXV is present in the amyloid plaques in Alzheimer's disease [1;17;19;20].

ELASTIC FIBERS

Tissue flexibility and extensibility are essential requirements in dynamic elastic connective tissues such as skin, tendons, lung and blood vessels. Elastic fibers are insoluble macromolecular structures that give resilience and the ability to stretch and recoil to connective tissue. Elastogenesis is a complex process that is not completely understood. The main components of elastic fibers are microfibrils composed of fibrillin-1 and -2 and an amorphous core of elastin. However, a large number of other ECM molecules are thought to be associated with or incorporated into the elastic fibers including fibulins, emilins, collagens and proteoglycans. Microfibril assembly is a cell-regulated process and independent of the tropoelastin pathway. Fibrillin is excreted by the cell and linear fibrillin arrays are formed on the cell surface. In this process calcium plays an important role in the folding of fibrillin. The fibrillin arrays are deposited in the ECM were they undergo maturation into beaded transglutaminase crosslinked microfibrils. The microfibrils form crosslinked microfibril bundles, which act as a scaffold for tropoelastin, the soluble precursor of elastin. Newly synthesized elastin is deposited onto the microfibrils, were it forms the core of an elastic fibre. In vitro elastin can self-assemble by a process called coascervation into an aggregate resembling the configuration of elastic fibre core in vivo. In vivo however, the tropoelastin is crosslinked by lysyl-oxidase-like proteins LOX and LOXL resulting in (mature) elastin with unique desmosine and isodesmosine crosslinks. The crosslinked elastin forms the core of the elastic fiber and is surrounded by microfibrillar bundles [21-31].

The elastic fibers' shape, deposition and function differ depending on the tissue, location and species, as illustrated by three examples. The elastic fibers in the reticular dermis of human skin are thick horizontally arranged fibers. The papillary dermis contains thin perpendicular orientated (candela structure) elastic fibers (elaunin fibers) that merge with a microfibrillar cascade (oxytalan fibers). Such organization

cannot be found in most other mammals, except for pig. In the skin of most mammals and avian species the elastic fibers perform a primary role in the movement of skin covering (hairs, feathers). In the aorta the elastic fibers form thick concentric lamellae giving resilience to the blood vessel. Relative little elastic fibers are present in tendons while they are abundant in flexible ligaments. In most tissues elastic fibers are designed to last a lifetime and only limited remodelling is possible. Elastic fibers are susceptible to a certain degree of degradation by enzymes such as neutrophil elastase and matrix metalloproteinases, which can lead to loss of elasticity of tissue in age dependant processes or sun induced elastosis [22;32-34].

TENASCINS

Tenascin-X is one member of a family of ECM glycoproteins that share a common general structure, but are distinguished by their patterns of expression in development and disease [35]. Tenascins consist of a N-terminal globular domain and heptad repeats, which facilitate multimerization; a number of epidermal growth factor (EGF) like repeats, a series of fibronectin type III (FNIII) repeats, and a C-terminal fibrinogen domain. There are four mammalian tenascins, each identified by more than one laboratory, leading to a variety of names depending on the context of discovery. For clarity, the mammalian genes are now called tenascin-C (TNC, formerly cytotactin, hexabrachion), tenascin-R (TNR, restrictin, janusin), tenascin-X (TNX, also tenascin-Y in chick), and the recently described tenascin-W (TNW, also tenascin-N) (figure 1) [36-46]. While many possible functions for these proteins have been proposed based on patterns of expression and studies in vitro, their functions in vivo remain poorly understood.

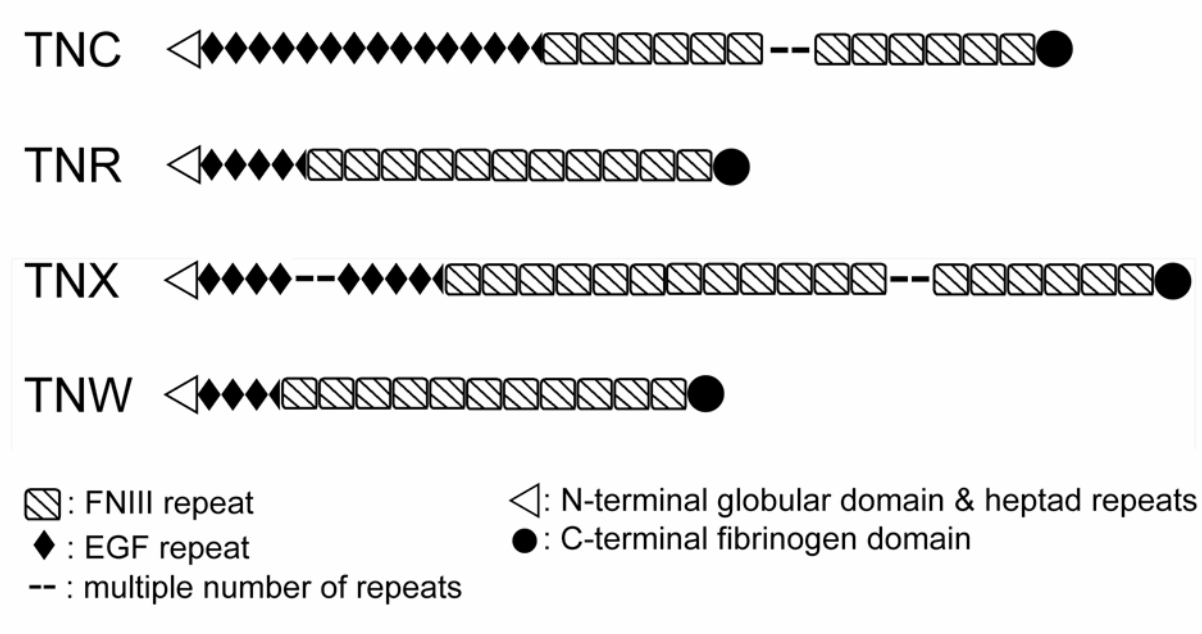

Figure 1: Mammalian tenascins.

Tenascins consist of a N-terminal globular domain and heptad repeats, which facilitate multimerization, a number of epidermal growth factor (EGF) like repeats, a series of fibronectin type III (FNIII) repeats, and a C-terminal fibrinogen domain. TNC has 14.5 EGF-like repeats and up to 15 FNIII repeats. TNR consists of 4.5 EGF-like repeats and 9 FNIII repeats. TNX, the largest tenascin thus far discovered, encompasses 18.5 EGF-like repeats and 29 to 32 FNIII repeats, depending on the species. Tenascin-W, identified in mice, has 3.5 EGF-like repeats and 9 FNIII repeats.

The findings that the TNC, TNR, and TNC/TNR double knockout mice lack an overt phenotype was both surprising and disappointing [47-49], and it remains uncertain whether this reflects redundant functions shared by the tenascins or whether the most important functions of these proteins are not during development but in adult responses to stress or injury. It was on this background, that the initial association of TNX deficiency with human Ehlers-Danlos syndrome (EDS) was made [50]. This observation was of particular interest not only because it revealed unique functions for at least one tenascin, but also because it demonstrated that genes beyond the fibrillar collagens and collagen modifying enzymes can cause EDS [51;52].

DISCOVERY OF TENASCIN-X

TNX was identified serendipitously because of its 3' overlap with the human *CYP21B* gene [38]. CYP21B encodes steroid 21-hydroxylase, an essential enzyme in cortisol and mineralocorticoid biosynthesis, deficiency of which leads to the recessive disorder, congenital adrenal hyperplasia (CAH) [53]. While trying to clone a mutant CYP21B cDNA from an adrenal library prepared from the adrenal gland of an affected fetus, Morel et al. [38] instead cloned a transcript overlapping CYP21B, but arising from the opposite DNA strand. This transcript was of low abundance that escaped previous recognition because of the 100-fold greater expression of CYP21B in the normal adrenal. Further analysis of this genomic locus on chromosome 6 showed that this transcript arose from a gene (*TNX*) that was partially duplicated along with CYP21 and C4 encoding the 4th component of serum complement. As shown in figure 2, these genes are arranged in the order: *C4A*/*CYP21A*/*XA*/*C4B*/*CYP21B*/*TNX* (fig. 2). Both *C4* genes are functional, while only the *CYP21B* gene is functional in humans.

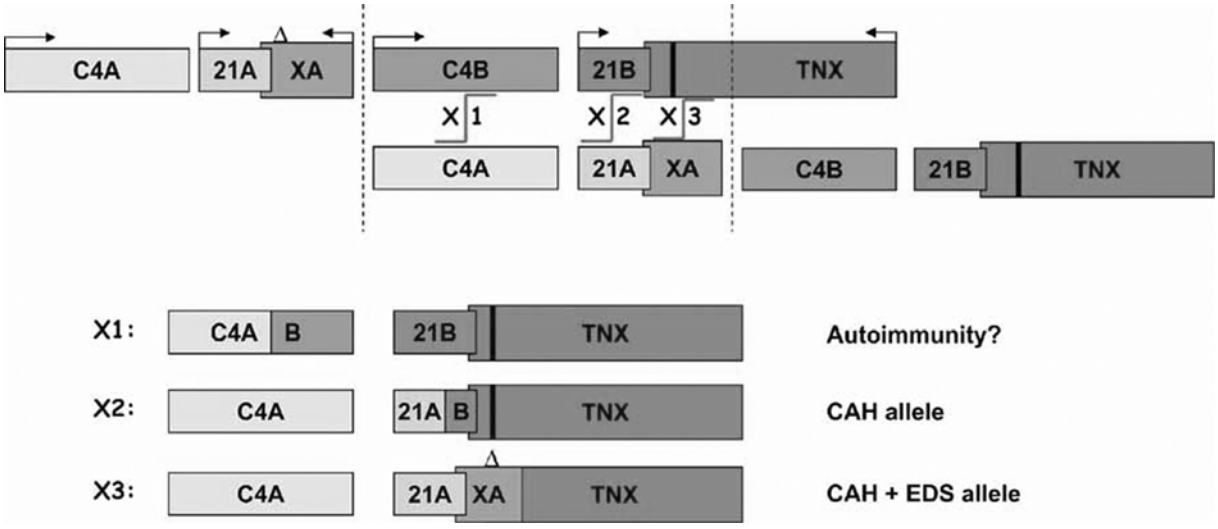

Figure 2: Deletions in the C4/CYP21/TNX locus.
The top panel shows the order of genes in this locus on human chromosome 6. The duplication event created complete duplicate copies of C4 and CYP21 and a partial duplicate of TNX (called XA). *CYP21A* and *XA* are non-functional pseudogenes. Unequal crossover events can occur through mis-alignment of the A and B regions during meiosis and produce alleles missing one 30 kb C4/CYP/TNX cassette. X1: Crossover between *C4* genes reduces C4 copy number, but is otherwise without effect. X2: Crossover between CYP21 genes inactivates CYP21B but TNX is unaffected. X3: Crossover between TNX and XA deletes CYP21B entirely and inactivates TNX because the small deletion in XA (d) truncates its open reading frame. This allele is associated with a contiguous gene syndrome consisting of congenital adrenal hyperplasia and EDS.

The duplication event truncated the duplicate *TNX* gene (called *XA*), which also contains a 121 basepair deletion that interrupts its open reading frame, rendering it non-functional [54]. Surprisingly, the *XA* gene is transcribed in the adrenal gland, but does not appear to encode protein [55]. However, a short adrenal specific transcript of *TNX* (*XB-S*) does encode protein [56].
Following this initial report, Matsumoto et al. [57] identified a cluster of fibronectin type III repeats in the class III region of the MHC that clearly represented an upstream portion of the *TNX* gene. Reports of the complete human gene and mouse cDNA soon followed, and included studies of expression that were consistent with important roles in development and matrix biology [40;41;57-59]. However, the large size of the TNX mRNA (12 kb) and protein (450 kDa) impeded functional studies and suggested to us that genetic strategies were most likely to identify unique functions for TNX.

THE EHLERS-DANLOS SYNDROME

The Ehlers-Danlos syndrome (EDS) is a heterogeneous group of heritable connective tissue disorders characterized by joint hypermobility and various degrees of tissue fragility. The classification of EDS is made according to the "1997 Villefranche nosology", which recognizes six major types. Classification of EDS is made on clinical grounds, biochemical and molecular analysis and mode of inheritance. The two most prevalent EDS types are the classical and hypermobility type EDS. Classical type EDS is characterised by joint hypermobility, skin hyperextensibility, poor wound healing with athropic scarring and easy bruising. Only 50% of the cases of classical type EDS can be explained by mutations in the *COL5A1*, *COL5A2* and *COL1A1* genes while the remainder of the mutations is unknown. Hypermobility type EDS is characterised by joint hypermobility and hyperextensible or smooth velvety skin. Often patients suffer from chronic musculoskeletal pain. The causative genetic defects are largly unknown. Vascular type EDS is the most severe and life-threatening type of EDS. Patients have thin translucent skin and fragile tissues resulting in the rupture of aorta, uterus and intestine. Skin hyperextsibility and joint hypermobility are minimal. The inheritance of classical, hypermobile and vascular type EDS is autosomal dominant. The kyphoscoliosis, dermatosparaxis and arthrochalasis types of EDS are relatively rare. The underlying genetic defects reside in collagen modifying enzymes lysyl hydroxylase (*PLOD*, kyphoscoliosis) and procollagen I N-terminal peptidase (dermatosparaxis) or in loss of functional protease cleavage sites in collagen type I caused by mutations in *COL1A1* and *COL1A2* (arthrochalasis) [60-63].

ASSOCIATION OF TENASCIN-X WITH RECESSIVE EDS

Burch et al. based their search for patients that might have disease caused by TNX on extensive prior work concerning the mechanism of disease in CAH. Specifically, it was well-known that 25% of CAH alleles carry deletions within the C4/CYP21/TNX locus that are usually inherited, but can arise de novo from unequal crossover events. In this model, there is misalignment of the 30 kb regions of homology in the A and B regions of the locus and recombination may occur anywhere in this region [64]. If recombination occurs between *C4* genes, an allele is produced containing a hybrid *C4A*/*B* gene, normal *CYP21B* and *TNX* genes, and lacking CYP21A and XA. This allele does not produce overt disease because the remaining *C4* gene, *CYP21B* and *TNX* genes are all functional, although reduced *C4* gene dosage may be associated with autoimmune disease [65]. When recombination occurs between *CYP21* genes, a hybrid *CYP21A/B* gene is produced. This allele is a CAH allele because the CYP21A/B hybrid will contain one or more truncating mutations found in the CYP21A pseudogene, while a normal *TNX* gene persists [66]. Many examples of these deleted C4 and CYP21 alleles exist, as well as the reciprocal triplicated alleles.

Based on these findings, Burch et al. postulated that recombination also occurs between TNX and XA. Such a recombination event would be a CAH allele because CYP21B is deleted and should also alter function of the *TNX* gene if the 3' end of XA (containing the 121 bp deletion) is retained. It was reasoned that such an allele might produce a contiguous gene syndrome consisting of CAH and a connective tissue disorder. A subsequent search identified such a patient: a 25-year-old man with salt-wasting CAH and EDS consisting of hyperextensible skin and joints, accompanied by prominent bruising and absence of atrophic scarring [50]. The index patient was found to share the predicted hybrid TNX/XA allele with his father and a sister, both of whom were phenotypically normal. Further studies showed complete absence of TNX mRNA and protein in the proband. These studies were most consistent with a recessive pattern of inheritance, but no mutation was identified on the proband's maternal TNX allele and a complex interaction between CAH or its treatment and TNX haploinsufficiency was not formally excluded.

In order to assess whether TNX deficiency independent of CAH is associated with EDS, a large number of patients needed to screened for TNX deficiency. To make this possible, Schalkwijk et al. developed a single dilution TNX ELISA. Screening was also facilitated by the observation that a 140 kDa C-terminal fragment of TNX circulates in serum and its absence is uniformly associated with absence of TNX mRNA and protein in dermal fibroblasts. Serum from 151 patients with isolated forms of EDS was screened and found 5 patients to be TNX-deficient [67]. Absence of TNX mRNA and protein was confirmed in skin fibroblasts and all had clinical findings of classical Ehlers-Danlos except that they had normal wound healing and lacked atrophic scars. Allele specific PCR demonstrated one patient (with CAH) was homozygous for the TNX deletion allele and another was heterozygous for the deletion. The remaining three patients carried homozygous inactivating mutations. This study confirmed the association of TNX deficiency with a recessive form of EDS and strongly suggested that TNX mutations were causative.

The published clinical findings of all known patients with TNX-deficient EDS are summarized in table 1. While the number remains small [50;67;68], several generalizations about the clinical features can be made. The first is that all known affected individuals have both hyperextensible skin and hypermobile joints, and none have atrophic scars. In these patients, bruising has been a very prominent feature. Together, these features strongly suggest TNX deficiency and should trigger genetic evaluation and serum testing for TNX deficiency. Some female heterozygotes will have isolated joint hypermobility (see below), so these findings in an affected patient's mother or daughter do not exclude the diagnosis of recessive TNX-deficiency. Large joint dislocations are the most frequent debilitating finding in patients identified to date, although other important complications including mitral valve prolapse, chronic obstructive pulmonary disease, and diverticulosis have each been found in several patients and deserve enhanced surveillance in TNX-deficient EDS. Aortic root dilation or dissection haven't been found in any TNX-deficient patient despite prominent expression of TNX in the adventitia of the normal aorta [58].

ASSOCIATION OF TENASCIN-X WITH HYPERMOBILITY-TYPE EDS

Following publication of these findings, Zweers et al. had the opportunity to examine many members of these families not originally available for study. Heterozygous deficient family members were found to have TNX levels ~50% of those of normal individuals and 9 of 20 had isolated joint hypermobility, representing nearly two-thirds of heterozygous women in the families [69]. No male TNX heterozygous were affected. Zweers et al. then evaluated TNX levels by ELISA in 80 unrelated Dutch patients with hypermobility-type EDS and found six

Table 1: Clinical findings in tenascin-X-deficient Ehlers-Danlos syndrome.

Patient, reference	Age (years), sex	Skin/joint laxity	Bruising	Wound healing	Other complications
Index, Burch et al.	26, M	++/+++	+++	Slow, NL scar	CAH, bronchiectasis, DJD
I-a, Schalkwijk et al.	43, F	++/++	++	NL	Joint pain, striae
I-b, Schalkwijk et al.	53, F	+++/+	++	NL	Goiter
II-a, Schalkwijk et al.	39, F	++/++	++	NL	Large joint dislocations, IgA deficiency
II-b, Schalkwijk et al.	44, F	++/++	++	NL	Large joint dislocations COPD
II-c, Schalkwijk et al.	43, M	++/++	++	NL	Hypertension
III, Schalkwijk et al.	32, F	++/++	++	NL	CAH
IV, Schalkwijk et al.	44, M	++/++	++	NL	Mitral prolapse/insuffic., large joint dislocations, GI bleeding
V, Schalkwijk et al.	48, F	++/++	++	NL	Atherosclerosis
VI, Lindor and Bristow	46, F	+++/+++	+++	NL	Rectal & uterine prolapse diverticulitis, COPD, mitral valve replacement
VII, Lindor and Bristow	37, M	+++/+++	+	Slow, NL scar	Diverticulitis, bowel perforation

Abbreviations: CAH, congenital adrenal hyperplasia; DJD, degenerative joint disease; COPD, chronic obstructive pulmonary disease.

individuals with TNX levels more than 2.5 standard deviations below the mean, a 10-fold excess over what might be expected by chance. Not unexpectedly, these patients had frequent joint subluxation and chronic arthralgias. Allele-specific PCR and sequencing of coding regions revealed two inactivating mutations in this group, supporting a causative role for TNX. The absence of coding-sequence mutations in the remaining four patients was surprising, but it was suggested that regardless of cause, the 50% reduction in TNX was likely to be responsible for disease. This study raised important questions of whether undefined TNX regulatory mutations might play an important role in this disorder.

TENASCIN-X KO MOUSE MODEL

Clinical studies of TNX deficient patients are limited in their scope due to ethical reasons and population size. In order to study the aspects and effects of TNX deficiency on a variety of processes and tissues two groups independently generated TNX knockout (KO) mice [70;71]. Matsumoto et al.reported that the TNX KO mice were grossly normal but tumour growth and metastasis were increased compared to wildtype (WT) mice [71]. Mao et al. also reported that TNX KO mice are viable and grossly normal at birth, but by weaning, their skin was noticeably hyperextensible. Biomechanical testing confirmed increased deformability and reduced tensile strength of TNX KO skin compared to WT littermates. Ultrastructural examination showed relatively normal size and shape of collagen fibrils, but the density of fibrils in dermis was significantly reduced, leading to a 30% reduction in collagen content in skin. TNX KO skin fibroblasts were studied in cell culture and found to have near normal collagen synthesis, but a significant deficit in the amount of collagen deposited into insoluble matrix. This led Mao et al. to the hypothesis that TNX-deficiency causes EDS not by interfering with collagen synthesis or processing, as has been described in other forms, but rather through regulation of fibril deposition into matrix by dermal fibroblasts [70].

While the skin phenotype of the TNX KO mouse was investigated, mobility of the joints was not investigated. Mouse models for joint laxity have been described previously for lumican- and fibromodulin deficient mice, which show a decrease in tendon stiffness and integrity. Furthermore mice that lack thrombospondin 2 have increased flexibility in tail tendons and ligaments, which permits tying a knot in the tail. This manipulation is not possible in WT mice. Abnormalities in these mice models have been associated with abnormal collagen fibrillogenesis [72;73].

It has long been known that collagen is deposited into widely varying tissue-specific forms, and while recent studies confirm that this process is highly regulated in fibroblasts, the molecular details of this process are not yet completely understood [9;10;74]. Mao et al. postulated that TNX participates in this pathway, and proposed that other genes playing a role in this process may be responsible for other Ehlers-Danlos variants [52].

TENASCIN-X AND THE COLLAGEN FIBRIL

Recently, several models have been proposed for TNX to interact with collagen fibrils. Bristow et al. proposed a model in which TNX might regulate the spacing between fibrils, and contribute to strength of the dermis, through direct binding to collagen fibrils [75]. Bristow et al. stated that several lines of evidence support this concept. First, Lethias et al. [76] cloned bovine TNX as a fibril-associated protein in dermal collagen preparations. Second, recent studies suggest that native TNX binds collagen and the native protein increased both the rate and extent of fibril formation in vitro [77]. Third, Lethias showed that the 10th and 11th fibronectin repeats of TNX interact with the dermatan sulfate chains of decorin, a small leucine-rich proteoglycan that binds collagen avidly and regulates fibrillogenesis [78;79]. Finally, immunogold labeling localizes TNX to the fibril surface in human dermis, while staining is absent from TNX-deficient skin [75]. Together these data strongly support physical interaction between TNX and collagen fibrils. However, if TNX specifically regulates inter-fibrillar distance, the protein must interact directly or indirectly with multiple fibrils. The simplest way for this to occur is if TNX is multimer. This is the case for both TNC and TNR and sequences at the N-terminus of these molecules that mediate oligomerization are conserved in TNX [39;41;80]. However, multimeric TNX complexes in extracts of tissue or fibroblast conditioned medium have not been demonstrated. Veit et al. demonstrated binding of TNX to collagen type XII and proposed a model in which collagen XII interacts with TNX, both bound to fibrils by decorin thus linking collagen fibers together

[81]. Following this report Lethias et al. demonstrated by rotary shadowing that recombinant TNX could form trimers. Furthermore they showed binding to several types of fibrillar and FACIT collagens, however trimerisation did not appear essential for binding as monomeric TNX extracted from bovine tissue exhibited the same binding properties [82].

TENASCIN-X, ELASTOGENESIS, AND MATRIX REMODELING

Zweers et al. [83] followed up molecular observations on TNX-deficient patients with ultrastructural analysis of their skin. They were able to confirm normal appearing fibrils and reduced collagen content, but also noticed irregular and immature elastin fibers containing few or no microfibrils. Elastin staining showed fragmentation and reduced branching of fine elastic fibers in papillary dermis and fragmented or clumped coarse elastic fibers in reticular dermis. Generalized elastic fiber abnormalities have not been shown in other forms of EDS, so it seems likely that the elastic fiber abnormalities are a direct result of TNX-deficiency and not a secondary consequence of altered collagen metabolism. What is still unclear is the extent to which the TNX-deficient phenotype is altered by co-existing elastin abnormalities.

Bristow et al. performed a microarray-based analysis of expression differences between TNX KO and WT mouse fibroblasts that may shed light in this phenomenon. They found significant up-regulation of fibrillin-2 and stromelysin-3 [M. Collier and J. Bristow, unpublished]. Stromelysin-3 is a protease whose primary known target is the α-1 proteinase inhibitor that in turn, normally binds and inhibits elastase [84]. The net consequence of these alterations may be activation of dermal elastic fiber remodeling that could account for the observed changes in vivo.

Recently reports of additional matrix alterations in TNX KO mice have emerged. Matsumoto et al. have reported adhesive defects in TNX KO fibroblasts, accumulation of triglycerides and altered expression of collagen VI, matrix metalloproteases 2 and 9 and altered composition of triglyceride associated fatty acids in independently derived TNX KO mice [71;85-89]. While the implications of these findings for TNX-deficient EDS are uncertain, these observations together suggest that TNX has effects on matrix synthesis and remodelling that extend beyond the fibrillar collagens.

AIMS OF THIS THESIS

Before the start of this project, Burch et al. [50] and Schalkwijk et al. [67] described clinical and genetic findings in a number of TNX-deficient patients and showed TNX deficiency causes a recessive form of EDS. Schalkwijk et al. [67] showed that a 140 kDa TNX species is present in serum and developed a sandwich ELISA to conveniently screen sera for TNX deficient patients. Mao et al. [70] generated a TNX KO mouse model and described an alteration in collagen deposition and fragile skin phenotype. However, how the absence of TNX resulted in the observed phenotypes remained unclear. The work described in this thesis was specifically aimed at answering the following questions:

1. Is TNX involved in the initial deposition of ECM components or in maturation and stability of the ECM?

2. Do TNX deficient mice exhibit joint hypermobility and if yes, which morphological changes are associated with increased mobility?

3. What are the interaction partners of TNX in the ECM and how does absence of TNX influence their deposition, maturation and stability?

4. Does TNX deficiency cause pathological conditions associated in humans other than skin laxity and joint hypermobility?

5. Which TNX fragments can be found in human serum and are they biological active?

In **chapters 2** (skin development), **3** (skin wound healing) and **4** (uterus remodeling) the role of TNX in deposition, maturation and stability of ECM components (aim #1) was investigated. Joint mobility of mice is investigated in **chapter 2** (aim #2). Biochemical evaluation of interaction partners of TNX is described in **chapters 5** (fibrillar collagens and elastin), **6** (collagen type XII) and **7** (serum TNX), while the effect of TNX deficiency on these interaction partners was investigated in **chapters 2, 3 and 4** (aim #3). **Chapter 3 and 4** describe the effect of TNX deficiency in patients on wound healing, pregnancy and uterus tissue stability (aim #4). Finally, TNX species present in human serum were investigated in **chapter 7** (aim #5).

REFERENCES

[1] Canty,E.G. & Kadler,K.E. (2005) Procollagen trafficking, processing and fibrillogenesis. *J. Cell Sci.* **118,** 1341-1353.

[2] Koch,M., Laub,F., Zhou,P., Hahn,R.A., Tanaka,S., Burgeson,R.E., Gerecke,D.R., Ramirez,F., & Gordon,M.K. (2003) Collagen XXIV, a vertebrate fibrillar collagen with structural features of invertebrate collagens: selective expression in developing cornea and bone. *J. Biol. Chem.* **278,** 43236-43244.

[3] Pace,J.M., Corrado,M., Missero,C., & Byers,P.H. (2003) Identification, characterization and expression analysis of a new fibrillar collagen gene, COL27A1. *Matrix Biol.* **22,** 3-14.

[4] Boot-Handford,R.P., Tuckwell,D.S., Plumb,D.A., Rock,C.F., & Poulsom,R. (2003) A novel and highly conserved collagen (pro(alpha)1(XXVII)) with a unique expression pattern and unusual molecular characteristics establishes a new clade within the vertebrate fibrillar collagen family. *J. Biol. Chem.* **278,** 31067-31077.

[5] Williams,B.R., Gelman,R.A., Poppke,D.C., & Piez,K.A. (1978) Collagen fibril formation. Optimal in vitro conditions and preliminary kinetic results. *J Biol Chem.* **253,** 6578-6585.

[6] GROSS,J. & KIRK,D. (1958) The heat precipitation of collagen from neutral salt solutions: some rate-regulating factors. *J. Biol. Chem.* **233,** 355-360.

[7] Fertala,A., Holmes,D.F., Kadler,K.E., Sieron,A.L., & Prockop,D.J. (1996) Assembly in vitro of thin and thick fibrils of collagen II from recombinant procollagen II. The monomers in the tips of thick fibrils have the opposite orientation from monomers in the growing tips of collagen I fibrils. *J. Biol. Chem.* **271,** 14864-14869.

[8] Kadler,K.E., Holmes,D.F., Trotter,J.A., & Chapman,J.A. (1996) Collagen fibril formation. *Biochem J* **316 (Pt 1),** 1-11.

[9] Canty,E.G., Lu,Y., Meadows,R.S., Shaw,M.K., Holmes,D.F., & Kadler,K.E. (2004) Coalignment of plasma membrane channels and protrusions (fibripositors) specifies the parallelism of tendon. *J. Cell Biol.* **165,** 553-563.

[10] Kadler,K. (2004) Matrix loading: assembly of extracellular matrix collagen fibrils during embryogenesis. *Birth Defects Res. C. Embryo. Today* **72,** 1-11.

[11] Kielty,C.M. & Grant,M.E. (2002) The collagen family: Structure, assembly, and organization in the extracellular matrix. In Connective Tissue and its Heritable Disorders, Molecular, Genetic and Medical Aspects (Royce P.M.and Steinmann,B., ed), pp. 159-221. Wiley-Liss , New York.

[12] Myllyharju,J. & Kivirikko,K.I. (2001) Collagens and collagen-related diseases. *Ann. Med.* **33,** 7-21.

[13] Koch,M., Foley,J.E., Hahn,R., Zhou,P., Burgeson,R.E., Gerecke,D.R., & Gordon,M.K. (2001) alpha 1(Xx) collagen, a new member of the collagen subfamily, fibril-associated collagens with interrupted triple helices. *J. Biol. Chem.* **276,** 23120-23126.

[14] Koch,M., Schulze,J., Hansen,U., Ashwodt,T., Keene,D.R., Brunken,W.J., Burgeson,R.E., Bruckner,P., & Bruckner-Tuderman,L. (2004) A novel marker of tissue junctions, collagen XXII. *J. Biol. Chem.* **279,** 22514-22521.

[15] Fitzgerald,J. & Bateman,J.F. (2001) A new FACIT of the collagen family: COL21A1. *FEBS Lett.* **505,** 275-280.

[16] Sato,K., Yomogida,K., Wada,T., Yorihuzi,T., Nishimune,Y., Hosokawa,N., & Nagata,K. (2002) Type XXVI collagen, a new member of the collagen family, is specifically expressed in the testis and ovary. *J. Biol. Chem.* **277,** 37678-37684.

[17] Myllyharju,J. & Kivirikko,K.I. (2004) Collagens, modifying enzymes and their mutations in humans, flies and worms. *Trends Genet.* **20,** 33-43.

[18] Veit,G., Kobbe,B., Keene,D.R., Paulsson,M., Koch,M., & Wagener,R. (2006) Collagen XXVIII, a novel von Willebrand factor A domain-containing protein with many imperfections in the collagenous domain. *J. Biol. Chem.* **281,** 3494-3504.

[19] Banyard,J., Bao,L., & Zetter,B.R. (2003) Type XXIII collagen, a new transmembrane collagen identified in metastatic tumor cells. *J. Biol. Chem.* **278,** 20989-20994.

[20] Hashimoto,T., Wakabayashi,T., Watanabe,A., Kowa,H., Hosoda,R., Nakamura,A., Kanazawa,I., Arai,T., Takio,K., Mann,D.M., & Iwatsubo,T. (2002) CLAC: a novel Alzheimer amyloid plaque component derived from a transmembrane precursor, CLAC-P/collagen type XXV. *EMBO J.* **21,** 1524-1534.

[21] Robb,B.W., Wachi,H., Schaub,T., Mecham,R.P., & Davis,E.C. (1999) Characterization of an in vitro model of elastic fiber assembly. *Mol. Biol. Cell* **10,** 3595-3605.

[22] Kielty,C.M., Sherratt,M.J., & Shuttleworth,C.A. (2002) Elastic fibres. *J. Cell Sci.* **115,** 2817-2828.

[23] Thomassin,L., Werneck,C.C., Broekelmann,T.J., Gleyzal,C., Hornstra,I.K., Mecham,R.P., & Sommer,P. (2005) The Pro-regions of lysyl oxidase and lysyl oxidase-like 1 are required for deposition onto elastic fibers. *J. Biol. Chem.* **280,** 42848-42855.

[24] Zhang,H., Hu,W., & Ramirez,F. (1995) Developmental expression of fibrillin genes suggests heterogeneity of extracellular microfibrils. *J. Cell Biol.* **129,** 1165-1176.

[25] Hill,C.H., Mecham,R., & Starcher,B. (2002) Fibrillin-2 defects impair elastic fiber assembly in a homocysteinemic chick model. *J. Nutr.* **132,** 2143-2150.

[26] Kozel,B.A., Wachi,H., Davis,E.C., & Mecham,R.P. (2003) Domains in tropoelastin that mediate elastin deposition in vitro and in vivo. *J. Biol. Chem.* **278,** 18491-18498.

[27] Jensen,S.A., Corbett,A.R., Knott,V., Redfield,C., & Handford,P.A. (2005) Ca2+-dependent interface formation in fibrillin-1. *J. Biol. Chem.* **280,** 14076-14084.

[28] Whiteman,P., Smallridge,R.S., Knott,V., Cordle,J.J., Downing,A.K., & Handford,P.A. (2001) A G1127S change in calcium-binding epidermal growth factor-like domain 13 of human fibrillin-1 causes short range conformational effects. *J. Biol. Chem.* **276,** 17156-17162.

[29] Kettle,S., Yuan,X., Grundy,G., Knott,V., Downing,A.K., & Handford,P.A. (1999) Defective calcium binding to fibrillin-1: consequence of an N2144S change for fibrillin-1 structure and function. *J. Mol. Biol.* **285,** 1277-1287.

[30] Reinhardt,D.P., Ono,R.N., & Sakai,L.Y. (1997) Calcium stabilizes fibrillin-1 against proteolytic degradation. *J. Biol. Chem.* **272,** 1231-1236.

[31] Reinhardt,D.P., Mechling,D.E., Boswell,B.A., Keene,D.R., Sakai,L.Y., & Bachinger,H.P. (1997) Calcium determines the shape of fibrillin. *J. Biol. Chem.* **272,** 7368-7373.

[32] Starcher,B. & Conrad,M. (1995) A role for neutrophil elastase in the progression of solar elastosis. *Connect. Tissue Res.* **31,** 133-140.

[33] Mecham,R.P., Broekelmann,T.J., Fliszar,C.J., Shapiro,S.D., Welgus,H.G., & Senior,R.M. (1997) Elastin degradation by matrix metalloproteinases. Cleavage site specificity and mechanisms of elastolysis. *J. Biol. Chem.* **272,** 18071-18076.

[34] Starcher,B., Aycock,R.L., & Hill,C.H. (2005) Multiple roles for elastic fibers in the skin. *J. Histochem. Cytochem.* **53,** 431-443.

[35] Jones,F.S. & Jones,P.L. (2000) The tenascin family of ECM glycoproteins: structure, function, and regulation during embryonic development and tissue remodeling. *Dev. Dyn.* **218,** 235-259.

[36] Grumet,M., Hoffman,S., Crossin,K.L., & Edelman,G.M. (1985) Cytotactin, an extracellular matrix protein of neural and non-neural tissues that mediates glia-neuron interaction. *Proc. Natl. Acad. Sci. U. S. A* **82,** 8075-8079.

[37] Pearson,C.A., Pearson,D., Shibahara,S., Hofsteenge,J., & Chiquet-Ehrismann,R. (1988) Tenascin: cDNA cloning and induction by TGF-beta. *EMBO J.* **7,** 2977-2982.

[38] Morel,Y., Bristow,J., Gitelman,S.E., & Miller,W.L. (1989) Transcript encoded on the opposite strand of the human steroid 21-hydroxylase/complement component C4 gene locus. *Proc. Natl. Acad. Sci. U. S. A* **86,** 6582-6586.

[39] Rathjen,F.G., Wolff,J.M., & Chiquet-Ehrismann,R. (1991) Restrictin: a chick neural extracellular matrix protein involved in cell attachment co-purifies with the cell recognition molecule F11. *Development* **113,** 151-164.

[40] Matsumoto,K., Ishihara,N., Ando,A., Inoko,H., & Ikemura,T. (1992) Extracellular matrix protein tenascin-like gene found in human MHC class III region. *Immunogenetics* **36,** 400-403.

[41] Bristow,J., Tee,M.K., Gitelman,S.E., Mellon,S.H., & Miller,W.L. (1993) Tenascin-X: a novel extracellular matrix protein encoded by the human XB gene overlapping P450c21B. *J. Cell Biol.* **122,** 265-278.

[42] Schachner,M., Taylor,J., Bartsch,U., & Pesheva,P. (1994) The perplexing multifunctionality of janusin, a tenascin-

related molecule. *Perspect. Dev. Neurobiol.* **2,** 33-41.

[43] Neidhardt,J., Fehr,S., Kutsche,M., Lohler,J., & Schachner,M. (2003) Tenascin-N: characterization of a novel member of the tenascin family that mediates neurite repulsion from hippocampal explants. *Mol. Cell Neurosci.* **23,** 193-209.

[44] Scherberich,A., Tucker,R.P., Samandari,E., Brown-Luedi,M., Martin,D., & Chiquet-Ehrismann,R. (2004) Murine tenascin-W: a novel mammalian tenascin expressed in kidney and at sites of bone and smooth muscle development. *J. Cell Sci.* **Pt**.

[45] Hagios,C., Koch,M., Spring,J., Chiquet,M., & Chiquet-Ehrismann,R. (1996) Tenascin-Y: a protein of novel domain structure is secreted by differentiated fibroblasts of muscle connective tissue. *J. Cell Biol.* **134,** 1499-1512.

[46] Tucker,R.P., Drabikowski,K., Hess,J.F., Ferralli,J., Chiquet-Ehrismann,R., & Adams,J.C. (2006) Phylogenetic analysis of the tenascin gene family: evidence of origin early in the chordate lineage. *BMC. Evol. Biol.* **6,** 60.

[47] Saga,Y., Yagi,T., Ikawa,Y., Sakakura,T., & Aizawa,S. (1992) Mice develop normally without tenascin. *Genes Dev.* **6,** 1821-1831.

[48] Forsberg,E., Hirsch,E., Frohlich,L., Meyer,M., Ekblom,P., Aszodi,A., Werner,S., & Fassler,R. (1996) Skin wounds and severed nerves heal normally in mice lacking tenascin-C. *Proc. Natl. Acad. Sci. U. S. A* **93,** 6594-6599.

[49] Weber,P., Bartsch,U., Rasband,M.N., Czaniera,R., Lang,Y., Bluethmann,H., Margolis,R.U., Levinson,S.R., Shrager,P., Montag,D., & Schachner,M. (1999) Mice deficient for tenascin-R display alterations of the extracellular matrix and decreased axonal conduction velocities in the CNS. *J. Neurosci.* **19,** 4245-4262.

[50] Burch,G.H., Gong,Y., Liu,W., Dettman,R.W., Curry,C.J., Smith,L., Miller,W.L., & Bristow,J. (1997) Tenascin-X deficiency is associated with Ehlers-Danlos syndrome. *Nat. Genet.* **17,** 104-108.

[51] Erickson,H.P. (1997) A tenascin knockout with a phenotype. *Nat. Genet.* **17,** 5-7.

[52] Mao,J.R. & Bristow,J. (2001) The Ehlers-Danlos syndrome: on beyond collagens. *J. Clin. Invest* **107,** 1063-1069.

[53] Speiser,P.W. & White,P.C. (2003) Congenital adrenal hyperplasia. *N. Engl. J. Med.* **349,** 776-788.

[54] Gitelman,S.E., Bristow,J., & Miller,W.L. (1992) Mechanism and consequences of the duplication of the human C4/P450c21/gene X locus. *Mol. Cell Biol.* **12,** 2124-2134.

[55] Bristow,J., Gitelman,S.E., Tee,M.K., Staels,B., & Miller,W.L. (1993) Abundant adrenal-specific transcription of the human P450c21A "pseudogene". *J. Biol. Chem.* **268,** 12919-12924.

[56] Tee,M.K., Thomson,A.A., Bristow,J., & Miller,W.L. (1995) Sequences promoting the transcription of the human XA gene overlapping P450c21A correctly predict the presence of a novel, adrenal-specific, truncated form of tenascin-X. *Genomics* **28,** 171-178.

[57] Matsumoto,K., Arai,M., Ishihara,N., Ando,A., Inoko,H., & Ikemura,T. (1992) Cluster of fibronectin type III repeats found in the human major histocompatibility complex class III region shows the highest homology with the repeats in an extracellular matrix protein, tenascin. *Genomics* **12,** 485-491.

[58] Burch,G.H., Bedolli,M.A., McDonough,S., Rosenthal,S.M., & Bristow,J. (1995) Embryonic expression of tenascin-X suggests a role in limb, muscle, and heart development. *Dev. Dyn.* **203,** 491-504.

[59] Matsumoto,K., Saga,Y., Ikemura,T., Sakakura,T., & Chiquet,E.R. (1994) The distribution of tenascin-X is distinct and often reciprocal to that of tenascin-C. *J. Cell Biol.* **125,** 483-493.

[60] Beighton,P., De Paepe,A., Steinmann,B., Tsipouras,P., & Wenstrup,R.J. (1998) Ehlers-Danlos syndromes: revised nosology, Villefranche, 1997. Ehlers-Danlos National Foundation (USA) and Ehlers-Danlos Support Group (UK). *Am. J. Med. Genet.* **77,** 31-37.

[61] Pepin,M., Schwarze,U., Superti-Furga,A., & Byers,P.H. (2000) Clinical and genetic features of Ehlers-Danlos syndrome type IV, the vascular type. *N. Engl. J. Med.* **342,** 673-680.

[62] Beighton,P., De Paepe,A., Danks,D., Finidori,G., Gedde-Dahl,T., Goodman,R., Hall,J.G., Hollister,D.W., Horton,W., McKusick,V.A., & . (1988) International Nosology of Heritable Disorders of Connective Tissue, Berlin, 1986. *Am. J. Med. Genet.* **29,** 581-594.

[63] Ramos-e-Silva, Libia Cardozo,P.A., Bastos,O.G., & Coelho da Silva,C.S. (2006) Connective tissue diseases: pseudoxanthoma elasticum, anetoderma, and Ehlers-Danlos syndrome in pregnancy. *Clin. Dermatol.* **24,** 91-96.

[64] Chung,E.K., Yang,Y., Rennebohm,R.M., Lokki,M.L., Higgins,G.C., Jones,K.N., Zhou,B., Blanchong,C.A., & Yu,C.Y. (2002) Genetic sophistication of human complement components C4A and C4B

and RP-C4-CYP21-TNX (RCCX) modules in the major histocompatibility complex. *Am. J. Hum. Genet.* **71,** 823-837.

[65] Yu,C.Y. & Whitacre,C.C. (2004) Sex, MHC and complement C4 in autoimmune diseases. *Trends Immunol.* **25,** 694-699.

[66] Koppens,P.F., Hoogenboezem,T., & Degenhart,H.J. (2002) Carriership of a defective tenascin-X gene in steroid 21-hydroxylase deficiency patients: TNXB - TNXA hybrids in apparent large-scale gene conversions. *Hum. Mol. Genet.* **11,** 2581-2590.

[67] Schalkwijk,J., Zweers,M.C., Steijlen,P.M., Dean,W.B., Taylor,G., Van Vlijmen,I.M., van Haren,B., Miller,W.L., & Bristow,J. (2001) A recessive form of the Ehlers-Danlos syndrome caused by tenascin-X deficiency. *N. Engl. J. Med.* **345,** 1167-1175.

[68] Lindor,N.M. & Bristow,J. (2005) Tenascin-X deficiency in autosomal recessive Ehlers-Danlos syndrome. *Am. J. Med. Genet. A* **135,** 75-80.

[69] Zweers,M.C., Bristow,J., Steijlen,P.M., Dean,W.B., Hamel,B.C., Otero,M., Kucharekova,M., Boezeman,J.B., & Schalkwijk,J. (2003) Haploinsufficiency of TNXB is associated with hypermobility type of Ehlers-Danlos syndrome. *Am. J. Hum. Genet.* **73,** 214-217.

[70] Mao,J.R., Taylor,G., Dean,W.B., Wagner,D.R., Afzal,V., Lotz,J.C., Rubin,E.M., & Bristow,J. (2002) Tenascin-X deficiency mimics Ehlers-Danlos syndrome in mice through alteration of collagen deposition. *Nat. Genet.* **30,** 421-425.

[71] Matsumoto,K., Takayama,N., Ohnishi,J., Ohnishi,E., Shirayoshi,Y., Nakatsuji,N., & Ariga,H. (2001) Tumour invasion and metastasis are promoted in mice deficient in tenascin-X. *Genes Cells* **6,** 1101-1111.

[72] Kyriakides,T.R., Zhu,Y.H., Smith,L.T., Bain,S.D., Yang,Z., Lin,M.T., Danielson,K.G., Iozzo,R.V., LaMarca,M., McKinney,C.E., Ginns,E.I., & Bornstein,P. (1998) Mice that lack thrombospondin 2 display connective tissue abnormalities that are associated with disordered collagen fibrillogenesis, an increased vascular density, and a bleeding diathesis. *J. Cell Biol.* **140,** 419-430.

[73] Jepsen,K.J., Wu,F., Peragallo,J.H., Paul,J., Roberts,L., Ezura,Y., Oldberg,A., Birk,D.E., & Chakravarti,S. (2002) A syndrome of joint laxity and impaired tendon integrity in lumican- and fibromodulin-deficient mice. *J. Biol. Chem.* **277,** 35532-35540.

[74] Wenstrup,R.J., Florer,J.B., Brunskill,E.W., Bell,S.M., Chervoneva,I., & Birk,D.E. (2004) Type V collagen controls the initiation of collagen fibril assembly. *J. Biol. Chem.* **279,** 53331-53337.

[75] Bristow,J., Carey,W., Egging,D., & Schalkwijk,J. (2005) Tenascin-X, collagen, elastin, and the Ehlers-Danlos syndrome. *Am. J. Med. Genet. C. Semin. Med. Genet.* **139,** 24-30.

[76] Lethias,C., Descollonges,Y., Boutillon,M.M., & Garrone,R. (1996) Flexilin: a new extracellular matrix glycoprotein localized on collagen fibrils. *Matrix Biol.* **15,** 11-19.

[77] Minamitani,T., Ikuta,T., Saito,Y., Takebe,G., Sato,M., Sawa,H., Nishimura,T., Nakamura,F., Takahashi,K., Ariga,H., & Matsumoto,K. (2004) Modulation of collagen fibrillogenesis by tenascin-X and type VI collagen. *Exp. Cell Res.* **298,** 305-315.

[78] Lethias,C., Elefteriou,F., Parsiegla,G., Exposito,J.Y., & Garrone,R. (2001) Identification and characterization of a conformational heparin-binding site involving two fibronectin type iii modules of bovine tenascin-x. *J. Biol. Chem.* **276,** 16432-16438.

[79] Elefteriou,F., Exposito,J., Garrone,R., & Lethias,C. (2001) Binding of tenascin-X to decorin. *FEBS Lett.* **495,** 44-47.

[80] Erickson,H.P. & Inglesias,J.L. (1984) A six-armed oligomer isolated from cell surface fibronectin preparations. *Nature* **311,** 267-269.

[81] Veit,G., Hansen,U., Keene,D.R., Bruckner,P., Chiquet-Ehrismann,R., Chiquet,M., & Koch,M. (2006) Collagen XII Interacts with Avian Tenascin-X through Its NC3 Domain. *J. Biol. Chem.* **281,** 27461-27470.

[82] Lethias,C., Carisey,A., Comte,J., Cluzel,C., & Exposito,J.Y. (2006) A model of tenascin-X integration within the collagenous network. *FEBS Lett.* **580,** 6281-6285.

[83] Zweers,M.C., Vlijmen-Willems,I.M., Van Kuppevelt,T.H., Mecham,R.P., Steijlen,P.M., Bristow,J., & Schalkwijk,J. (2004) Deficiency of tenascin-x causes abnormalities in dermal elastic fiber morphology. *J. Invest Dermatol.* **122,** 885-891.

[84] Amano,T., Fu,L., Sahu,S., Markey,M., & Shi,Y.B. (2004) Substrate specificity of Xenopus matrix metalloproteinase stromelysin-3. *Int. J. Mol. Med.* **14,** 233-239.

[85] Matsumoto,K., Sato,T., Oka,S., Inokuchi,J., & Ariga,H. (2004) Comparison of the compositions of phospholipid-associated fatty acids in wild-type and

extracellular matrix tenascin-X-deficient mice. *Biol. Pharm. Bull.* **27,** 1447-1450.

[86] Matsumoto,K., Minamitani,T., Orba,Y., Sato,M., Sawa,H., & Ariga,H. (2004) Induction of matrix metalloproteinase-2 by tenascin-X deficiency is mediated through the c-Jun N-terminal kinase and protein tyrosine kinase phosphorylation pathway. *Exp. Cell Res.* **297,** 404-414.

[87] Matsumoto,K., Sato,T., Oka,S., Orba,Y., Sawa,H., Kabayama,K., Inokuchi,J., & Ariga,H. (2004) Triglyceride accumulation and altered composition of triglyceride-associated fatty acids in the skin of tenascin-X-deficient mice. *Genes to Cells* **9,** 737-748.

[88] Minamitani,T., Ariga,H., & Matsumoto,K. (2002) Adhesive defect in extracellular matrix tenascin-x-null fibroblasts: a possible mechanism of tumor invasion. *Biol. Pharm. Bull.* **25,** 1472-1475.

[89] Minamitani,T., Ariga,H., & Matsumoto,K. (2004) Deficiency of tenascin-X causes a decrease in the level of expression of type VI collagen. *Exp. Cell Res.* **297,** 49-60.

CHAPTER 2

DERMAL CONNECTIVE TISSUE DEVELOPMENT IN MICE: AN ESSENTIAL ROLE FOR TENASCIN-X

This chapter has been previously published:
Egging DF, van Vlijmen I, Starcher B, Gijsen Y, Zweers MC, Blankevoort L, Bristow J, Schalkwijk J. Dermal connective tissue development in mice: an essential role for tenascin-X. Cell Tissue Res. 2006 Mar;323(3):465-74. Reprinted with permission.

Cell Tissue Res
DOI 10.1007/s00441-005-0100-5

REGULAR ARTICLE

D. F. Egging · I. van Vlijmen · B. Starcher · Y. Gijsen · M. C. Zweers · L. Blankevoort · J. Bristow · J. Schalkwijk

Dermal connective tissue development in mice: an essential role for tenascin-X

Received: 28 September 2005 / Accepted: 10 October 2005

Abstract Deficiency of the extracellular matrix protein tenascin-X (TNX) causes a recessive form of Ehlers–Danlos syndrome (EDS) characterized by hyperextensible skin and hypermobile joints. It is not known whether the observed alterations of dermal collagen fibrils and elastic fibers in these patients are caused by disturbed assembly and deposition or by altered stability and turnover. We used biophysical measurements and immunofluorescence to study connective tissue properties in TNX knockout and wild-type mice. We found that TNX knockout mice, even at a young age, have greatly disturbed biomechanical properties of the skin. No joint abnormalities were noted at any age. The spatio-temporal expression of TNX during normal mouse skin development, during embryonic days 13–19 (E13–E19), was distinct from tropoelastin and the dermal fibrillar collagens type I, III, and V. Our data show that TNX is not involved in the earliest phase (E10–E14) of the deposition of collagen fibrils and elastic fibers during fetal development. From E15 to E19, TNX starts partially to colocalize with the dermal collagens and elastin, and in adult mice, TNX is present in the entire dermis. In adult TNX knockout mice, we observed an apparent increase of elastin. We conclude that TNX knockout mice only partially recapitulate the phenotype of TNX-deficient EDS patients, and that TNX could potentially be involved in maturation and/or maintenance of the dermal collagen and elastin network.

Keywords Tenascin-X · Collagen · Elastin · Development · Ehlers-Danlos syndrome · Mouse (TNX knockout)

D. F. Egging (✉) · I. van Vlijmen · M. C. Zweers · J. Schalkwijk
Department of Dermatology Nijmegen,
Centre for Molecular Life Sciences,
Radboud University Nijmegen Medical Centre,
P.O. Box 9101, 6500 HB Nijmegen, The Netherlands
e-mail: d.egging@derma.umcn.nl

B. Starcher
Department of Biochemistry,
University of Texas Health Center at Tyler,
Tyler, TX, USA

Y. Gijsen · L. Blankevoort
Department of Orthopedics,
Orthotrauma Research Center Amsterdam,
Academic Medical Center,
University of Amsterdam,
Amsterdam, The Netherlands

J. Bristow
Department of Pediatrics, University of California,
San Francisco, CA, USA

J. Bristow
Department of Genome Sciences,
Lawrence Berkeley National Laboratory,
Berkeley, CA, USA

Introduction

TNX is a large extracellular matrix glycoprotein (Bristow et al. 1993; Lethias et al. 1996; Elefteriou et al. 1997; Ikuta et al. 1998) that is expressed in a variety of tissues including skin, joints, heart, and blood vessels. Complete deficiency of TNX in humans leads to a recessive form of Ehlers-Danlos syndrome (EDS), and TNX haploinsufficiency is a cause of hypermobility type EDS (Burch et al. 1997; Schalkwijk et al. 2001; Zweers et al. 2003). Adult TNX-deficient patients show abnormal elastic fibers and reduced collagen deposition in skin (Zweers et al. 2004). We have recently found that a high serum TNX concentration is a risk indicator for abdominal aorta aneurysm (Zweers et al. 2005). TNX-deficient patients appear to have normal vessel wall compliance and distensibility of the large arteries; however, two out of nine described patients underwent surgery for mitral valve replacement (Peeters et al. 2004; Lindor and Bristow 2005).

Two groups have independently generated TNX knockout mice (Matsumoto et al. 2001; Mao et al. 2002). Mao et al. (2002) have shown that TNX knockout mice mimic EDS

through alterations in collagen deposition, as seen in TNX-deficient patients. Matsumoto et al. (2004a–c) have demonstrated altered fatty acid composition in TNX knockout mice compared with wild-type mice and increased MMP2 activation. The same group have found that tumour invasion and metastasis are enhanced in TNX knockout mice (Matsumoto et al. 2001, 2002). The enhanced tumor invasion found in TNX knockout mice is supported by the data on cutaneous malignant melanoma in MeLiM swine. These melanoma cells show a dramatic downregulation of TNX, which could account in part for the invasive phenotype of this tumor (Geffrotin et al. 2000).

In our previous study of the dermal abnormalities of five adult TNX index patients (Schalkwijk et al. 2001), we could not determine whether these alterations were attributable to developmental defects in the collagen and elastic fibre network, or to post-natal instability or breakdown. Here, we have investigated TNX expression in wild-type and TNX knockout mice during fetal skin development in relation to the expression of fibrillar collagens type I, III, and V and elastin. Our results indicate that the TNX knockout mouse is a suitable model for skin fragility but not for joint hypermobility. The reduced biomechanical strength of the skin in adult TNX knockout mice can be found in juvenile mice but is unlikely to be caused in the initial phase of deposition of the collagenous and elastic fibre network.

Materials and methods

Test animals

TNX knockout mice were obtained as described previously (Mao et al. 2002). For all studies, except for measurements of the medial collateral ligament (MCL), we used +/+, +/–, and –/– offspring from heterozygous parents obtained by the backcrossing of TNX knockout mice with four generations of C57/BL6 mice. For optical coherence tomography and measurements of the stiffness of the MCL, littermates (3–6 months old) were used from TNX heterozygous parents obtained by backcrossing with two generations of C57/BL6 mice. The number of mice for each test is indicated in the results. The experimental design was approved by the animal use committee of Radboud University, Nijmegen.

Processing of samples

At each time point, adult mice were killed in a sealed compartment by exposure to a mixture of carbogen gas and increasing concentrations of CO_2. Mouse fetuses were killed by decapitation. Complete hind legs of mice were stored at –20°C prior to measurements of the MCL and were processed as previously described (Gijssen et al. 2004). Skin samples for paraffin sections were fixed in buffered formalin for 4 h. Skin samples for frozen sections were embedded in Tissue–Tek O.C.T. compound (Sakura Finetek Europe, The Netherlands) and snap-frozen in liquid nitrogen. The breaking strength of mouse skin samples was measured immediately after the animals had been killed.

Histochemistry and immunohistochemistry

Staining of elastic fibers was performed by a modified Hart's method on paraffin sections (7 μm thick; Starcher et al. 2005). Paraffin and frozen sections (7 μm thick) were stained with antibodies against TNX, tropoelastin (TE), and collagens type I, III, and V. Detection was performed with antibodies conjugated to fluorescein isothiocyanate (FITC, green) and Alexa Fluor 594 (AF594, red; Table 1). Cell nuclei were counterstained with 4,6-diamidino-2-phenylindole (DAPI; Molecular Probes, The Netherlands; blue).

Computational analysis of (tropo) elastin and elastic fiber density

Each micrograph was analyzed by using IPlab software (Scanalytics, US). Once a representative "region of interest" (ROI), excluding hair follicles, had been chosen, all positive segments in the ROI were marked with a specific color. The surface of the colored area was divided by the ROI surface to determine the signal density.

Measurement of the stiffness of the MCL

The stiffness of the MCL was determined as previously described (Gijssen et al. 2004). Briefly, the tibia and femur of the mouse leg were clamped in a tensile tester. All tissues were removed from the femur and tibia with the exception of the MCL. Forces were applied in the longitudinal direction of the tibia and MCL.

Measurement of the cross-sectional area of the MCL by optical coherence tomography

Optical coherence tomography, which is the optical equivalent of ultasound imaging, is a noninvasive cross-sectional imaging technique for biological systems (Huang et al. 1991). For the imaging of the MCL, a reference point was visually determined at approximately the midpoint of the ligament, in between the tibia and femoral insertion (approximately 1 mm distal to the joint cavity). Images were taken from 2 mm distal to 2 mm proximal to the reference point to cover the full length of the MCL (approximately 3.5 mm). Cross-sectional images (β-scans) were made at 0.2-mm intervals to obtain a series of 21 β-scans along the full length of the ligament. The cross-sectional area of a MCL was calculated with custom analysis software written in Labview 7 (National Instruments, US) by using β-scans 8–15 in which the MCL was clearly visible and of constant dimensions. Optical coherence tomography has been previously validated for ligaments and tendons (Martin et al. 2003).

Table 1 Antibodies used for immunofluorescence studies

ECM constituents	Primary antibody mixture	Secondary antibody mixture
Elastin and TNX	Goat polyclonal anti-rat (tropo)elastin[a]	Chick polyclonal anti-goat AF594[f]
	Guinea pig anti-human TNX[b]	Rabbit polyclonal anti-guinea pig FITC[g]
Collagens type I and TNX	Goat polyclonal anti-human collagen I[c]	Chick polyclonal anti-goat AF594[f]
	Guinea pig anti-human TNX[b]	Rabbit polyclonal anti-guinea pig FITC[g]
Collagen type III and TNX	Goat polyclonal anti-human collagen III[d]	Chick polyclonal anti-goat AF594[f]
	Guinea pig anti-human TNX[b]	Rabbit polyclonal anti-guinea pig FITC[g]
Collagen type V and TNX	Goat polyclonal anti-human collagen V[e]	Chick polyclonal anti-goat AF594[f]
	Guinea pig anti-human TNX[b]	Rabbit polyclonal anti-guinea pig FITC[g]

[a]Elastin Products, USA
[b]Schalkwijk et al. 2001
[c]SouthernBiotech, USA
[d]SouthernBiotech, USA
[e]SouthernBiotech, USA
[f]Molecular Probes, The Netherlands
[g]Dakocytomation, Denmark

Flexibility of the tail

Increased flexibility of tail ligaments and tendons, as described for the TSP2-null mouse (Kyriakides et al. 1998), was ascertained for the TNX knockout mouse. In a blind randomized test, the animals were maintained under anesthesia at an isofluran dose of 2.5%–3.0% in a N_2O_2 gas mixture (50%–65% O_2) while the investigator attempted to tie a knot in the mouse tail.

Breaking strength

A rectangular strip of dorsal skin (7 mm × 3.5 cm) was prepared from the killed mice by using a custom-made apparatus. The skin segment was clamped in a device that exerted a continuously increasing force in a longitudinal direction. The breaking strength was defined as the peak force necessary to induce tearing of a tissue segment and was expressed in grams (1000 g is equivalent to 9.281 N), as described previously (Waard de et al. 1995).

Biochemical analysis of hydroxyproline and desmosine content

Desmosine analysis of mouse skin samples was used to measure the elastin content of the skin. After removal of the hair, a 3-mm biopsy punch was obtained from the caudal dorsal skin of the mice and placed in a secure-lock microfuge tube. The sample was hydrolyzed in 500 µl 6 N HCl at 105°C for 24 h. The hydrolysate was evaporated to dryness, re-dissolved in 200 µl water, and microfuged to remove insoluble material. A 20-µl aliquot was removed for desmosine analysis by radioimmunoassay (Starcher and Conrad 1995), and 1 µl was used for protein determination by a ninhydrin-based assay as described previously (Starcher 2001). Hydroxyproline (OHP) analysis was used as a method for measuring the collagen content of the skin. The OHP content was determined by amino acid analysis from the same hydrolysate as the desmosine analysis.

Results

Biomechanical properties of skin and joints in TNX knockout and wild-type mice

Littermates –/–, –/+, and +/+ for TNX were used to measure skin and joint biomechanical properties. Figure 1 shows the applied force required for skin failure (breaking strength). The breaking strength of TNX knockout mouse skin was significantly lower than that of heterozygous or wild-type littermates. The phenotype was appreciable even at the earliest possible age that could be investigated (2 weeks neonatal), and the difference in skin strength between wild-type and TNX knockout mice increased with age (Fig. 1). Wild-type and heterozygous mice did not significantly differ. To investigate joint laxity in these animals, we performed two tests. First, we tested whether

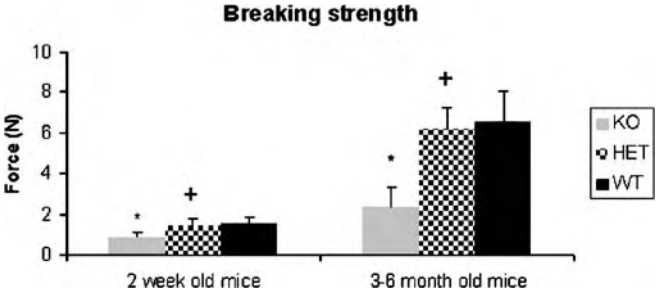

Fig. 1 Breaking strength of mouse skin. TNX knockout mice (*KO*) have weaker skin compared with that of heterozygous (*HET*) and wild-type (*WT*) littermates. The difference is appreciable even at a young age and increases over time (for comparisons of adult mice of 3–6 months of age, n=12 for knockout, n=6 for heterozygous, and n=5 for wild-type mice; for mice of 2 weeks of age, n=6 for knockout, n=8 for heterozygous, and n=10 for wild-type mice). For all comparisons to wild-type mouse, *P<0.001 when compared with knockout mice (+ not significant when compared with heterozygous mice)

Table 2 Biomechanical properties of the MCL of TNX knockout and wild-type littermates. The MCL of TNX knockout and wild-type littermates were the same in thickness and stiffness (for all comparisons, + not significant)

Character	Genotype	Mean	SD	*n*
Stiffness of MCL (N/mm)	Wild-type	5.08^{+}	1.12	8
	TNX knockout	4.96	1.50	7
Cross-sectional area MCL (mm^2)	Wild-type	0.058^{+}	0.008	8
	TNX knockout	0.052	0.010	5

the laxity of the tail ligaments of the –/– mice was such to permit tying a knot in the tail; this is not possible in wild-type mice but has been described for the thrombospondin-2 knockout mouse (Kyriakides et al. 1998). We found, however, that this manipulation was not possible in the $TNX^{-/-}$ mouse (not shown). Secondly, as a measure for joint hypermobility, the stiffness of the MCL in the knee joint was analyzed. As shown in Table 2, our measurements did not reveal a difference in ligament stiffness between TNX knockout mice and wild-type littermates. In order to exclude the possibility of a thicker MCL in TNX knockout mice as a compensatory mechanism, we measured the mean thickness of the ligament by optical coherence tomography. The MCL thickness in TNX knockout mice did not significantly differ from wild-type littermates (Table 2). Histological analysis of wild-type and TNX knockout ligaments revealed no obvious differences (data not shown).

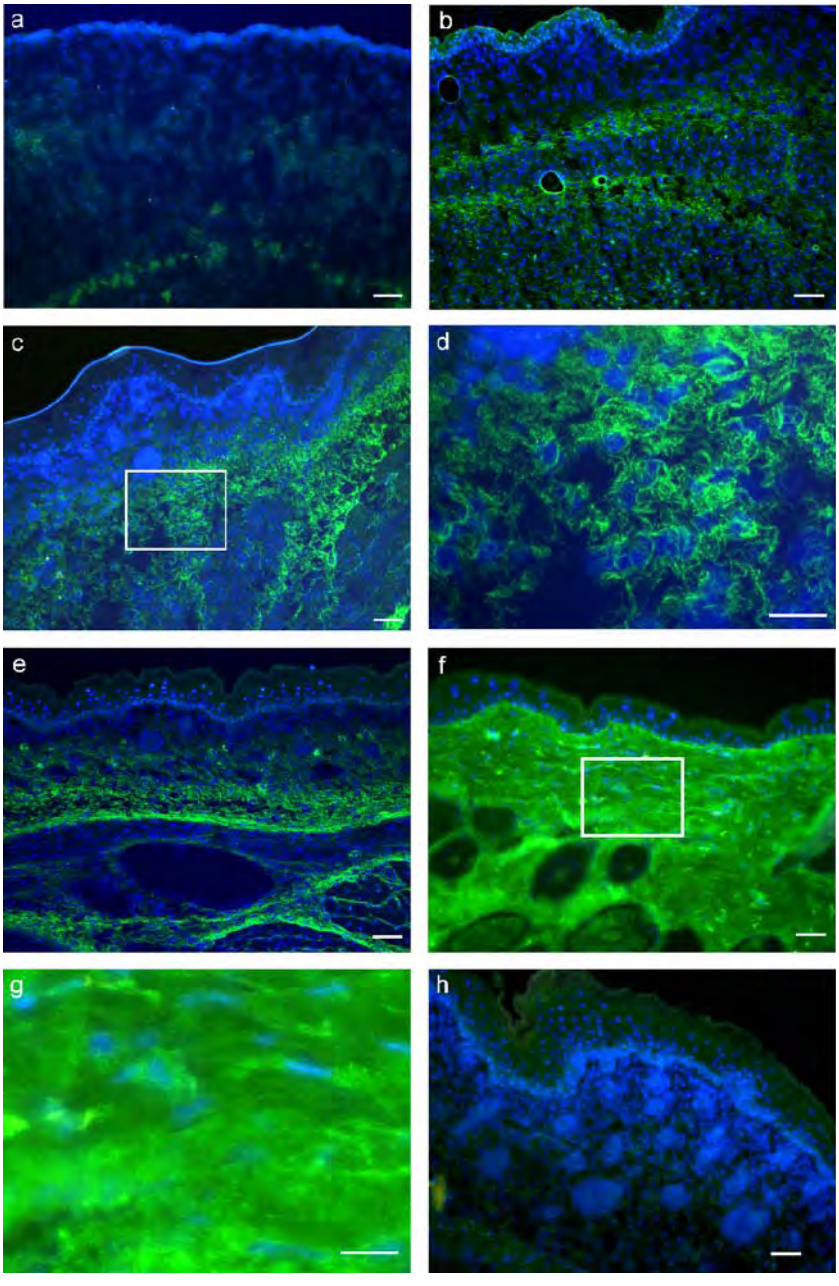

Fig. 2 TNX immunofluorescent staining of the developing skin of wild-type mice. **a** At stage E14, no significant signal in the prospective dermis is detected (*blue* nuclear staining with DAPI). **b** By stage E15, TNX expression (*green*) is visible in the developing reticular dermis and around the fascia of the carnosus muscle layer. **c**, **e** At E18 and in 1-day-old neonatal mice, respectively, expression of TNX has extended further into the dermis. **d** Higher magnification of the *rectangle* in **c**; TNX is expressed in the fetal mouse in a distinct fibre-like pattern. **f** In adult mouse skin, TNX is observed throughout the dermis in a more homogeneous pattern. **g** Higher magnification of the *rectangle* in **f**. **h** The specificity of the anti-TNX serum is demonstrated in TNX knockout mice skin (E18), which is devoid of signal. *Bars* 50 μm (**a**–**c**, **e**, **f**, **h**), 25 μm (**d**, **g**)

Expression of TNX in fetal and adult mouse skin

Sections of fetal, viz., embryonic day 13–20 (E13–E20), and adult skin were immunostained to reveal the expression of TNX at various developmental stages. The epidermis was devoid of signal at all stages, except for occasional non-specific staining of the stratum corneum. At E14, no significant signal was detected in the prospective dermis (Fig. 2a). From stage E15 onward, TNX expression was found in the lower dermis and around the fascia surrounding the panniculus carnosus beneath the developing dermis (Fig. 2b). TNX expression extended toward the

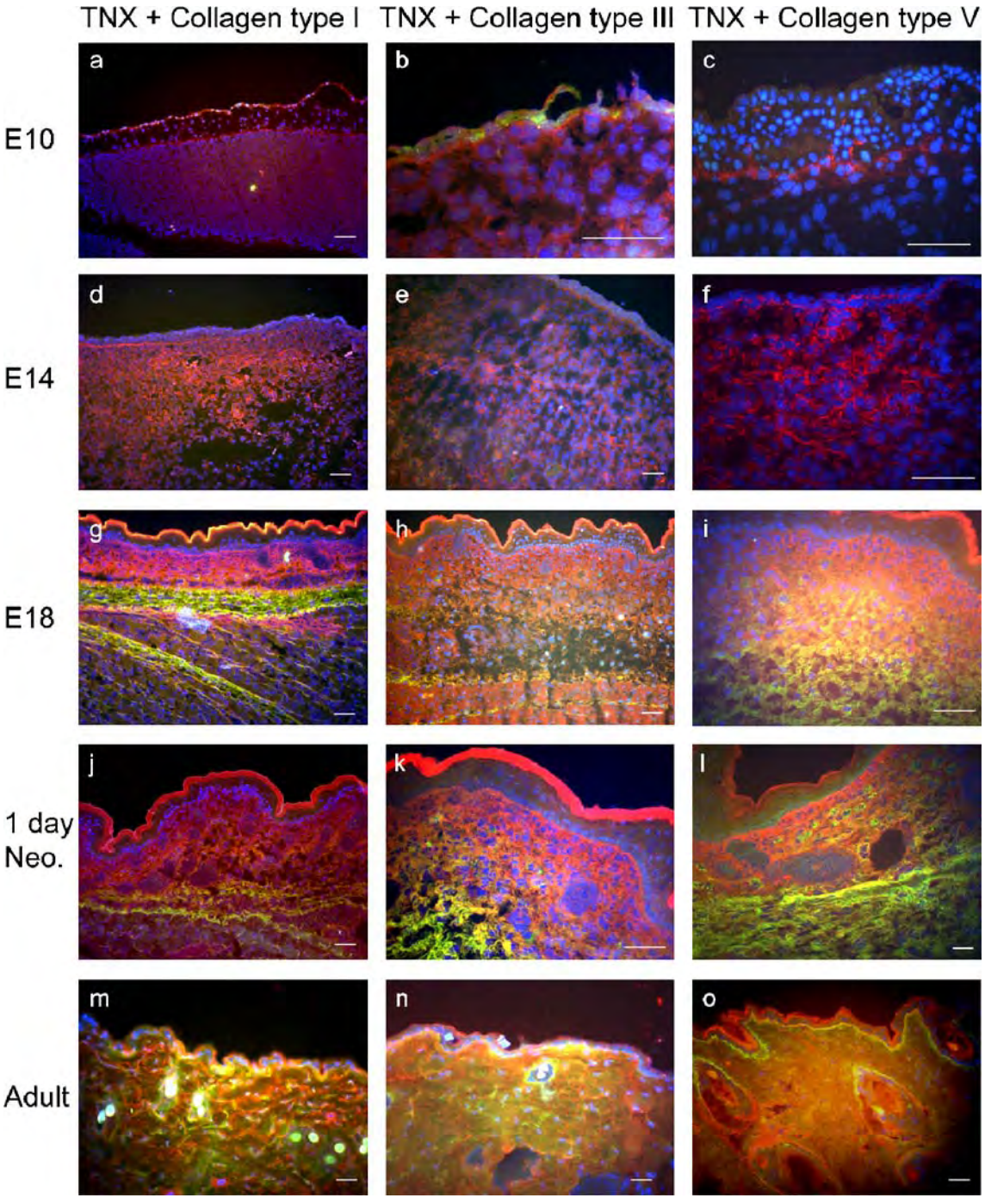

Fig. 3 Merged micrographs showing immunofluorescent double-staining for TNX (*green*) and collagens (*red*) type I (**a**, **d**, **g**, **j**, **m**), III (**b**, **e**, **h**, **k**, **n**), or V (**c**, **f**, **i**, **l**, **o**) in developing skin of wild-type mice. Nuclei are stained *blue* with DAPI. The different types of collagen are expressed even at fetal stages E10 (**a–c**) and E14 (**d–f**) in the prospective dermis. At E18 (**g–i**) and 1-day-old neonatal (*1 day Neo.*) mice (**j–l**), TNX starts to colocalize with the various types of collagens (*orange*, *yellow*). In adult mice, TNX is expressed in the entire dermis and overlaps with collagens type I (**m**), III (**n**), and V (**o**). Non-specific staining of the stratum corneum was present in some sections. *Bars* 50 μm

Table 3 Hydroxyproline (*OHP*) content in skin of adult (8–9 months old) mice as a measure for total collagen (^{+}P=0.09, ^{++}P=0.07)

Amount OHP	Genotype	Mean	SD	*n*
Content in nmol per mg protein	Wild-type	281.4^{+}	42.7	7
	TNX knockout	253.8	38.9	10
Content in nmol per mm^2 skin	Wild-type	31.6^{++}	10.4	7
	TNX knockout	24.7	8.3	10

upper part of the developing dermis at E18 and neonatal stages (Fig. 2c,e) and appeared in a fibre-like pattern (E18, Fig. 2d). In the adult mouse (Fig. 2f), the distinct fibre-like pattern was less clear, and the entire dermis exhibited a strong diffuse pattern (Fig. 2g). The specifity of our anti-TNX serum is illustrated in Fig. 2h, which shows the complete absence of staining at the E18 stage of a TNX knockout mice.

Differences in spatio-temporal appearance of TNX and the dermal fibrillar collagens

To address the question of whether TNX is involved in the assembly of collagen fibrils during normal dermal differentiation, we examined the appearance of collagens type I, III, and V in comparison with TNX. Collagens type I, III, and V were weakly present on E10 (Fig. 3a–c) in the undifferentiated dermal mesenchyme beneath the periderm of normal mouse fetuses (red signal). Expression of these collagens was abundant at E14 (Fig. 3d–f) before the start of TNX expression. The fibre-associated expression pattern of TNX, however, overlapped with the collagen network in the reticular dermis (orange signal) and around the fascia of the panniculus carnosus (orange and yellow signals), as shown in the overlays of the immunofluorescent stainings from E18 and 1-day-old neonatal mice (Fig. 3g–l). In the papillary dermis, the various collagen types were stained red, and TNX expression had not yet started in this compartment (Fig. 3g–l). In adult mice, TNX was expressed diffusely throughout the dermis and overlapped with collagens type I, III, and V, which were also expressed throughout the dermis (orange and yellow signals; Fig. 3m–o). No obvious differences in expression of the various collagen types and TNX were noted between TNX knockout and wild-type mice during development (data not shown).

Previous studies in mouse and human have shown that collagen content is reduced in adult skin of TNX-deficient individuals (Mao et al. 2002; Schalkwijk et al. 2001). Because immunofluorescent staining of dermal collagens could not be used to quantify collagen content, we performed an analysis of OHP content in TNX knockout and wild-type mouse skin. We found a slight reduction in collagen content, but this was not as prominent as in previous studies (Table 3).

Differences in spatio-temporal appearance of TNX and elastin

To address the question of whether TNX is involved in the assembly of elastic fibers during dermal differentiation, we used an antibody directed against TE as a marker for developing elastic fibers. A thin discontinuous layer of TE expression was present even in the undifferentiated dermal mesenchyme at E10 (red staining in Fig. 4a). Thereafter, TE staining was strong and continuous in the fascia lining the developing muscle cells of the panniculus carnosus. At E18, many TE-positive fibers were found in the outer layer of the fascia and scattered throughout the prospective reticular dermis as witnessed by the orange-yellow staining in merged double-staining images (Fig. 4b). Clearly, TNX expression differed temporally and spatially from TE expression in the developing mouse skin. However, from E15 onward, TNX started partially to colocalize with elastin. The TNX fibre-like pattern found at this stage overlapped with the pattern of TE-positive fibers around the fascia of the panniculus carnosus and in the prospective reticular dermis (Fig. 4b). In adult mouse skin, TNX was present diffusely throughout the entire dermis and therefore by definition overlaps with TE staining (Fig. 4c).

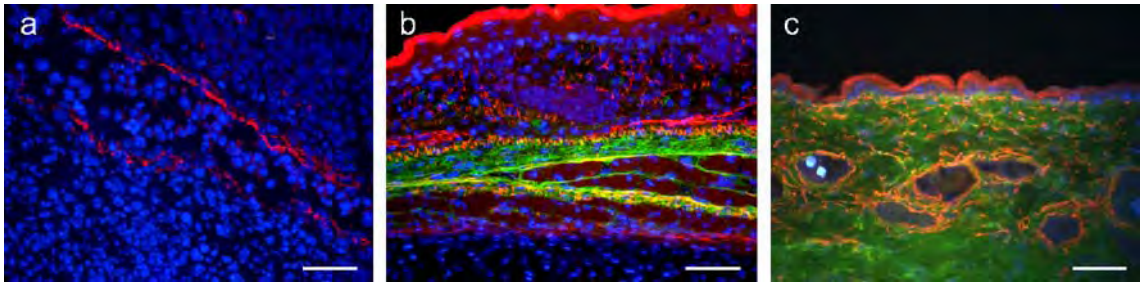

Fig. 4 Merged micrographs of immunofluorescent double-staining for TNX (*green*) and tropoelastin (TE; *red*) in developing skin in wild-type mice. TE is expressed in the undifferentiated mesenchyme at the earliest investigated stage, E10 (**a**). The signals for TE and TNX partially overlap (*orange*, *yellow*) in the developing mice skin around the fascia of the carnosus muscle at E18 (**b**). In adult mice (**c**), the entire dermis is stained positively for TNX with overlapping signal for TE (*orange*, *yellow*). *Bars* 50 μm

Difference in TE expression in knockout mice compared with heterozygous and wild-type mice

In adult TNX-deficient EDS patients, we have previously observed the fragmentation and clumping of elastic fibers (Zweers et al. 2004). We therefore examined the appearance of elastic fibers in adult knockout mice compared with heterozygous and wild-type mice by using immunofluorescent staining for TE. We did not observe obvious differences in the morphology or spatial distribution of the TE-positive elastic fibers, although the difference in density of the fibers was appreciable between adult wild-type and TNX knockout mice. Image analysis followed by computational quantitation showed that the signal intensity for TE was significantly higher in TNX knockout (Fig. 5c) mice than in heterozygous (Fig. 5b) and wild-type (Fig. 5a) littermates. The difference in density appeared at 3–6 months of age (Fig. 5e). Wild-type and heterozygous mice did not significantly differ in signal intensity. We subsequently investigated whether the differences in density of TE-positive fibers were reflected in the density of mature elastic fibers as determined histochemically by

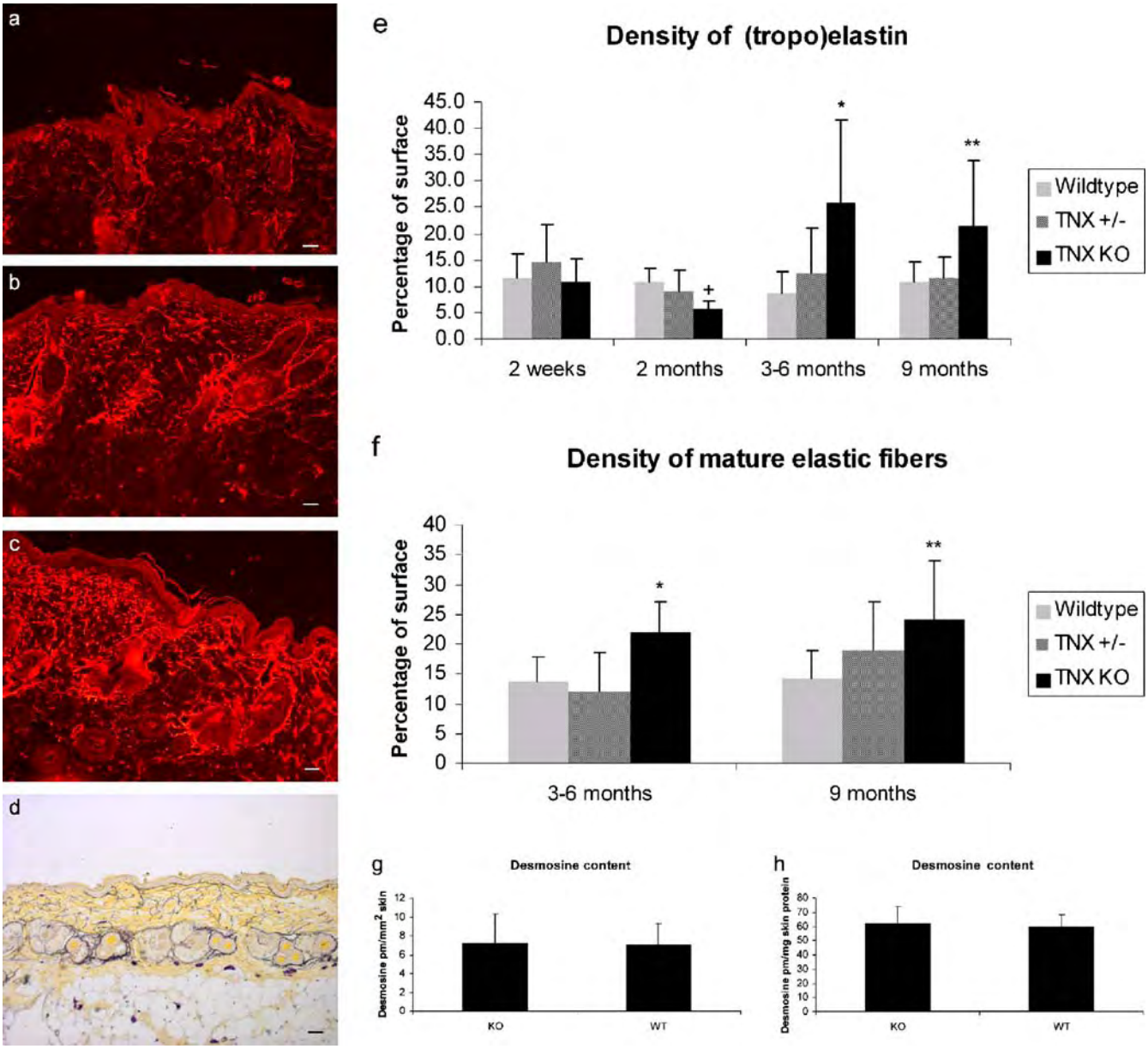

Fig. 5 Analysis of elastin and elastic fibers. Immunostaining for TE on paraffin sections of 9-month-old mice (**a**–**c**). At 3–6 months, TNX knockout mice (**c**) show a higher density of TE in their dermis than do wild-type (**a**) and heterozygous (**b**) mice (represented graphically in **e**). The density of mature elastic fibers made visible by modified Hart's staining in TNX knockout skin (not shown) compared with wild-type mice (**d**) is increased (**f**). No differences in desmosine content expressed per milligram protein (**h**) or per mm^2 (**g**) skin were found between the different phenotypes in adult mice. *P<0.01, **P<0.05, + not significant. For all comparisons, n=12 for each genotype for mice at 3–6 months, n=6 (or more) for mice at 2 weeks and 9 months. For 2-month-old mice, n=8 for heterozygous mice, n=4 for TNX knockout mice and n=3 for wild-type mice (*KO* knockout, *WT* wild-type, +/− heterozygous)

modified Hart's staining (shown for wild-type in Fig. 5d). Although the differences between wild-type and TNX knockout mice were not as obvious as for the TE immunostaining, computational analysis showed a significant difference in the densities of mature elastic fibers between TNX knockout and wild-type mice (Fig. 5f). To investigate these differences between wild-type and knockout mice further, we measured the amount of desmosine, a tetrafunctional crosslink specific for elastin, in mouse skin. Desmosine content did not differ between wild-type and knockout mice, irrespective of whether it was expressed per milligram protein or per skin surface area (Fig. 5g,h).

Discussion

The aim of our investigations was to provide a detailed study of TNX expression in skin and to examine the consequences of TNX deficiency at the functional and morphological levels. We have found no obvious differences in tail mobility and MCL stiffness, which we have used as a measure for joint hypermobility, between wild-type and knockout mice. We conclude that TNX knockout mice show a similar skin phenotype as human TNX-deficient patients but that these mice are not a suitable model to investigate joint hypermobility. On the basis of colocalization studies, we surmise that TNX is more likely to be involved in the maturation and maintenance of the collagen and elastin network than in its initial deposition.

TNX expression has not yet been studied in depth during the development of the skin. Geffrotin et al. (1995) have reported TNX transcripts in 87-day-old pig fetuses. Matsumoto et al. (1994) have demonstrated TNX transcripts in mice at E17 and staining of the dermis, but this is less strong toward the dermis at E15.5. This is in accordance with our data. However, no data from other fetal stages have been published, and TNX expression has not been studied at the protein level. We show that expression starts at E15 and progresses from the reticular dermis toward the papillary dermis during development. TNX is expressed in a fiber-like network during development, but this network is lost in adulthood. This suggests a possible difference in function for TNX during the development of skin and in mature skin.

We suggest that TNX is not involved in the initial deposition of collagen fibrils or elastic fibers because expression of the dermal fibrillar collagens and expression of TE starts well before TNX is expressed in the dermis. However, during development, the characteristic fiber-like pattern of TNX colocalizes with the collagens type I, III, and V networks; this is in accordance with previously results showing that TNX colocalizes with banded collagen fibrils in bovine fetal skin (Lethias et al. 1996; Elefteriou et al. 1997). The expression of the various types of fibrillar collagens in developing mouse skin has not been comprehensively studied in detail at the protein level. Van Exan and Hardy (1984) have found that fibrils are present at the earliest of investigated fetal stages (E12), and Niederreither et al. (1995) have demonstrated, by using in situ hybridization, that collagens type I and III are expressed in dermatomes at E10.5 and E12.5 in the presumptive dermis of whole mouse fetuses. The expression of collagen type V appears to mimic that of collagen type I, and transcripts are localized to dermal cells (Garrone et al. 1997; Andrikopoulos et al. 1992). These data are in accordance with our findings at the protein level.

A reduction in collagen occurs in the skin of adult TNX knockout mice (Mao et al. 2002) similar to that in TNX-deficient patients (Zweers et al. 2004). Although we have found a small difference in OHP content between TNX knockout and wild-type mice, the differences are not as profound as observed by Mao et al. (2002). Of note, the TNX null allele used in our study is on a different (homogenous C57Black6) background than that used by Mao et al. (2002). Together with the reduction of collagen, Mao et al. (2002) have found a decrease in the stress-strain properties of adult TNX knockout mice. We have confirmed this alteration of skin biomechanical properties in a test of skin breaking strength. We have found that, even at the youngest possible investigated age (2-week-old mice), skin strength is severely disturbed. Although no gross abnormalities of the collagen fibrils have been observed, a minor increase in size variation has been reported (Mao et al. 2002). Moreover, Minamitani et al. (2004) have found an increase in thickness of collagen fibrils in 3-month-old mice. Differences in skin mechanical properties between wild-type and TNX knockout are probably not solely caused by differences in the collagen density of the skin; qualitative differences in, for example, crosslinking and interaction between collagen fibrils might also play a role.

In TNX-deficient patients, we have previously observed altered elastic fibers in sections stained by Elastica von Gieson stain (Zweers et al. 2004). This stain appears ill-suited for the visualization of fetal and neonatal elastic fibers in mice. We have instead used a TE antibody, which recognizes both soluble TE and cross-linked elastin. In addition, we have used modified Hart's stain, a histochemical stain suitable for the visualization of elastic fibers in mouse skin. Immunofluorescence on paraffin sections has revealed an increased density of TE/elastin in TNX knockout mice compared with heterozygous TNX and wild-type mice at 3–6 months of age. This difference in density for TE/elastin is reflected, although less prominently, in mature elastic fibers in the dermis detected by modified Hart's staining. The quantification of desmosine content, however, has revealed no significant differences, suggesting a lower amount of desmosine crosslinks per elastic fiber in TNX knockout mice, which might possibly lead to less stable elastic fibers. This could in turn lead to increased synthesis as a possible compensatory mechanism. The elastic fibers of the TNX knockout mice might also be more susceptible to breakdown, since the differences in TE/elastin density appear in adulthood, in which case the TE/elastin might pick up elastin breakdown products from elastic fibers. Once again, the TNX knockout mice might compensate for this by (over) producing new elastic fibers, but this awaits further investigation. The elastic fiber phenotype in the TNX knockout mice does not resemble the phenotype found in humans. The organization and cellular source of elastic fibers in mice is known to

differ from those in humans (Starcher et al. 1999, 2005). Both in humans and in mice, TNX appears to be involved in the maintenance of normal elastic fibers. However, TNX does not seem to be associated with the initial deposition of TE/elastin, as immureactivity to the TE antibody is detected in the dermis before TNX expression starts. TNX could nevertheless be involved in the maturation of elastic fibers, since mature elastic fibers only start to appear approximately 5 days post partum in mice, coinciding with the start of hair growth (Starcher et al. 2005).

The morphological and biochemical abnormalities in TNX-deficient skin are mild compared with the strongly disturbed biomechanical properties. This suggests that TNX exerts more subtle functions that contribute to connective tissue stability. Studies by others have previously indicated that TNX interacts with various other matrix molecules (Elefteriou et al. 1997, 1999, 2001; Ikuta et al. 2000; Lethias et al. 2001; Matsumoto et al. 1994; Minamitani et al. 2004). Obviously, the biomechanical properties of the matrix will be affected by these interactions, and this is clearly an area of future research.

Acknowledgements The authors acknowledge the assistance of Dirk J. Faber and Ton G. van Leeuwen of the Laser Center at the Academic Medical Center, Amsterdam, with the optical coherence tomography measurements.

References

Andrikopoulos K, Suzuki HR, Solursh M, Ramirez F (1992) Localization of pro-alpha 2(V) collagen transcripts in the tissues of the developing mouse embryo. Dev Dyn 195:113–120

Bristow J, Tee MK, Gitelman SE, Mellon SH, Miller WL (1993) Tenascin-X: a novel extracellular matrix protein encoded by the human XB gene overlapping P450c21B. J Cell Biol 122:265–278

Burch GH, Gong Y, Liu W, Dettman RW, Curry CJ, Smith L, Miller WL, Bristow J (1997) Tenascin-X deficiency is associated with Ehlers–Danlos syndrome. Nat Genet 17:104–108

Elefteriou F, Exposito J, Garrone R, Lethias C (2001) Binding of tenascin-X to decorin. FEBS Lett 495:44–47

Elefteriou F, Exposito JY, Garrone R, Lethias C (1997) Characterization of the bovine tenascin-X. J Biol Chem 272:22866–22874

Elefteriou F, Exposito JY, Garrone R, Lethias C (1999) Cell adhesion to tenascin-X mapping of cell adhesion sites and identification of integrin receptors. Eur J Biochem 263:840–848

Exan RJ van, Hardy MH (1984) The differentiation of the dermis in the laboratory mouse. Am J Anat 169:149–164

Garrone R, Lethias C, LeGuellec D (1997) Distribution of minor collagens during skin development. Microsc Res Tech 38:407–412

Geffrotin C, Garrido JJ, Tremet L, Vaiman M (1995) Distinct tissue distribution in pigs of tenascin-X and tenascin-C transcripts. Eur J Biochem 231:83–92

Geffrotin C, Horak V, Crechet F, Tricaud Y, Lethias C, Vincent-Naulleau S, Vielh P (2000) Opposite regulation of tenascin-C and tenascin-X in MeLiM swine heritable cutaneous malignant melanoma. Biochim Biophys Acta 1524:196–202

Gijssen Y, Sierevelt I, Kooloos J, Blankevoort L (2004) Stiffness of the healing medial collateral ligament of the mouse. Connect Tissue Res 45:190–195

Huang D, Swanson EA, Lin CP, Schuman JS, Stinson WG, Chang W, Hee MR, Flotte T, Gregory K, Puliafito CA, Fujimoto JG (1991) Optical coherence tomography. Science 254:1178–1181

Ikuta T, Ariga H, Matsumoto K (2000) Extracellular matrix tenascin-X in combination with vascular endothelial growth factor B enhances endothelial cell proliferation. Genes Cells 5:913–927

Ikuta T, Sogawa N, Ariga H, Ikemura T, Matsumoto K (1998) Structural analysis of mouse tenascin-X: evolutionary aspects of reduplication of FNIII repeats in the tenascin gene family. Gene 217:1–13

Kyriakides TR, Zhu YH, Smith LT, Bain SD, Yang Z, Lin MT, Danielson KG, Iozzo RV, LaMarca M, McKinney CE, Ginns EI, Bornstein P (1998) Mice that lack thrombospondin 2 display connective tissue abnormalities that are associated with disordered collagen fibrillogenesis, an increased vascular density, and a bleeding diathesis. J Cell Biol 140:419–430

Lethias C, Descollonges Y, Boutillon MM, Garrone R (1996) Flexilin: a new extracellular matrix glycoprotein localized on collagen fibrils. Matrix Biol 15:11–19

Lethias C, Elefteriou F, Parsiegla G, Exposito JY, Garrone R (2001) Identification and characterization of a conformational heparin-binding site involving two fibronectin type iii modules of bovine tenascin-X. J Biol Chem 276:16432–16438

Lindor NM, Bristow J (2005) Tenascin-X deficiency in autosomal recessive Ehlers–Danlos syndrome. Am J Med Genet A 135:75–80

Mao JR, Taylor G, Dean WB, Wagner DR, Afzal V, Lotz JC, Rubin EM, Bristow J (2002) Tenascin-X deficiency mimics Ehlers–Danlos syndrome in mice through alteration of collagen deposition. Nat Genet 30:421–425

Martin SD, Patel NA, Adams SB, Roberts MJ, Plummer S, Stamper DL, Brezinski ME, Fujimoto JG (2003) New technology for assessing microstructural components of tendons and ligaments. Int Orthop 27:184–189

Matsumoto K, Saga Y, Ikemura T, Sakakura T, Chiquet ER (1994) The distribution of tenascin-X is distinct and often reciprocal to that of tenascin-C. J Cell Biol 125:483–493

Matsumoto K, Takayama N, Ohnishi J, Ohnishi E, Shirayoshi Y, Nakatsuji N, Ariga H (2001) Tumour invasion and metastasis are promoted in mice deficient in tenascin-X. Genes Cells 6:1101–1111

Matsumoto K, Takahashi K, Yoshiki A, Kusakabe M, Ariga H (2002) Invasion of melanoma in double knockout mice lacking tenascin-X and tenascin-C. Jpn J Cancer Res 93:968–975

Matsumoto K, Minamitani T, Orba Y, Sato M, Sawa H, Ariga H (2004a) Induction of matrix metalloproteinase-2 by tenascin-X deficiency is mediated through the c-Jun N-terminal kinase and protein tyrosine kinase phosphorylation pathway. Exp Cell Res 297:404–414

Matsumoto K, Sato T, Oka S, Inokuchi J, Ariga H (2004b) Comparison of the compositions of phospholipid-associated fatty acids in wild-type and extracellular matrix tenascin-X-deficient mice. Biol Pharm Bull 27:1447–1450

Matsumoto K, Sato T, Oka S, Orba Y, Sawa H, Kabayama K, Inokuchi J, Ariga H (2004c) Triglyceride accumulation and altered composition of triglyceride-associated fatty acids in the skin of tenascin-X-deficient mice. Genes Cells 9:737–748

Minamitani T, Ikuta T, Saito Y, Takebe G, Sato M, Sawa H, Nishimura T, Nakamura F, Takahashi K, Ariga H, Matsumoto K (2004) Modulation of collagen fibrillogenesis by tenascin-X and type VI collagen. Exp Cell Res 298:305–315

Niederreither K, DSouza R, Metsaranta M, Eberspaecher H, Toman PD, Vuorio E, DeCrombrugghe B (1995) Coordinate patterns of expression of type I and III collagens during mouse development. Matrix Biol 14:705–713

Peeters ACTM, Kucharekova M, Timmermans J, Berkmortel FWPJ van den, Boers GH, Novakova IRO, Egging D, Heijer M den, Schalkwijk J (2004) A clinical and cardiovascular survey of Ehlers–Danlos syndrome patients with complete deficiency of tenascin-X. Neth J Med 62:23–25

Schalkwijk J, Zweers MC, Steijlen PM, Dean WB, Taylor G, Van Vlijmen IM, Haren B van, Miller WL, Bristow J (2001) A recessive form of the Ehlers–Danlos syndrome caused by tenascin-X deficiency. N Engl J Med 345:1167–1175

Starcher B (2001) A ninhydrin-based assay to quantitate the total protein content of tissue samples. Anal Biochem 292:125–129
Starcher B, Conrad M (1995) A role for neutrophil elastase in the progression of solar elastosis. Connect Tissue Res 31:133–140
Starcher B, Pierce R, Hinek A (1999) UVB irradiation stimulates deposition of new elastic fibers by modified epithelial cells surrounding the hair follicles and sebaceous glands in mice. J Invest Dermatol 112:450–455
Starcher B, Aycock RL, Hill CH (2005) Multiple roles for elastic fibers in the skin. J Histochem Cytochem 53:431–443
Waard JWD de, Wobbes T, Deman BM, Linden CJ van der, Hendriks T (1995) Postoperative levamisole may compromise early healing of experimental intestinal anastomoses. Br J Cancer 72:456–460
Zweers MC, Bristow J, Steijlen PM, Dean WB, Hamel BC, Otero M, Kucharekova M, Boezeman JB, Schalkwijk J (2003) Haploinsufficiency of TNXB is associated with hypermobility type of Ehlers–Danlos syndrome. Am J Hum Genet 73:214–217
Zweers MC, Vlijmen–Willems IM, Van Kuppevelt TH, Mecham RP, Steijlen PM, Bristow J, Schalkwijk J (2004) Deficiency of tenascin-X causes abnormalities in dermal elastic fiber morphology. J Invest Dermatol 122:885–891
Zweers MC, Peeters ACTM, Graafsma S, Kranendonk S, Vliet JA van der, Heijer M den, Schalkwijk J (2005) A high tenascin-X serum concentration is a risk indicator for abdominal aortic aneurysm. Circulation (in press)

CHAPTER 3

WOUND HEALING IN TENASCIN-X DEFICIENT MICE SUGGESTS THAT TENASCIN-X IS INVOLVED IN MATRIX MATURATION RATHER THAN MATRIX DEPOSITION

This chapter has been previously published:
Egging D, van Vlijmen-Willems I, van Tongeren T, Schalkwijk J, Peeters A. Wound healing in tenascin-X deficient mice suggests that tenascin-X is involved in matrix maturation rather than matrix deposition. Connect Tissue Res. 2007;48(2):93-8. Reprinted with permission.

Connective Tissue Research, 48:93–98, 2007

ISSN: 0300-8207 print / 1521-0456 online
DOI: 10.1080/03008200601166160

informa
healthcare

Wound Healing in Tenascin-X Deficient Mice Suggests that Tenascin-X is Involved in Matrix Maturation Rather than Matrix Deposition

David Egging, Ivonne van Vlijmen-Willems
Department of Dermatology, Nijmegen Centre for Molecular Life Sciences, Radboud University Nijmegen Medical Centre, Nijmegen, the Netherlands
Anita Peeters
Department of Endocrinology, Radboud University Nijmegen Medical Centre, Nijmegen, the Netherlands
Tomas van Tongeren, Joost Schalkwijk
Department of Dermatology, Nijmegen Centre for Molecular Life Sciences, Radboud University Nijmegen Medical Centre, Nijmegen, the Netherlands

Tenascin-X (TNX) is an extracellular matrix glycoprotein whose absence in humans leads to a recessive form of Ehlers-Danlos Syndrome (EDS). TNX deficient patients have hypermobile joints and fragile skin, but unlike the classical type of EDS, no atrophic scars were observed. Anecdotal evidence suggested that wound healing in TNX deficient patients is abnormal, but no detailed study has been performed so far. To address the role of TNX in wound healing, we analyzed skin wound morphology and mechanical properties of scars in TNX knockout (KO) mice. Breaking strength of unwounded skin of KO mice is significantly lower (<50%) than that of wild-type (WT) mice. In the early stage of wound healing when TNX is hardly expressed in WT wounds (day 7), WT and KO skin are of similar strength. After 14 days, when TNX starts to be expressed at moderate levels in wounds of WT mice, the WT scars gain a further increase in breaking strength, whereas KO scars do not progress beyond the mechanical strength of uninjured KO skin. No obvious differences between KO and WT mice were noted in the rate of wound closure, or in expression of fibrillar collagens during wound healing. We conclude that TNX is unlikely to be involved in matrix deposition in the early phase of wound healing, but it is required in the later phase when remodeling and maturation of the matrix establishes and improves its biomechanical properties.

Keywords Tenascin-X, Collagen, Elastin, Wound Healing, Ehlers-Danlos Syndrome

INTRODUCTION

Tenascin-X (TNX) is a large, multi domain, extracellular matrix (ECM) glycoprotein composed of EGF like-repeats, fibronectin type III repeats and a C-terminal fibrinogen domain [1–5]. TNX abnormalities are associated with several pathological conditions [6–8]. Complete deficiency of TNX in humans leads to a recessive form of Ehlers-Danlos Syndrome (EDS) and TNX haploinsufficiency is a cause of hypermobility-type EDS. The skin of TNX-deficient patients is markedly lax with poor recoil properties and shows easy bruising. The collagen density appears reduced and the elastic fibers are abnormal in the dermis of these patients [6–10]. The first patient with a known TNX deficiency was described as having poor wound healing [6]. In general, coagulation time of TNX-deficient patients is within normal range and cannot explain the easy bruising [9].

Wound healing in TNX deficient patients has not been studied extensively, but on the basis of clinical observation of our 5 index patients and 3 additional patients, it was noted they lack the atrophic scars ("cigarette paper-like skin") that are common in classic-type EDS [7, 10]. On closer inspection some of our patients exhibited widened scars and sutures are kept in longer than normal. We therefore wanted to perform a more detailed study on the role of TNX in wound healing, under standardized conditions in an experimental model. We analyzed general morphology, expression of ECM proteins, and biomechanical tissue properties during wound healing of incisional and excisional skin wounds in TNX (KO) [11] and WT mice. The wounds of KO mice healed at approximately the same rate as WT mice, but the restoration of biomechanical properties suggests that TNX has a role in remodeling and maturation of the neomatrix.

MATERIALS AND METHODS

TNX-Deficient Patients

We investigated and photographed the scars of our 8 previously described TNX deficient index patients [7]. The study

Received 10 October 2006; accepted 7 December 2006.
Address correspondence to David Egging, P.O. Box 9101, 6500 HB, Nijmegen, the Netherlands. E-mail: d.egging@derma.umcn.nl

protocol was approved by the local medical ethics committee, and written informed consent was obtained from the patients.

Experimental Animals

TNX KO mice were obtained as described previously [12]. For all studies we used TNX KO mice obtained by backcrossing of TNX KO mice with six generations of C57/BL6 N mice. Wild type C57/BL6 mice were used as a control. All mice were between 3 to 6 months of age. The experimental design was approved by the animal use committee of the Radboud University Nijmegen.

Wounds

During infliction of the wounds, the animals were maintained anesthetized with isofluran doses of 2.5–3.0% in an N_2/O_2 gas mixture (50–65% O_2). Incisional wounds (2 cm) were made in the dorsal skin (cranial side) and closed by means of two surgical staples placed 1cm apart. Excisional wounds were made in the dorsal skin (caudal side) using an 8 mm biopsy punch and were left to heal by secondary intention.

Processing of Samples

At each time point, the mice were sacrificed in a sealed compartment by exposure to a mixture of carbogen gas and increasing concentrations of CO_2. Skin samples for frozen sections were embedded in Tissue-Tek O.C.T. compound (Sakura Finetek Europe B.V., NL) and snap frozen in liquid nitrogen. Skin samples for paraffin sections were fixed in 4% buffered formalin for 4 hr. Breaking strength of noninjured mouse skin and skin with incisional wounds was measured immediately after sacrificing the animals.

Histochemistry and Immunohistochemistry

Staining of elastic fibers was performed by modified Hart's stain on paraffin sections (7 μm) [13]. Paraffin sections also were stained with Sirius Red and H&E stain to assess collagen distribution and wound morphology. Frozen sections (7 μm) were stained with antibodies against TNX [11] and collagen types I, III, and V (SouthernBiotech, US) as previously described by us [11]. Specificity of the TNX antibody in mouse and human tissue has previously been demonstrated by us [7, 11, 14].Detection was performed with fluorescein isothiocyanate (FITC, green, Dakocytomation, DK) and Alexa Fluor 594 (AF594, red, Molecular Probes, NL)-labeled antibodies. Cell nuclei were made visible with a DAPI (blue) (Molecular Probes, NL) counterstaining.

Breaking Strength

The breaking strength was measured as previously described [11]. Briefly, a rectangular strip of dorsal skin (7mm $\times$ 3.5 cm) was prepared from the sacrificed mice using a custom made stance. The skin segment was clamped in a device that exerts a continuously increasing force in a longitudinal direction. The breaking strength is defined as the peak force necessary to induce tearing of a tissue segment and expressed in grams (1000 g equals 9.3 N), as described previously [11, 15]. The breaking strength of skin strips containing incisional wounds and uninjured skin was measured. Force was applied perpendicular to the incisional wound, and care was taken that the incisional wound ran along the entire width of the skin strip.

RESULTS

Wound Healing in TNX-Deficient Patients

Index patients (8 in total) were examined for skin abnormalities including abnormal scars. All patients had hyperextensible skin, easy bruising, and all but 1 had velvety skin. None of the patients had atrophic scars, as is the case in classic-type EDS. On closer inspection however, some of our patients exhibited widened scars (Figure 1) and some reported that sutures had to be kept in longer than normal. In general, however, patients did not report delayed wound healing. Due to the small number of patients and limited availability of tissue, it is difficult to make general assumptions regarding TNX deficiency and wound healing. We therefore used the TNX KO mouse as a model to study the effect of TNX deficiency on wound healing.

Morphological Analysis in TNX KO Mice

Excisional wounds in both TNX KO mice and WT mice healed macroscopically at approximately the same rate (not shown) and no visual differences in scar tissue were noted. Mouse wounds tend to contract extensively and heal very rapidly, which makes it nearly impossible to trace the wound area with absolute certainty beyond day 14 in C57/B6N mice. In histological tissue sections the wound area, even from an 8 mm excisional would, is very small due to contraction. Careful examination of skin sections allows identification of the wound

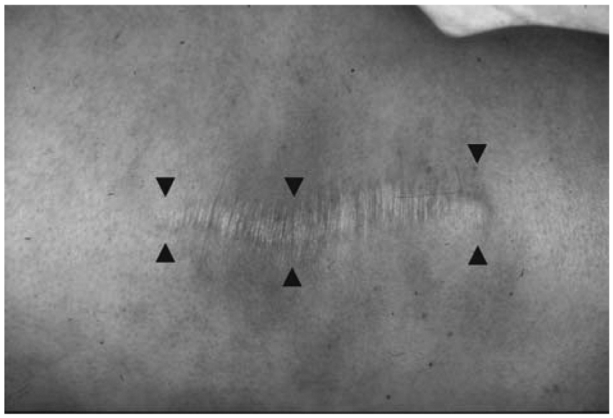

FIG. 1. Widened scar in TNX deficient patient. An example of a widened scar with irregular boundaries, indicated by arrows, on the arm of a TNX-deficient patient. This is found in some of our TNX-deficient patients, but not in all patients. Atrophic scars (cigarette paper-like skin) were never observed in these patients.

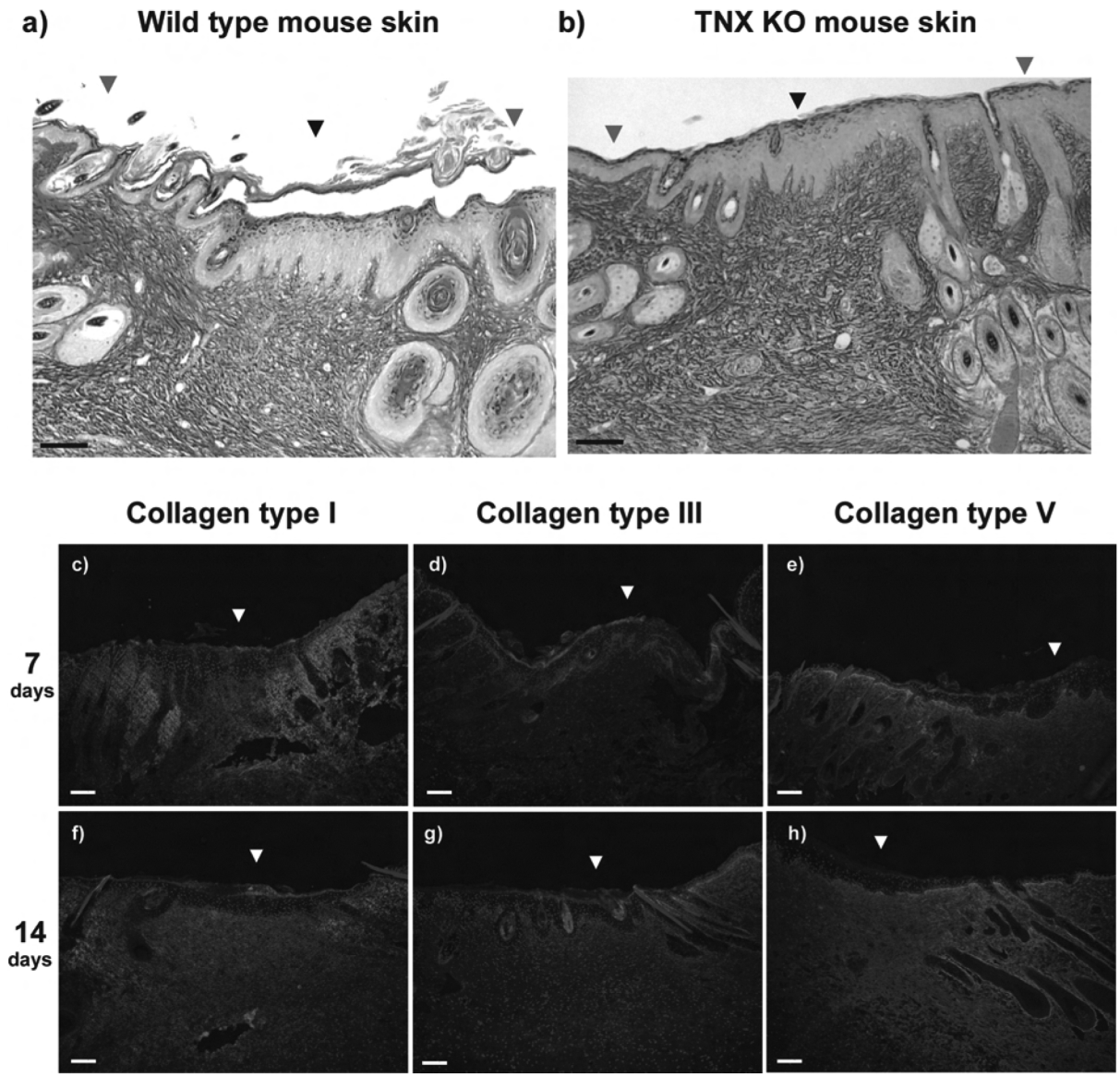

FIG. 2. Collagen distribution in the wound area. In (a) and (b) collagen is stained red/pink by Sirius red staining. The wound area is indicated by black arrows. The collagen fibrils in the dermis under the wound area are packed less tight compared with uninjured skin (indicated by grey arrows). No obvious differences in collagen density in the wound area between WT (a) and TNX KO (b) mice were noted as is shown for a 14-day-old wound area. Immunofluorescent staining (red) of collagen type I (c, f), III (d, g) and V (e, h) are abundantly expressed in a 7-day (c–e) and 14-day (f–h) wound area (as shown for WT skin). The area under white arrows indicates the wounded skin. Hair follicles are absent in the wound area but present in uninjured skin. Positive staining of the outer layer of the epidermis (stratum corneum) is nonspecific. [Bars in a, b are 25 μm, bars in c-h are 100 μm].

area through absence of hair follicles and carnosus muscle. The distribution of collagen does not appear to differ between WT and TNX KO mice both in uninjured skin and in the wound area on histological examination.

Collagen types I, III, and V were found to be expressed throughout the entire dermis. The collagen density in the wound area is less than in the uninjured skin (Figure 2a and 2b shown in 14-day-old wound area) in both mouse strains. Collagen I, III and V are abundantly expressed in a 7- and 14-day-old wound area and uninjured skin in WT and TNX KO mice (Figure 2c–2h, data shown for WT skin). In WT mice, TNX expression is very low to nonexistent in the wound area at day 7 compared with the adjacent unwounded skin (Figure 3a). At day 14, low to moderate TNX expression is visible in the wound area, but it is still much weaker than in the uninjured skin of WT mice (Figure 3b). The specificity of the anti-TNX antibody is demonstrated in TNX KO skin in Figure 3c. TNX is putatively involved in elastic fiber assembly or stability. Using modified Hart's staining, no elastic fibers could be detected in a 14-day-old wound area of WT or KO mice (Figure 3d and 3e). This is in accordance with

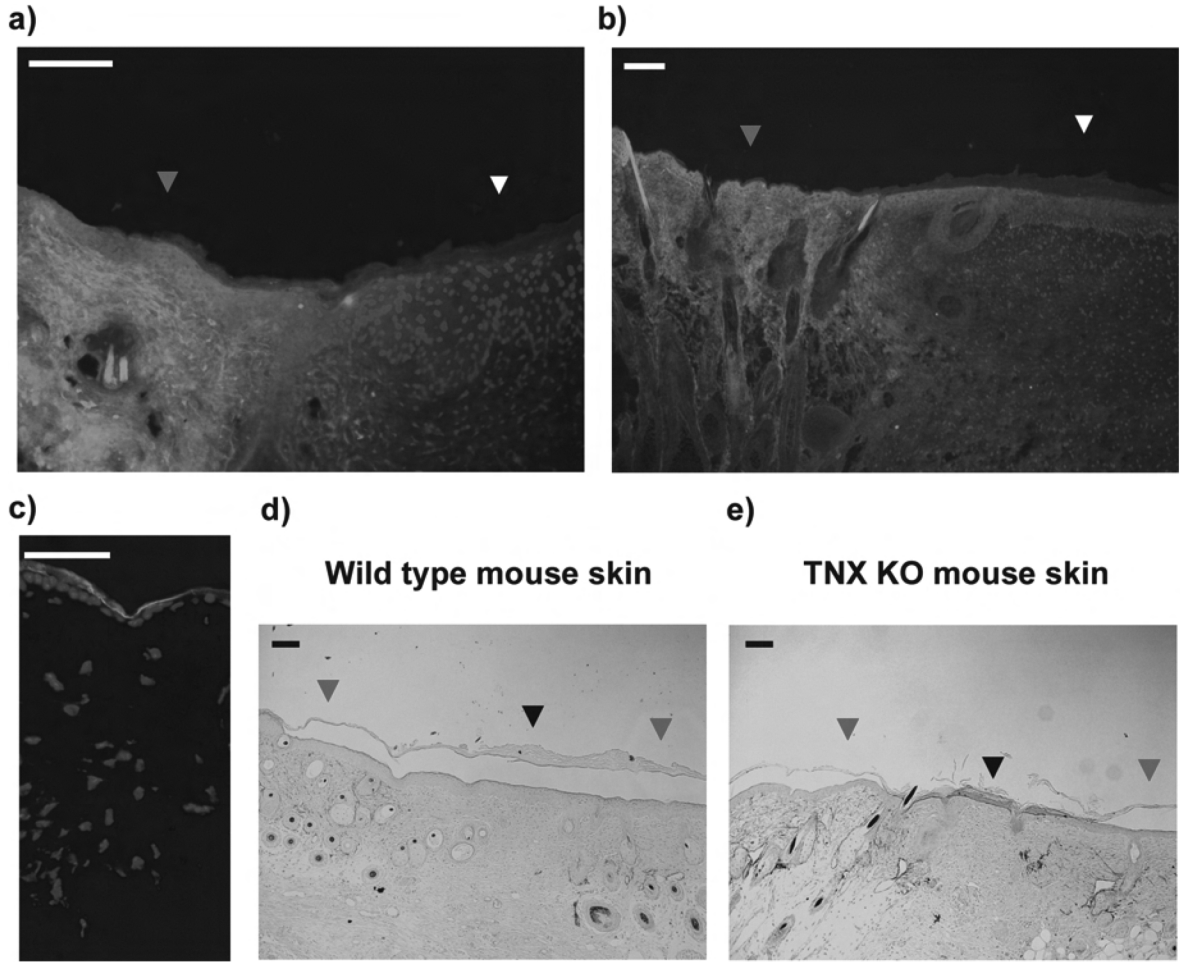

FIG. 3. Low expression of TNX and absence of elastic fibers in wound tissue. White arrows indicate the wound area in sections (a) and (b). Red arrows indicate uninjured skin. TNX expression is very low/not present in a 7-day-old wound area of WT skin (a). TNX expression (green) can be observed in a 14-day-old wound area of WT skin but it is far less strong than in the adjacent normal skin (b). The specificity of the anti-TNX antibody is demonstrated in TNX KO skin, which is devoid of signal (c). Note that staining of the stratum corneum is nonspecific (a–c). No elastic fibers can be detected in a 14-day-old wound area as shown by modified Hart's staining for WT skin (d) and TNX KO skin. Black arrows indicate the wound area, white. [Bars in (a), (b), (d), and (e) are 100 μm and 50 μm in c)].

previous observations that regeneration of elastic fibers happens very slowly [16, 17].

Biomechanical Analysis in TNX KO Mice

In a previous study we have shown that the biomechanical strength of TNX KO skin is significantly diminished compared with WT mice [11]. Here we extended this study to analyze the breaking strength of skin strips that contained healing incisional wounds of both mouse strains at 7, 19, 33, and 62 days after wounding. An incision of 2 cm was made and sutured with two staples. Healing in both groups was uncomplicated, and no macroscopical difference in healing was observed between KO and WT mice. Figure 4 shows that after 1 week there is no difference in strength between KO and WT wounds, and neither of them can withstand forces over 1 Newton. As wound healing progresses WT wound strength starts to differ from the strength of KO wounds.

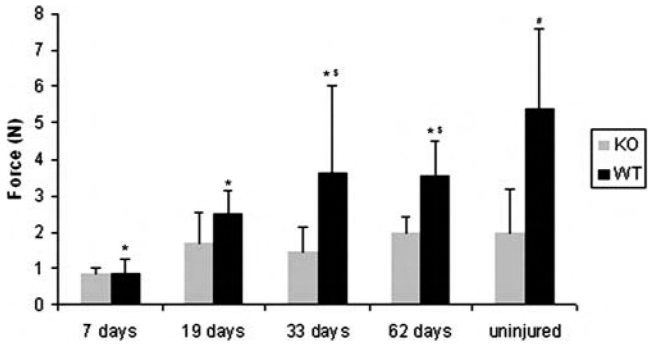

FIG. 4. Breaking strength of healing wounds uninjured TNX KO skin is significantly weaker than WT mouse skin ($^{\#}p < 0.0001$). From day 33 onward the healing WT skin is significantly stronger than the KO skin ($^{\$}p < 0.05$). Healing WT skin does not regain the biomechanical properties of normal skin in the time frame studied here ($*p < 0.02$). At least 6 mice were used for all time points. Analysis of variance was performed, followed by Duncan's multiple range posthoc test.

Remarkably, in the period of wound healing studied here (day 7 to day 62), no significant difference was found between wounded KO skin and uninjured KO skin at any time (ANOVA and Duncan's multiple range posthoc test). Although the mechanical strength of healing WT skin increased with time, it was found to be significantly reduced at all times, compared with uninjured WT skin (ANOVA and Duncan's multiple range posthoc test). It appears that from day 7 onward, the KO skin wounds have attained their maximum strength, which is similar to that of uninjured KO skin. In contrast, the WT skin wounds, although stronger than the KO wounds, have not regained their full biomechanical properties.

DISCUSSION

The fact that TNX deficiency in humans is a rare condition, and/or obvious ethical reasons, has so far precluded a detailed investigation of a potential role of TNX in human wound healing. The expression and presumed function of TNX strongly suggest involvement in matrix assembly and/or maintenance, and for this reason TNX could play a role in wound healing processes. Although the number of patients available is small and TNX deficient patients do not exhibit delayed healing or atrophic scars, clinical observations provided a rationale to study TNX function in a mouse model for wound healing.

Healing TNX KO skin returns to the strength of uninjured skin within 19 days, at which point healing WT skin becomes stronger than KO skin. Collagens type I, III, and V are already abundantly expressed as of day 7, but TNX expression is virtually absent in WT wounds at that stage. This expression pattern is consistent with the data on the well-studied tenascin family member tenascin-C (TNC). TNC expression is distinct and often reciprocal to TNX [18, 19]. TNC in normal skin is only associated with basement membranes and hair follicle dermal sheats, whereas TNX is abundantly expressed in dermis. In contrast, TNC is strongly expressed in healing skin wounds [20]. As shown in our study TNX expression is low in a wound area. The amount of TNX in the wound area increases over time followed by an increase in biomechanical strength of the healing wound area.

We have shown that TNX is not involved in the initial deposition of dermal fibrillar collagens type I, III, and V during fetal development [11]. This observation is similar to our present findings that collagens type I, III, and V are expressed abundantly in the initial phase of wound healing wound before TNX expression starts. In TNX deficient patients the collagen density appears reduced [6, 7, 21, 22]. However, we found no obvious differences in collagen deposition in the skin of TNX KO and WT mice using Sirius red staining, as has been previously reported by Mao et al. [12]. Our data are similar to those of Minnamitani et al. who found no differences in the density of collagen fibrils at the ultrastructural level [23]. Furthermore, in a previous study [11] we found no reduction of the amount of collagen in TNX KO skin as described by Mao et al. [12]. We must note that Mao et al. used mice with a different genetic background than in our studies, as did Minnamitani et al [11, 12, 23]. There appears to be an increase in size variation in the collagen fibrils in TNX KO mice [12, 23]. Although the reduction of collagen density in TNX KO mice as found in TNX-deficient patients [6, 7, 21, 22] remains debatable, previous studies have indicated a large reduction in skin strength of TNX KO mice [11, 12], which appears to increase with age [11]. Fragile skin is a hallmark of EDS and is observed in TNX-deficient patients [6, 7, 10]. Taking all data into consideration it is attractive to hypothesize that TNX itself is responsible for increasing the biomechanical strength of skin after deposition of a collagen matrix, through stabilization and maturation of the extracellular matrix [18, 22–30].

CONCLUSION

Although absence of TNX does not appear to hinder wound healing per se, we would caution that the fragility of the skin of TNX-deficient patients could cause complications in scar formation or surgery, as is often the case in other forms of EDS.

ACKNOWLEDGMENTS

Prof. Dr Jim Bristow is acknowledged for providing the TNX KO mice. Our work was supported by a grant from the Dutch Program Tissue Engineering (DPTE).

REFERENCES

1. Bristow, J., Tee, M.K., Gitelman, S.E., Mellon, S.H., and Miller, W.L. (1993). Tenascin-X: a novel extracellular matrix protein encoded by the human XB gene overlapping P450c21B. *J. Cell Biol.*, 122, 265–278.
2. Lethias, C., Descollonges, Y., Boutillon, M.M., and Garrone, R. (1996). Flexilin: a new extracellular matrix glycoprotein localized on collagen fibrils. *Matrix Biol.*, 15, 11–19.
3. Elefteriou, F., Exposito, J.Y., Garrone, R., and Lethias, C. (1997). Characterization of the bovine tenascin-X. *J. Biol. Chem.*, 272, 22866–22874.
4. Ikuta, T., Sogawa, N., Ariga, H., Ikemura, T., and Matsumoto, K. (1998). Structural analysis of mouse tenascin-X: evolutionary aspects of reduplication of FNIII repeats in the tenascin gene family. *Gene*, 217, 1–13.
5. Tucker, R.P., Drabikowski, K., Hess, J.F., Ferralli, J., Chiquet-Ehrismann, R., and Adams, J.C. (2006). Phylogenetic analysis of the tenascin gene family: evidence of origin early in the chordate lineage. *BMC. Evol. Biol.*, 6, 60.
6. Burch, G.H., Gong, Y., Liu, W., Dettman, R.W., Curry, C.J., Smith, L., Miller, W.L., and Bristow, J. (1997). Tenascin-X deficiency is associated with Ehlers-Danlos syndrome. *Nat. Genet.*, 17, 104–108.
7. Schalkwijk, J., Zweers, M.C., Steijlen, P.M., Dean, W.B., Taylor, G., Van Vlijmen, I.M., van Haren, B., Miller, W.L., and Bristow, J. (2001). A recessive form of the Ehlers-Danlos syndrome caused by tenascin-X deficiency. *N. Engl. J. Med.*, 345, 1167–1175.
8. Zweers, M.C., Bristow, J., Steijlen, P.M., Dean, W.B., Hamel, B.C., Otero, M., Kucharekova, M., Boezeman, J.B., and Schalkwijk, J. (2003). Haploinsufficiency of TNXB is associated with hypermobility type of Ehlers-Danlos syndrome. *Am. J. Hum. Genet.*, 73, 214–217.
9. Peeters, A.C.T.M., Kucharekova, M., Timmermans, J., Van Den Berkmortel, F.W.P.J., Boers, G.H., Novakova, I.R.O., Egging, D., den Heijer, M., and Schalkwijk, J. (2004). A clinical and cardiovascular survey of Ehlers-Danlos

syndrome patients with complete deficiency of tenascin-X. *Neth. J. Med.*, 62, 23–25.
10. Lindor, N.M., and Bristow, J. (2005). Tenascin-X deficiency in autosomal recessive Ehlers-Danlos syndrome. *Am. J. Med. Genet. A*, 135, 75–80.
11. Egging, D.F., van Vlijmen, I., Starcher, B., Gijsen, Y., Zweers, M.C., Blankevoort, L., Bristow, J., and Schalkwijk, J. (2006). Dermal connective tissue development in mice: an essential role for tenascin-X. *Cell Tissue Res.*, 323, 465–474.
12. Mao, J.R., Taylor, G., Dean, W.B., Wagner, D.R., Afzal, V., Lotz, J.C., Rubin, E.M., and Bristow, J. (2002). Tenascin-X deficiency mimics Ehlers-Danlos syndrome in mice through alteration of collagen deposition. *Nat. Genet.*, 30, 421–425.
13. Starcher, B., Aycock, R.L., and Hill, C.H. (2005). Multiple roles for elastic fibers in the skin. *J. Histochem. Cytochem.*, 53, 431–443.
14. Zweers, M.C., Schalkwijk, J., Van Kuppevelt, T.H., Vlijmen-Willems, I.M., Bergers, M., Lethias, C., and Lamme, E.N. (2005). Transplantation of reconstructed human skin on nude mice: a model system to study expression of human tenascin-X and elastic fiber components. *Cell Tissue Res.*, 319, 279–287.
15. Waard de, J.W.D., Wobbes, T., Deman, B.M., Linden van der, C.J., and Hendriks, T. (1995). Postoperative levamisole may compromise early healing of experimental intestinal anastomoses. *Br. J. Cancer*, 72, 456–460.
16. Schwartz, D. (1977). The proliferation of elastic fibres after skin incisions in albino mice and rats: a light and electron microscopic study. *J. Anat.*, 124, 401–411.
17. Zheng, Q., Choi, J., Rouleau, L., Leask, R.L., Richardson, J.A., Davis, E.C., and Yanagisawa, H. (2006). Normal wound healing in mice deficient for fibulin-5, an elastin binding protein essential for dermal elastic fiber assembly. *J. Invest. Dermatol.*, 126, 2707–2714.
18. Matsumoto, K., Saga, Y., Ikemura, T., Sakakura, T., and Chiquet, E.R. (1994). The distribution of tenascin-X is distinct and often reciprocal to that of tenascin-C. *J. Cell Biol.*, 125, 483–493.
19. Geffrotin, C., Garrido, J.J., Tremet, L., and Vaiman, M. (1995). Distinct tissue distribution in pigs of tenascin-X and tenascin-C transcripts. *Eur. J. Biochem.*, 231, 83–92.
20. Mackie, E.J., Halfter, W., and Liverani, D. (1988). Induction of tenascin in healing wounds. *J. Cell Biol.*, 107, 2757–2767.
21. Zweers, M.C., Vlijmen-Willems, I.M., Van Kuppevelt, T.H., Mecham, R.P., Steijlen, P.M., Bristow, J., and Schalkwijk, J. (2004). Deficiency of tenascin-x causes abnormalities in dermal elastic fiber morphology. *J. Invest Dermatol.*, 122, 885–891.
22. Bristow, J., Carey, W., Egging, D., and Schalkwijk, J. (2005). Tenascin-X, collagen, elastin, and the Ehlers-Danlos syndrome. *Am. J. Med. Genet. C. Semin. Med. Genet.*, 139, 24–30.
23. Minamitani, T., Ikuta, T., Saito, Y., Takebe, G., Sato, M., Sawa, H., Nishimura, T., Nakamura, F., Takahashi, K., Ariga, H., and Matsumoto, K. (2004). Modulation of collagen fibrillogenesis by tenascin-X and type VI collagen. *Exp. Cell Res.*, 298, 305–315.
24. Elefteriou, F., Exposito, J.Y., Garrone, R., and Lethias, C. (1999). Cell adhesion to tenascin-X mapping of cell adhesion sites and identification of integrin receptors. *Eur. J. Biochem.*, 263, 840–848.
25. Elefteriou, F., Exposito, J., Garrone, R., and Lethias, C. (2001). Binding of tenascin-X to decorin. *FEBS Lett.*, 495, 44–47.
26. Hagios, C., Koch, M., Spring, J., Chiquet, M., and Chiquet-Ehrismann, R. (1996). Tenascin-Y: a protein of novel domain structure is secreted by differentiated fibroblasts of muscle connective tissue. *J. Cell Biol.*, 134, 1499–1512.
27. Hagios, C., Brown, L.M., and Chiquet, E.R. (1999). Tenascin-Y, a component of distinctive connective tissues, supports muscle cell growth. *Exp. Cell Res.*, 253, 607–617.
28. Lethias, C., Elefteriou, F., Parsiegla, G., Exposito, J.Y., and Garrone, R. (2001). Identification and characterization of a conformational heparin-binding site involving two fibronectin type iii modules of bovine tenascin-x. *J. Biol. Chem.*, 276, 16432–16438.
29. Veit, G., Hansen, U., Keene, D.R., Bruckner, P., Chiquet-Ehrismann, R., Chiquet, M., and Koch, M. (2006). Collagen XII Interacts with Avian Tenascin-X through Its NC3 Domain. *J. Biol. Chem.*, 281, 27461–27470.
30. Egging, D., Van Den, B.F., Taylor, G., Bristow, J., and Schalkwijk, J. (2006). Interactions of human tenascin-X domains with dermal extracellular matrix molecules. *Arch. Dermatol. Res.*

CHAPTER 4

ANALYSIS OF OBSTETRIC COMPLICATIONS AND UTERINE CONNECTIVE TISSUE IN TENASCIN-X DEFICIENT HUMANS AND MICE: A CLINICAL AND MORPHOLOGICAL STUDY

This chapter has been submitted:
Egging DF, van Vlijmen-Willems I, Choi J, Peeters ACTM, van Rens D, Veit G, Koch M, Davis EC, Schalkwijk J. Analysis of obstetric complications and uterine connective tissue in tenascin-X deficient humans and mice: a clinical and morphological study. CTR, submitted.

ANALYSIS OF OBSTETRIC COMPLICATIONS AND UTERINE CONNECTIVE TISSUE IN TENASCIN-X DEFICIENT HUMANS AND MICE: A CLINICAL AND MORPHOLOGICAL STUDY

[a]David F. Egging, [a]Ivonne van Vlijmen-Willems, [b]Jiwon Choi, [c]Anita C.T.M. Peeters, [a]Desiree van Rens, [d]Guido Veit, [d,e]Manuel Koch, [b]Elaine C. Davis, [*a]Joost Schalkwijk

[a]Department of Dermatology, Nijmegen Centre for Molecular Life Sciences, Radboud University Nijmegen Medical Centre, Nijmegen, the Netherlands
[b]Department of Anatomy & Cell Biology, McGill University, Montreal, Quebec, Canada
[c]Department of Endocrinology, Radboud University Nijmegen Medical Centre, Nijmegen, the Netherlands
[d]Center for Biochemistry, Medical faculty, University of Cologne, Cologne, Germany
[e]Department of Dermatology and Center for Molecular Medicine Cologne , Medical faculty, University of Cologne, Cologne, Germany
*corresponding author. E-mail address: j.schalkwijk@derma.umcn.nl. P.O. Box 9101, 6500 HB, Nijmegen, the Netherlands

Keywords: Ehlers-Danlos syndrome, tenascin-X, collagen, elastin, pregnancy

ABSTRACT

Tenascin-X (TNX) is a large, multi-domain, extracellular matrix (ECM) glycoprotein. Complete deficiency of TNX in humans leads to a recessive form of Ehlers-Danlos syndrome (EDS) and TNX haploinsufficiency is a cause of hypermobility type EDS. EDS patients appear to have a higher risk for several complications during pregnancy such as pelvic instability, premature rupture of membranes and postpartum hemorrhage. Here we present a study on genitourinary and obstetric complications in TNX-deficient women of reproductive age. We found several complications that are in line with previous findings as observed in other EDS types. In TNX knockout (KO) mice, we found mild pregnancy-related abnormalities. Morphological and immunohistological analysis of uterine tissues did not reveal obvious quantitative or spatial differences between TNX KO and wildtype (WT) mice with respect to collagen types I, III, V and XII or elastic fibers. We conclude that TNX deficiency leads to impaired biomechanical properties of the connective tissue, such as laxity of the vaginal wall, uterus or ligaments, leading to an increased risk for obstetric complications.

INTRODUCTION

Tenascin-X (TNX) is a large, multi-domain, extracellular matrix (ECM) glycoprotein composed of EGF like-repeats, fibronectin type III repeats and a C-terminal fibrinogen domain [1-5]. Complete deficiency of TNX in humans leads to a rare recessive form of Ehlers-Danlos Syndrome (EDS) and TNX haploinsufficiency is a cause of hypermobility type EDS. Patients of both EDS types exhibit mild to severe joint hypermobility. The skin of TNX-deficient patients is markedly lax with poor recoil properties and shows easy bruising. The collagen density appears reduced in the dermis of these patients and the elastic fibers are abnormal [6-10]. Most literature concerning pregnancy in EDS uses the old classification of nine subgroups. In our study, we use the revised classification of six subtypes of EDS [11]. Tissue fragility is a hallmark of EDS and is present in all different subtypes. EDS patients appear to have a higher risk of several complications during pregnancy such as pelvic instability, premature rupture of membranes and postpartum hemorrhage. Pregnancy in classical and hypermobility type EDS has a relative favorable maternal and neonatal outcome. Pregnancy in vascular type EDS patients is associated with severe complications including maternal mortality [12-19]. The effect of TNX deficiency on pregnancy has not been studied so far and only one case report of pregnancy in a TNX-deficient woman has been reported in the literature [10]. Here we present a study of all known pregnancies and genito-

urinary (GU) abnormalities in TNX-deficient woman of reproductive age identified [7] in our clinic and in literature [7;10]. Furthermore, we extended our studies to a TNX knockout (KO) mouse model in which we studied uterine development during pregnancy. We previously established that TNX is essential for development of tissue strength in skin and is able to bind to elastin, a major component of elastic fibers, and collagens type I, III, V and XII [20-22]. We investigated expression of these molecules at the protein level.

MATERIALS AND METHODS

TNX-deficient patients

We investigated pregnancies and GU abnormalities in all currently identified female tenascin-X deficient patients of reproductive age identified in our clinic and in literature. The study protocol was approved by the local medical ethics committee, and written informed consent was obtained from the patients.

Experimental animals

TNX knockout mice were obtained as described previously [23]. For all studies, we used TNX KO mice that were crossed back with six generations of C57/BL6N mice. Wild type C57/BL6 (WT) mice were used as a control. All mice used to investigate pregnancy abnormalities and morphological changes in uterus tissue were between 2 to 6 months of age, reflecting a normal age distribution of a breeding mice population. Skin samples were taken from 2 month and 9 month old mice, aortic tissue was obtained from 9 month old mice. The experimental design was approved by the animal use committee of the Radboud University Nijmegen.

Breeding

Breeding pairs were kept in a five to one female:male ratio. Females were inspected daily for vaginal plugs and those with plugs were isolated and inspected each day for abnormalities and progression of pregnancy. Litter size was determined after birth. Neonatal survival is defined as the difference in litter size after partus and 2 weeks postpartum.

Processing of samples for (immuno)histochemistry

Mice were sacrificed in a sealed compartment by exposure to a mixture of carbogen gas and increasing concentrations of CO_2. Skin samples for frozen sections were embedded in Tissue-Tek O.C.T. compound (Sakura Finetek Europe B.V., NL) and snap frozen in liquid nitrogen. Skin samples for paraffin sections were fixed in 4% buffered formalin for four hours.

Affinity purified TNX antibody production

TNX FNIII repeats 27-32 were amplified by PCR (forward primer 5'-GGAATTCGAGCT ACCTCCCCAC-3', reverse primer 5'-CAGGTCGACTCAGGTGAAAGAGGTGG A-3') using a previously described 2.7 kb human TNX cDNA as a template [24]. The PCR product was ligated into the pCR2.1TOPO vector (Invitrogen, Breda, NL) according to the manufacturer's instructions for easy digestion with restriction enzymes. The pCR2.1 TOPO vector with insert was digested with EcoRI and SalI. The region coding for FNIII27-32 was inserted into the EcoRI/SalI site of the pET28(a)+ plasmid (Brunschwig Chemie B.V., Amsterdam, NL). The sequence of the TNX domains was verified by dideoxy sequencing with a 3730 DNA analyser (Applied Biosystems, Nieuwekerk a/d IJssel, NL). TNX FNIII27-32 protein was expressed and purified according to the manufacturer's instructions (Brunschwig Chemie B.V., Amsterdam, NL). Purified TNX FNIII27-32 protein was used for immunization of a rabbit. Aliquots of 500 µg TNX FNIII27-32 in 500 µL of PBS were mixed with an equal volume of Freund's complete adjuvant for the first injection and Freund's incomplete adjuvant for boosters. Three injections were administered subcutaneously at 3-week intervals. Polyclonal antibodies against TNX FNIII27-32 were purified by affinity chromatography on a column with antigen coupled to CNBr-activated sepharose 4B (GE Healthcare Life Sciences, Diegem, BE).

Histochemistry and immunohisto-chemistry

Staining of elastic fibers was performed by modified Hart's stain on paraffin sections (7 μm) [25]. Paraffin sections were also stained with H&E stain to assess uterus morphology. Frozen sections (7 μm) were stained with antibodies against collagen types I, III and V (SouthernBiotech, US) and elastin (Elastin Products Company Inc., US) as previously described by us [20]. Collagen XII was stained as previously described [22]. TNX was stained with affinity-purified antibodies directed against FNIII27-32 of TNX. Detection was performed with fluorescein isothiocyanate (FITC, green, Dakocytomation, DK) and Alexa Fluor 594 (AF594, red, Molecular Probes, NL) labeled antibodies. Cell nuclei were made visible with a DAPI (blue) (Molecular Probes, NL) counterstaining.

Table 1: Pregnancy in TNX-deficient woman.

#	Sex/Age (yr)	G#P#	GU	*Specification
1	F/50	G1P1	-	
2	F/60 Sister of #1	G2P2	+ VUE after uterine prolapse (at age 49) + Vaginal prolapse 2 weeks after VUE	
3	F/46*	G0P0	-	*Was born premature (week 35) with shoulder luxation, rectal prolapse at age 1
4	F/51 Sister of #3	G3P3	+ One incident of hemorrhage post partum (>1000 ml blood loss)	
5	F/38	G0P0*	-	*CAH
6	F/51*	G3P2	+ IUD (24 weeks) with relatively large blood loss + Undefined prolapse (at age 36)	*Deceased at age 51, severe co-morbidity including cardiomyopathy, arrhythmia, arteriosclerosis and amputation of left leg [7]
7	F/57*	G4P4	+ Precipitious second stage at term for all births + Uterine prolapse (at age 20), also recurrent rectal prolapses	*Lindor et al. [10]

G#P#: Gravida # Para #, GU: Genito-Urinary, VUE: Vaginal Uterine Extirpation, IUD: Intra Uterine Death, CAH: Congenital Adrenal Hyperplasia.

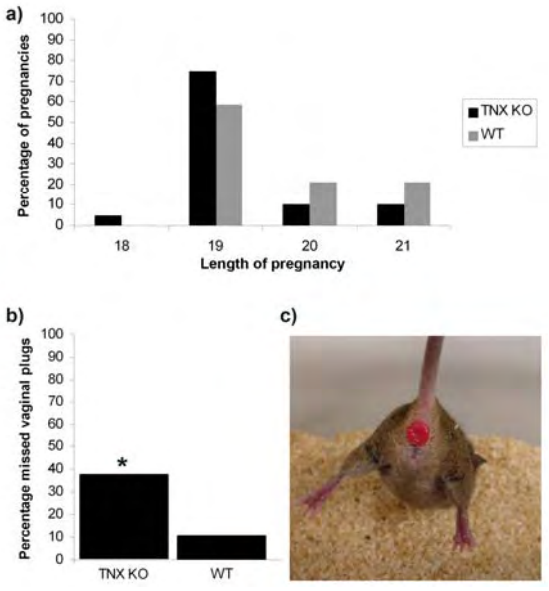

Figure 1: TNX KO mice abnormalities.

(a) Although the difference in the length of pregnancy between TNX KO and WT mice is found non-significant by Fisher exact test, a decreasing trend in the length of pregnancy of TNX KO mouse compared to WT mice can be observed. Vaginal plugs, which are present after mating, are much more difficult to asses in TNX KO mice than in WT mice. This results in a significant increase of pregnancies in which the insemination date was unknown as shown in panel (b). In this study no uterine prolapses have been observed, however, some TNX KO mice suffer from a rectal prolapse as shown in panel (c). Rectal prolapses are also observed in TNX-deficient patients, although the incidence in TNX KO mouse appears low. (* $p<0.025$, chi square test).

Electron microscopy

For electron microscopy, WT and TNX KO samples from uterine wall at 3 weeks post-partum, skin from 2 month-old and 9 month-old mice, and aortas from 9 month-old mice were fixed in 3% glutaraldehyde in 0.1 M sodium cacodylate overnight, and washed in 0.1 M sodium cacodylate buffer. The tissues were then sequentially treated with osmium tetroxide, tannic acid and uranyl acetate, then dehydrated and embedded in epon as previously described [26]. Thin sections (60 nm) were counterstained with 7% uranyl acetate in absolute methanol and lead citrate, and examined using a Tecnai 12 transmission electron microscope at 120kV.

Statistics

For statistical analyses, the Fisher's exact or chi-square tests were used where appropriate for proportional data. Student's t-test was used to compare mean litter size after partus and neonatal survival (difference in litter size after partus and 2 weeks postpartum). A *p*-value of <0.05 was considered statistically significant.

RESULTS

Pregnancy in TNX-deficient patients

We investigated pregnancy and GU abnormalities in TNX-deficient woman of reproductive age. General reproduction characteristics and GU abnormalities of female TNX-deficient patients are presented in table 1. Maternal and neonatal outcome was generally normal; one out of thirteen pregnancies resulted in an intrauterine death of the fetus. Tissue laxity of TNX-deficient patients is demonstrated by the occurrence of vaginal, uterine and rectal prolapses, even at a relative young age. One case of postpartum hemorrhage was observed in twelve childbirths. None of our patients had urinary incontinence symptoms. TNX-deficient EDS is an autosomal recessive disorder, therefore all offspring of a TNX-deficient patient and an unaffected individual are obligatory heterozygotes. We have previously found that approximately 60% of adult females that are haploinsufficient for TNX suffer from hypermobility type EDS or benign joint hypermobility syndrome [8]. We found no obvious abnormalities (e.g. floppy infant syndrome, premature birth) in the neonates (obligatory heterozygotes) of our TNX-deficient population however, some TNX-deficient patients themselves were born prematurely (table 1, [10]).

Pregnancy in TNX KO mice

We investigated GU and pregnancy-related abnormalities in TNX KO and WT mice ranging between 2-6 months of age. Litter size (TNX KO: 7 ± 2 pups, WT: 7 ± 3 pups) and neonatal survival (TNX KO: $74\% \pm 36\%$, WT: $54\% \pm 40\%$) did not differ significantly (student's t-test). GU abnormalities of the TNX KO and WT mice are presented in table 2. Overall, we noted relatively few pregnancy-related abnormalities. Obstruction of the uterine or vaginal canals during partus resulting in a failure to deliver pups was noted more often in WT mice compared to TNX KO mice, but the difference was not significant (Chi-square test). A decrease in the length of term for the TNX KO mice can be observed in figure 1a, although this trend is not significant (Fisher's exact test).

Table 2: Pregnancy in TNX-deficient mice.

	TNX KO mice number of mice	**WT mice** number of mice
Maternal death during pregnancy	1	0
Miscarriage	2	0
Obstruction during partus	1	3
Excessive bleeding of vagina (as seen at vaginal plug check)	2	0
Cannibalism after partus	1	1
Total number of evaluated pregnancies	36	31

A striking difference between TNX KO and WT was found for the location of the vaginal plug that is present after mating. Generally, the vaginal plug in TNX KO mice was located much deeper in the vaginal canal than in WT mice. This made identification of vaginal plugs in TNX KO mice markedly more difficult, resulting in a significant increase in pregnancies with unknown length of pregnancy (figure 1b, Chi-square test). No uterine or rectal prolapses were observed in this particular study (67 pregnancies of KO and WT mice). We did, however, occasionally observe rectal prolapse in the breeding colony of our TNX KO mice population (shown in figure 1c).

Structure of the mouse uterus

In figure 2, H&E stained sections of the uterus of WT (figure 2a) and TNX KO mice (figure 2b) are shown. The mouse uterus consists of three layers: an outer layer, that includes the single-cell layered perimetrium and a thin layer of connective tissue; a muscular layer, the myometrium, composed of two oppositely orientated layers of muscle; and an endometrium, consisting of loose connective tissue covered by epithelium, which undergoes remodeling during the menstrual cycle and pregnancy. No differences in structure of the uterus were noticeable between TNX KO and WT mice (figure 2, as shown for uteri 1 day postpartum).

Immunostaining of TNX in the mouse uterus

TNX is present throughout the uterus of virgin mice and in the uterus during and after pregnancy (figure 3a-c). Immunostaining of TNX appears weak and discontinuous in the perimetrium (figure 3a-c and f). TNX is present in the endometrium, although the epithelium, which lines the endometrium, is negative for TNX (figure 3d). TNX is abundantly present in the layers of connective tissue ensheathing muscle bundles of the myometrium (figure 3f). Overall, no change in the localization of TNX immunostaining was observed during and after pregnancy. Specificity of our TNX antibody is demonstrated by the complete absence of positive staining in the TNX KO mouse tissues (figure 3e and g).

Immunostaining of collagen in the mouse uterus

We previously demonstrated binding and colocalization of TNX in skin with collagen type I, II and V [20;21]. In the uterus, TNX also colocalizes with major fibrillar collagens type I, III and V as is shown for uteri 3 weeks postpartum (figure 4). The collagens are present in the perimetrium, endometrium and the layers of connective tissue ensheathing muscle bundles of the myometrium. Similar results were obtained for uteri from virgin, 13 days pregnant and 1-day postpartum mice. No difference in collagen type I, III and V immunostaining was found between WT and TNX KO mice (data not shown), which is in line with our observations in skin [20]. Collagen type XII, an interaction partner of TNX [22], is present throughout the uterus (figure 5). The immunostaining appears the strongest in the transverse muscle bundles of the myometrium around blood vessels (BV) and around the lumen although the signal intensity is not always completely continuous around the lumen and blood vessels. TNX and collagen type XII are both present throughout the entire uterus, however, the strongest collagen type XII immunostaining is observed in the transverse muscle bundles of the

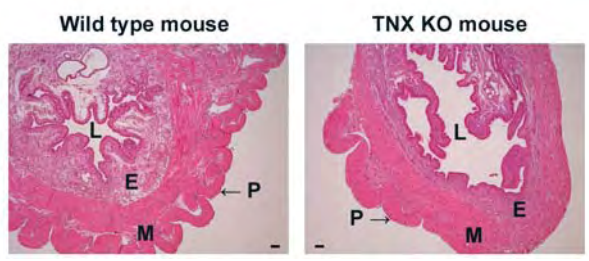

Figure 2: Structure of the TNX KO and WT uterus. H&E stained sections of the uterus of WT mice (a) and of TNX KO mice (b) are shown. No differences in structure of the uterus were noticeable between TNX KO and WT mice. The uterus of mice consists of a thin outer layer, the perimetrium (denoted as P). A muscle layer, the myometrium (denoted as M), consist of two oppositely orientated layers of muscle, although this is difficult to distinguish in H&E stained slides. The endometrium (denoted as E) consist of loose connective tissue. The endometrium is separated from the lumen (denoted as L) by an epithelium. Bars are 0.01 mm.

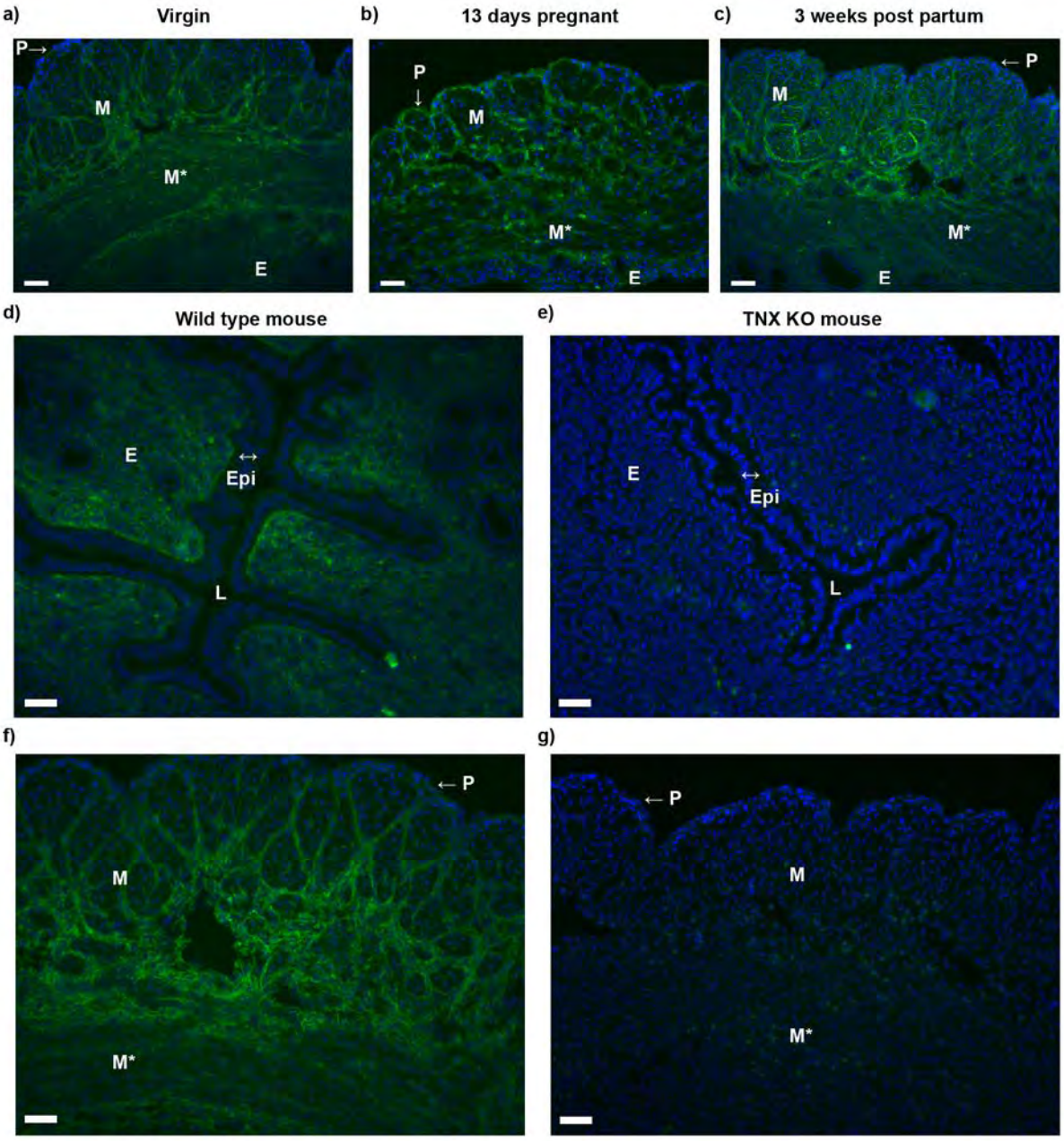

Figure 3: Immunostaining of TNX in the uterus.
TNX (green) is present throughout the uterus of virgin mice (a) and in the uterus during and after pregnancy (shown for 13 days pregnant (b) and 3 weeks postpartum (c) uteri). Cell nuclei are stained with DAPI (blue). TNX is present in the endometrium (d) and the layers of connective tissue ensheathing muscle bundles of the myometrium (f). The TNX staining of the perimetrium can be relatively weak (a-c and f). The epithelium of the lumen is negative for TNX (d). Specificity of our TNX antibody is demonstrated in figures (e) and (g). Panels (d-g) are from uteri 3 weeks postpartum. Bars are 50 µm (P = perimetrium, M = myometrium; longtidunal muscle bundles, M* = myometrium; transverse muscle bundles, E = endometrium, Epi = epithelium of the lumen, L = lumen).

myometrium, whereas the TNX immunostaining in the ECM of these bundles is relatively weak compared to the rest of the uterus (figure 3a-c,f). No differences in the collagen type XII localization in the uterus between WT (figure 5a) and TNX KO (figure 5b) mice were observed.

Elastic fibers in mouse tissues

Elastic fibers in the skin of TNX-deficient patients are known to be abnormally shaped [27] and thus we investigated their structure in TNX KO mouse tissues. Elastic fibers in the uterus are mostly located in the myometrium and perimetrium (figure 6a and b).

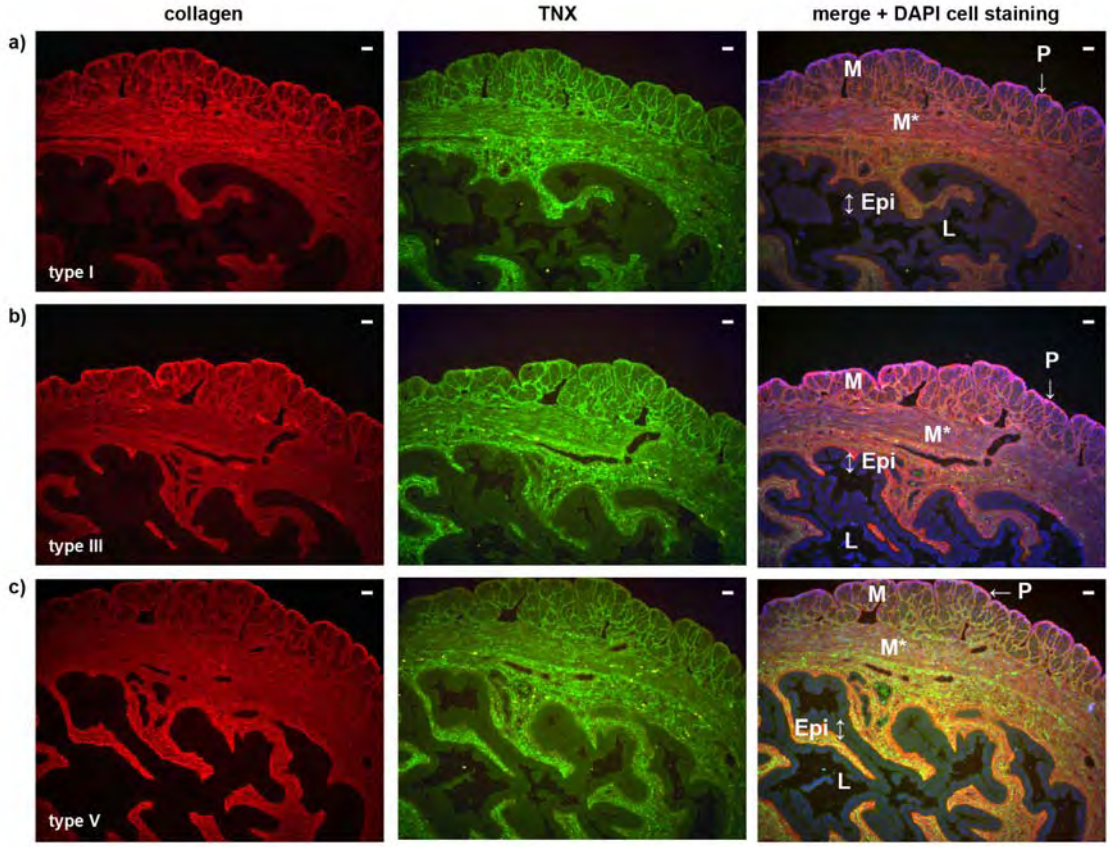

Figure 4: TNX colocalizes with major fibrillar collagens type I, III and V.
TNX (green) and collagen types I (a), III (b) and V (c) (red) colocalize (yellow to orange) as is shown for uteri 3 weeks postpartum. Similar results were obtained for uteri from virgin, 13 days pregnant and 1-day postpartum mice. No difference in collagen type I, III and V immunostaining was found between WT and TNX KO mice (data not shown). Bars are 50 µm (P = perimetrium, M = myometrium; longtidunal muscle bundles, M* = myometrium; transverse muscle bundles, E = endometrium, Epi = epithelium of the lumen, L = lumen).

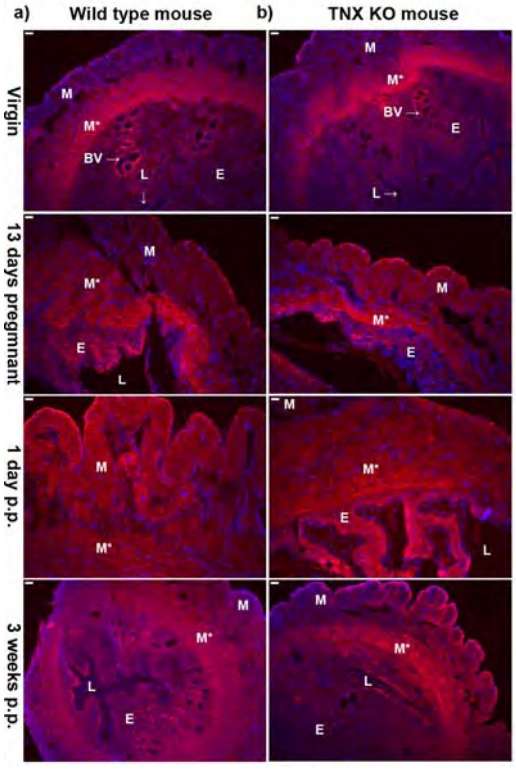

Figure 5: Immunostaining of collagen type XII in uterus.
Collagen XII (red) is present throughout the uterus. The immunostaining appears the strongest in the transverse muscle bundles of the myometrium (M*), around blood vessels (BV) and around the lumen (L), although the signal intensity is not always completely continuous. No differences in the collagen type XII localization in the uterus between WT (a) and TNX KO (b) mice were observed. Bars are 50 µm (P = perimetrium, M = myometrium; longtidunal muscle bundles, M* = myometrium; transverse muscle bundles, BV = blood vessel, E = endometrium, L = lumen).

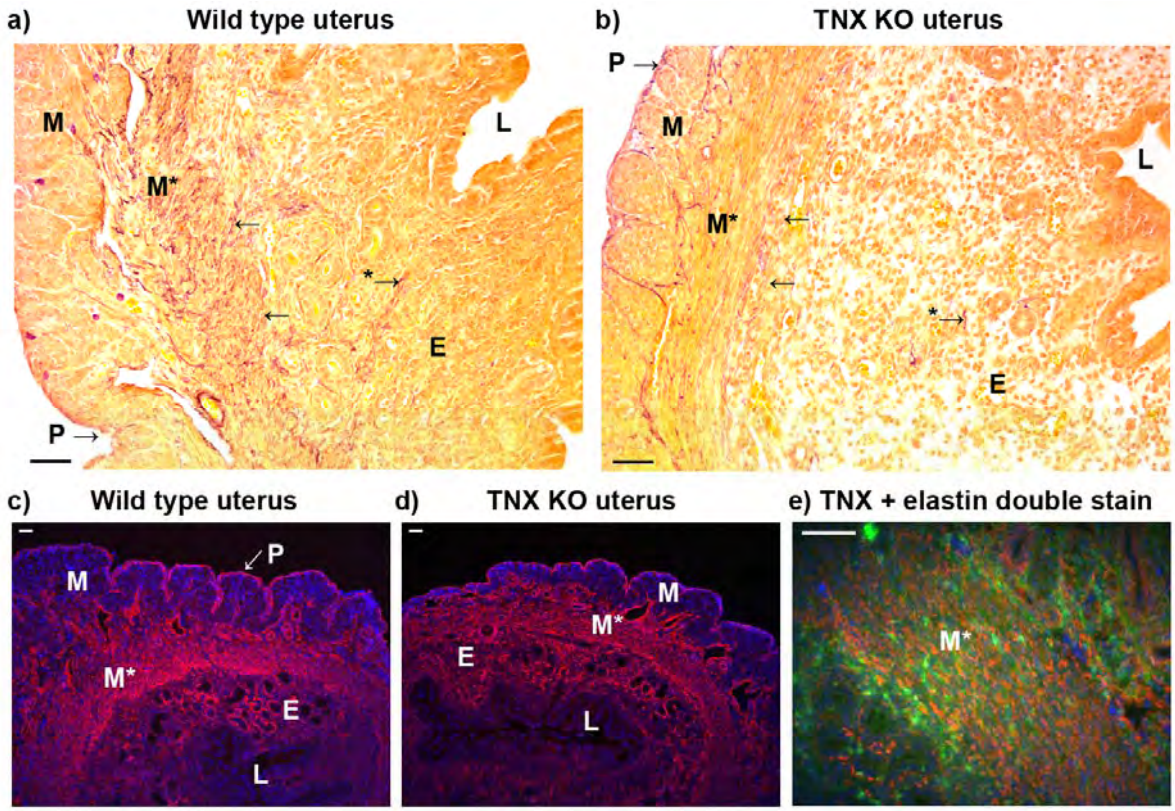

Figure 6: Elastin and elastic fibers in the uterus.
Elastic fibers (purple, modified Hart's staining) are mostly located in the myometrium (M, M*) and perimetrium (P), whereas the endometrium (E) appears to contain fewer elastic fibers as shown for WT (a) and TNX KO mice (b). No elastic fiber abnormalities were found in the TNX KO mice. Elastin (red) immunostaining is observed in the myometrium, predominantly in the transverse bundles (M*) as shown in panels (c) and (d). The layers of connective tissue ensheathing muscle bundles of the myometrium (M) and perimetrium (P) are stained positive for elastin (red). Strong elastin staining is also seen in the endometrium (E). Elastin immunoreactivity was similar for WT (c) and TNX KO mice (d). Elastin (red) colocalizes (orange) with TNX (green) as shown in the myometrium (M*) (e). Not all TNX colocalizes with elastin as TNX also colocalizes with different collagen types (fig. 4). Bars are 50 µm (P = perimetrium, M = myometrium; longtidunal muscle bundles, M* = myometrium; transverse muscle bundles, BV = blood vessel, E = endometrium, L = lumen).

The endometrium contains few elastic fibers as shown for WT (figure 6a) and TNX KO mice (figure 6b). In the myometrium and perimetrium, positive staining for elastin is seen predominantly in the layers of connective tissue ensheathing the transverse muscle bundles (figure 6c and d). Despite the relative low abundance of mature elastic fibers seen in the endometrium, the presence of elastin could be detected by immunohistochemistry, possibly a consequence of sensitivity of the detection methods (figure 6c-d). Elastin localization was similar for WT (figure 6c) and TNX KO mice (figure 6d). We previously demonstrated binding of TNX with elastin and the colocalization of these two proteins in skin [20;21]. Consistent with these findings, elastin also colocalizes with TNX in the uterus as shown in the myometrium (figure 6e). In previous work, we showed an increase in elastin positive material in the skin of aging TNX KO mice [20;21]. Although by light microscopy, the elastic fibers in the TNX KO mouse skin did not appear to be abnormally shaped, an increase in staining could have resulted from an increase in less mature or less organized elastin fibers, an increase in soluble tropoelastin within the matrix and/or the consequence of more immunoreactive epitopes being available due to an increased susceptibility for degradation. These results are consistent with our past observations of elastic fibers in the skin of TNX-deficient patients, where irregular and immature elastic fibers and fibers devoid of microfibrils could be seen at the ultrastructural level [20;27].

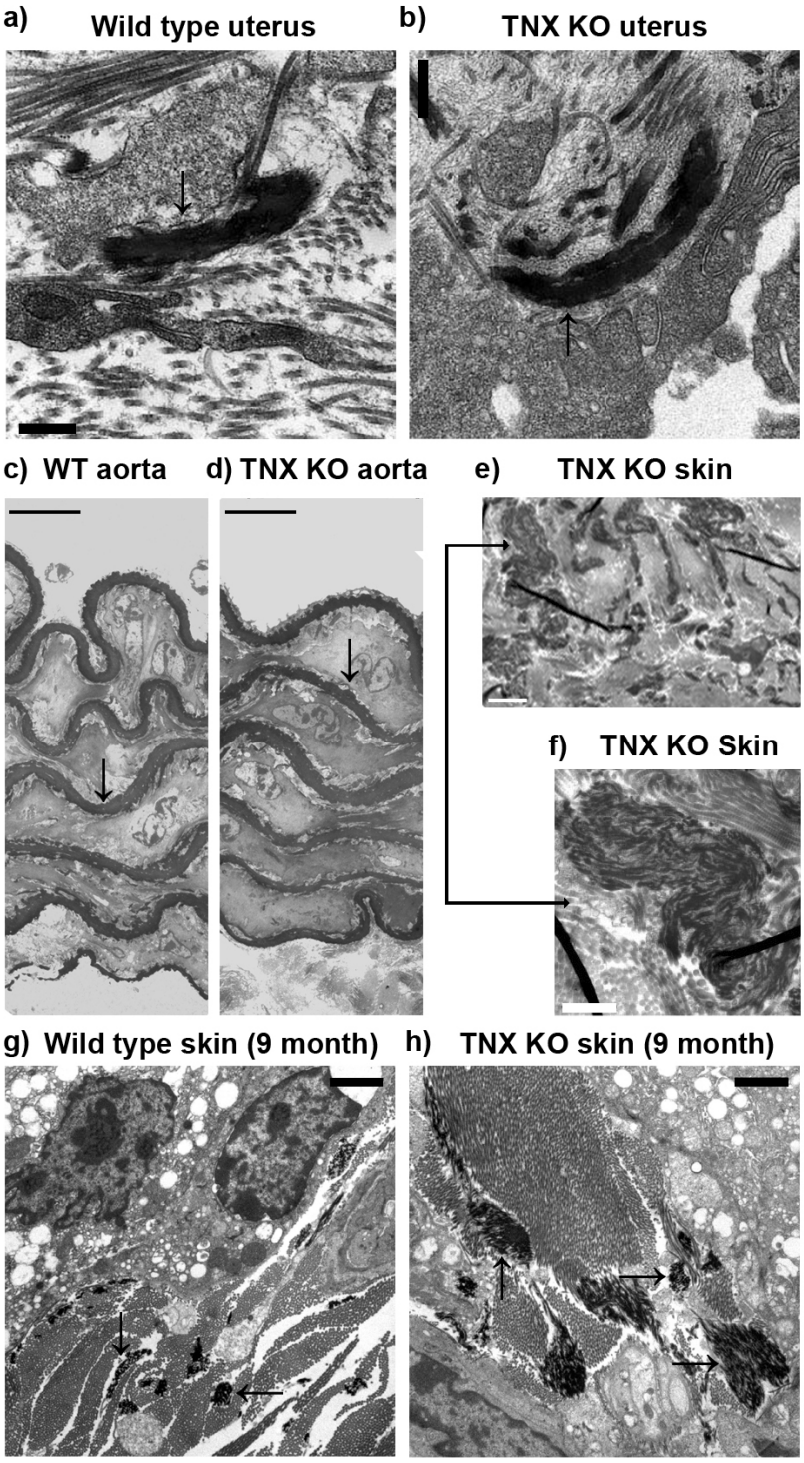

Figure 7: Ultrastructural evaluation of elastic fibers. Elastic fibers in WT (a) and TNX KO mice (b) uterus do not appear to differ in shape or size. The dark structures indicated by arrows are elastic fibers (shown for uterus 3 weeks postpartum). The elastic laminae (one indicated by an arrow in each slide) in the aorta of WT (c) and TNX KO mice (d) are similar in shape and number (aorta of 9 month-old mice). Skin of older TNX KO mice (9 months old) show differences in elastic fibers compared to WT skin. Irregular elastin aggregates can be observed in the TNX KO mouse skin (e, near a sebaceous gland). An enlargement of an elastin aggregate, indicated by an arrow, is shown in (f). These aggregates were not found in skin of 2 month old TNX KO mice nor in 9 month old WT mice. No irregularities in the shape of elastic fibers are observed in 9 month old TNX KO mice skin, however, larger elastic fibers than in WT mice (g) are often observed in the TNX KO mice (h, arrows indicate elastic fibers). Bars in panel (a) and (b) are 0.5 µm, in panel (c) and (d) 10 µm, in panel (e), (g) and (h) 2 µm and in panel (f) 1 µm.

Thus, to further expand these findings in skin and to investigate the elastic fibers in the uterus, we performed an ultrastructural analysis of the elastic fibers in several tissues. Elastic fibers in WT (figure 7a) and TNX KO mice (figure 7b) uteri do not appear to differ in shape or size (shown for uterus 3 weeks postpartum). Similarly, in aorta the elastic laminae (one indicated by an arrow in each slide) of WT (figure 7c) and TNX KO mice (figure 7d) are similar in shape and number (aorta of 9 month old mice). In skin of older TNX KO mice (9 months old), however, a difference in elastic fiber ultrastructure was observed compared to WT skin. In addition to normal appearing elastic fibers, irregular elastin aggregates, as seen in the skin of TNX-deficient patients [27], could be observed (figure 7e and f). These elastin aggregates were not found in skin of 2 month old TNX KO mice or in 9 month old

WT mice. Interestingly, elastic fibers in skin of 9 month old TNX KO mice often appear larger compared to WT mice of the same age (compare figures 7g and h).

DISCUSSION

GU complications occur frequently in patients with various types of EDS [12;13;16-19]. In classical and hypermobility types of EDS, which are the most common, the outcome of pregnancy is generally favorable. Maternal complications however, such as postpartum hemorrhage and pelvic instability, are more common than in the general population [16;18;19]. Furthermore, EDS patients appear to have an elevated risk of uterine prolapse [13;17]. Pregnancy in patients with vascular type EDS may even lead to maternal death through uterus or vessel rupture [12]. We investigated pregnancies and GU abnormalities in all known TNX-deficient woman of reproductive age. Generally, pregnancy was without major complications in TNX-deficient patients apart from one incident of postpartum hemorrhage. However, uterine and vaginal prolapse regularly occur in TNX-deficient women, even at a young age, suggesting laxity of GU tissues. Premature rupture of fetal membranes is a risk in pregnancy with EDS affected fetuses [17;19]. No premature births were observed in the offspring of the TNX-deficient patients, however, some TNX-deficient patients had been born premature.

Complete TNX deficiency in humans is a rare condition, and so far only few patients have been identified. We therefore investigated pregnancy and uterine tissue structure in our TNX KO mouse model. No gross, significant differences were found in abnormalities during pregnancy or reproduction between the TNX KO and WT mice. There was a trend towards a reduction in the length of pregnancy in TNX KO mice. The only significant difference was observed in the location of the vaginal plugs, which suggests laxity in the vaginal wall.

In a previous study, we did not find any differences in cutaneous collagen deposition between TNX KO and WT mice [20], as has been observed in the skin of TNX-deficient patients [7;27]. Alterations in collagen deposition in the skin of TNX KO mice is, however, a matter of debate [20;23;28]. In the present study, we found elastin aggregates and enlarged elastic fibers in 9 month old skin of TNX KO mice at the ultrastructural level, which is in accordance with our previous published data on increased elastin staining in aging TNX KO mouse skin [20]. We found no differences in elastic fibers in the uterus or elastic laminae of the abdominal aorta between TNX KO and WT mice suggesting a specific role for TNX in the maturation or maintenance of elastic fibers in skin. However, abnormal elastic fibers might not be present in the uterus since the ECM is constantly being remodeled in the menstrual cycle and in pregnancy.

Although the TNX KO mice appear to have a much milder phenotype compared to TNX-deficient humans, the skin of TNX KO mice is significantly weaker and more lax compared to WT mice [6;7;10;20;23;27-30]. Our data suggest a more lax vaginal canal in TNX-deficient patients and to a certain degree in TNX KO mice. It is attractive to speculate, considering the observations from all our studies in mice, that TNX is essential for tissue integrity, independent of the quantity of collagen deposition or elastic fiber structure. In conclusion, we would advise obstetricians and gynecologists to monitor TNX-deficient patients more closely as they are likely to have weaker GU connective tissue, could therefore be at risk for GU complications.

ACKNOWLEDGEMENTS

We are grateful to Ilona van den Brink, Geert Poelen, Debby Smits and Brenda van Vliet of the Central Animal laboratory of the Radboud University Nijmegen for their technical assistance. Willeke Blokx of the department of Pathology of the UMC Nijmegen, is acknowledged for advice and discussion. Jim Bristow of the Lawrence Berkeley National Laboratory, USA, is acknowledged for providing the original TNX KO mice and discussion. This work was supported by grants from the Dutch Program Tissue Engineering (DPTE) and the Canadian Institutes of Health

Research (CIHR). ECD is a Canada Research Chair.

REFERENCES

[1] Bristow,J., Tee,M.K., Gitelman,S.E., Mellon,S.H., & Miller,W.L. (1993) Tenascin-X: a novel extracellular matrix protein encoded by the human XB gene overlapping P450c21B. *J. Cell Biol.* **122,** 265-278.

[2] Lethias,C., Descollonges,Y., Boutillon,M.M., & Garrone,R. (1996) Flexilin: a new extracellular matrix glycoprotein localized on collagen fibrils. *Matrix Biol.* **15,** 11-19.

[3] Elefteriou,F., Exposito,J.Y., Garrone,R., & Lethias,C. (1997) Characterization of the bovine tenascin-X. *J. Biol. Chem.* **272,** 22866-22874.

[4] Ikuta,T., Sogawa,N., Ariga,H., Ikemura,T., & Matsumoto,K. (1998) Structural analysis of mouse tenascin-X: evolutionary aspects of reduplication of FNIII repeats in the tenascin gene family. *Gene* **217,** 1-13.

[5] Tucker,R.P., Drabikowski,K., Hess,J.F., Ferralli,J., Chiquet-Ehrismann,R., & Adams,J.C. (2006) Phylogenetic analysis of the tenascin gene family: evidence of origin early in the chordate lineage. *BMC. Evol. Biol.* **6,** 60.

[6] Burch,G.H., Gong,Y., Liu,W., Dettman,R.W., Curry,C.J., Smith,L., Miller,W.L., & Bristow,J. (1997) Tenascin-X deficiency is associated with Ehlers-Danlos syndrome. *Nat. Genet.* **17,** 104-108.

[7] Schalkwijk,J., Zweers,M.C., Steijlen,P.M., Dean,W.B., Taylor,G., Van Vlijmen,I.M., van Haren,B., Miller,W.L., & Bristow,J. (2001) A recessive form of the Ehlers-Danlos syndrome caused by tenascin-X deficiency. *N. Engl. J. Med.* **345,** 1167-1175.

[8] Zweers,M.C., Bristow,J., Steijlen,P.M., Dean,W.B., Hamel,B.C., Otero,M., Kucharekova,M., Boezeman,J.B., & Schalkwijk,J. (2003) Haploinsufficiency of TNXB is associated with hypermobility type of Ehlers-Danlos syndrome. *Am. J. Hum. Genet.* **73,** 214-217.

[9] Peeters,A.C.T.M., Kucharekova,M., Timmermans,J., van den Berkmortel,F.W.P.J., Boers,G.H., Novakova,I.R.O., Egging,D., den Heijer,M., & Schalkwijk,J. (2004) A clinical and cardiovascular survey of Ehlers-Danlos syndrome patients with complete deficiency of tenascin-X. *Neth. J. Med.* **62,** 23-25.

[10] Lindor,N.M. & Bristow,J. (2005) Tenascin-X deficiency in autosomal recessive Ehlers-Danlos syndrome. *Am. J. Med. Genet. A* **135,** 75-80.

[11] Beighton,P., De Paepe,A., Steinmann,B., Tsipouras,P., & Wenstrup,R.J. (1998) Ehlers-Danlos syndromes: revised nosology, Villefranche, 1997. Ehlers-Danlos National Foundation (USA) and Ehlers-Danlos Support Group (UK). *Am. J. Med. Genet.* **77,** 31-37.

[12] Pepin,M., Schwarze,U., Superti-Furga,A., & Byers,P.H. (2000) Clinical and genetic features of Ehlers-Danlos syndrome type IV, the vascular type. *N. Engl. J. Med.* **342,** 673-680.

[13] Carley,M.E. & Schaffer,J. (2000) Urinary incontinence and pelvic organ prolapse in women with Marfan or Ehlers Danlos syndrome. *Am. J. Obstet. Gynecol.* **182,** 1021-1023.

[14] Roop,K.A. & Brost,B.C. (1999) Abnormal presentation in labor and fetal growth of affected infants with type III Ehlers-Danlos syndrome. *Am. J. Obstet. Gynecol.* **181,** 752-753.

[15] Wegrowski,Y., Bellon,G., Quereux,C., & Maquart,F.X. (1999) Biochemical alterations of uterine leiomyoma extracellular matrix in type IV Ehlers-Danlos syndrome. *Am. J. Obstet. Gynecol.* **180,** 1032-1034.

[16] Ramos-e-Silva, Libia Cardozo,P.A., Bastos,O.G., & Coelho da Silva,C.S. (2006) Connective tissue diseases: pseudoxanthoma elasticum, anetoderma, and Ehlers-Danlos syndrome in pregnancy. *Clin. Dermatol.* **24,** 91-96.

[17] Lind,J. & Wallenburg,H.C. (2002) Pregnancy and the Ehlers-Danlos syndrome: a retrospective study in a Dutch population. *Acta Obstet. Gynecol. Scand.* **81,** 293-300.

[18] Kuczkowski,K.M. (2005) Ehlers-Danlos syndrome in the parturient: an uncommon disorder--common dilemma in the delivery room. *Arch. Gynecol. Obstet.* **273,** 60-62.

[19] Parry,S. & Strauss,J.F., III (1998) Premature rupture of the fetal membranes. *N. Engl. J. Med.* **338,** 663-670.

[20] Egging,D.F., van Vlijmen,I., Starcher,B., Gijsen,Y., Zweers,M.C., Blankevoort,L., Bristow,J., & Schalkwijk,J. (2006) Dermal connective tissue development in mice: an essential role for tenascin-X. *Cell Tissue Res.* **323,** 465-474.

[21] Egging,D., van den,B.F., Taylor,G., Bristow,J., & Schalkwijk,J. (2006) Interactions of human tenascin-X domains with dermal extracellular matrix molecules. *Arch. Dermatol. Res.* **298,** 389-396.

[22] Veit,G., Hansen,U., Keene,D.R., Bruckner,P., Chiquet-Ehrismann,R., Chiquet,M., & Koch,M. (2006) Collagen XII Interacts with Avian Tenascin-X through Its NC3 Domain. *J. Biol. Chem.* **281,** 27461-27470.

[23] Mao,J.R., Taylor,G., Dean,W.B., Wagner,D.R., Afzal,V., Lotz,J.C., Rubin,E.M., & Bristow,J. (2002) Tenascin-X deficiency mimics Ehlers-Danlos syndrome in mice through alteration of collagen deposition. *Nat. Genet.* **30,** 421-425.

[24] Morel,Y., Bristow,J., Gitelman,S.E., & Miller,W.L. (1989) Transcript encoded on the opposite strand of the human steroid 21-hydroxylase/complement component C4 gene locus. *Proc. Natl. Acad. Sci. U. S. A* **86,** 6582-6586.

[25] Starcher,B., Aycock,R.L., & Hill,C.H. (2005) Multiple roles for elastic fibers in the skin. *J. Histochem. Cytochem.* **53,** 431-443.

[26] Davis,E.C. (1993) Smooth muscle cell to elastic lamina connections in developing mouse aorta. Role in aortic medial organization. *Lab Invest* **68,** 89-99.

[27] Zweers,M.C., Vlijmen-Willems,I.M., Van Kuppevelt,T.H., Mecham,R.P., Steijlen,P.M., Bristow,J., & Schalkwijk,J. (2004) Deficiency of tenascin-x causes abnormalities in dermal elastic fiber morphology. *J. Invest Dermatol.* **122,** 885-891.

[28] Minamitani,T., Ikuta,T., Saito,Y., Takebe,G., Sato,M., Sawa,H., Nishimura,T., Nakamura,F., Takahashi,K., Ariga,H., & Matsumoto,K. (2004) Modulation of collagen fibrillogenesis by tenascin-X and type VI collagen. *Exp. Cell Res.* **298,** 305-315.

[29] Bristow,J., Carey,W., Egging,D., & Schalkwijk,J. (2005) Tenascin-X, collagen, elastin, and the Ehlers-Danlos syndrome. *Am. J. Med. Genet. C. Semin. Med. Genet.* **139,** 24-30.

[30] Matsumoto,K., Takayama,N., Ohnishi,J., Ohnishi,E., Shirayoshi,Y., Nakatsuji,N., & Ariga,H. (2001) Tumour invasion and metastasis are promoted in mice deficient in tenascin-X. *Genes Cells* **6,** 1101-1111.

CHAPTER 5

INTERACTIONS OF HUMAN TENASCIN-X DOMAINS WITH DERMAL EXTRACELLULAR MATRIX MOLECULES

This chapter has been previously published:
Egging D, van den Berkmortel F, Taylor G, Bristow J, Schalkwijk J. Interactions of human tenascin-X domains with dermal extracellular matrix molecules. Arch Dermatol Res. 2007 Jan;298(8):389-96. Reprinted with permission.

Arch Dermatol Res
DOI 10.1007/s00403-006-0706-9

ORIGINAL PAPER

Interactions of human tenascin-X domains with dermal extracellular matrix molecules

David Egging · Franka van den Berkmortel · Glen Taylor · Jim Bristow · Joost Schalkwijk

Received: 5 July 2006 / Revised: 28 August 2006 / Accepted: 2 September 2006

Abstract Tenascin-X (TNX) is a large 450 kDa extracellular matrix protein expressed in a variety of tissues including skin, joints and blood vessels. Deficiency of TNX causes a recessive form of Ehlers–Danlos syndrome characterized by joint hypermobility, skin fragility and hyperextensible skin. Skin of TNX deficient patients shows abnormal elastic fibers and reduced collagen deposition. The mechanism by which TNX deficiency leads to connective tissue alterations is unknown. Here we report that C-terminal domains of human TNX bind to major dermal fibrillar collagens and tropoelastin. We have mapped these interactions to the fibronectin type III repeat 29 (FNIII29) and the C-terminal fibrinogen domain (FbgX) of TNX. In addition we found that FNIII29 of TNX accelerates collagen fibrillogenesis in vitro. We hypothesize that TNX contributes to matrix stability and is possibly involved in collagen fibril formation.

Electronic supplementary material Supplementary material is available in the online version of this article at http://dx.doi.org/10.1007/s00403-006-0706-9 and is accessible for authorized users.

D. Egging (✉) · F. van den Berkmortel · J. Schalkwijk
Department of Dermatology, Nijmegen Centre for Molecular Life Sciences, Radboud University Nijmegen Medical Centre, P.O. Box 9101, 6500 HB Nijmegen, The Netherlands
e-mail: d.egging@derma.umcn.nl

G. Taylor · J. Bristow
Department of Pediatrics, University of California, San Francisco, CA, USA

J. Bristow
Department of Genome Sciences, Lawrence Berkeley National Laboratory, Berkeley, CA, USA

Keywords Tenascin-X · Collagen · Elastin · Fibrillogenesis · Ehlers–Danlos syndrome

Introduction

Tenascin-X is a large extracellular matrix glycoprotein composed of EGF like-repeats, fibronectin type III (FNIII) repeats and a C-terminal fibrinogen domain (FbgX) [1, 5, 6, 12]. TNX abnormalities are associated with several pathological conditions [2, 22, 27]. Complete deficiency of TNX in humans leads to a recessive form of Ehlers Danlos syndrome (EDS) and TNX haploinsufficiency is a cause of hypermobility type EDS. The skin of TNX deficient patients is markedly lax with poor recoil properties and shows easy bruising [2, 14, 20, 22, 27]. We have previously shown TNX to be present in the entire dermis of healthy individuals. During development in mice TNX colocalises with the major fibrillar collagens and elastic fibers in the dermis [3, 22]. Adult TNX deficient patients show abnormal elastic fibers and reduced collagen deposition in skin [28]. The mechanism by which TNX deficiency leads to alterations in the extracellular matrix (ECM) is unknown. Mapping of TNX domains that interact with components of the elastic fibers or collagen is therefore an important step to define the role of TNX in connective tissue biology of human skin.

It has previously been shown that bovine and murine TNX bind to heparin [13, 16]. In bovine TNX a conformational heparin-binding site has been identified involving FNIII repeats 10 and 11 in the N-terminal half of the molecule. This heparin-binding site is also involved in the binding of TNX to decorin, and it was proposed that TNX interacts with collagen through

decorin [4]. Minamitani et al. showed that the short isoform of murine TNX binds directly to collagen type I, probably through interaction with one of the fibronectin type III repeats. This short isoform was found to promote collagen fibrillogenesis in vitro [18].

The aim of our study was to investigate the molecular mechanisms of the observed phenotype in TNX-deficient EDS patients. We therefore analyzed interactions of human TNX with elastic fiber components and with the major fibrillar collagens in the dermis (collagen type I, III and V). We found that the C-terminus of TNX harbors potential interaction sites with collagens type I, III and V and tropoelastin (TE), which are constituents of the anatomical structures that are abnormal in the dermis of these patients.

Materials and methods

Expression and purification of recombinant TNX fragments

The TNX fragments were amplified by PCR with the primers listed in Table 1 using a previously described 2.7 kb human TNX cDNA [19] as a template. PCR products were ligated into the pCR2.1TOPO vector (Invitrogen, Breda, NL) according to the manufacturer's instructions for easy digestion with restriction enzymes. The pCR2.1 TOPO vectors with inserts were digested with *Eco*RI and *Sal*I and cloned into the *Eco*RI/*Sal*I site of the pMal-c2X plasmid (Westburg B.V., Leusden, NL). Subsequently the DNA sequences coding for FNIII29 and FNIII29–30 of TNX were cloned into the *Eco*RI/*Sal*I site of the pGex-4T1 plasmid (GE Healthcare Life Sciences, Diegem, BE). The sequence of the TNX domains was verified by dideoxy sequencing with a 3730 DNA analyzer (Applied Biosystems, Nieuwekerk a/d IJssel, NL). TNX fragments were obtained as maltose binding protein (MBP) fusion proteins using E.coli TOP10F' cells (Invitrogen) according to the manufacturer's instructions. MBP fusion proteins were isolated on amylose resin columns and analyzed for purity with SDS-PAGE. MBP fusion proteins were incubated with factor Xa (Westburg B.V.) in an attempt to remove the MBP tag from the fusion protein according to the manufacturer's instructions. FNIII29–30 without tag was obtained by proteolytic cleavage of FNIII29–30 from a glutathione-*S*-transferase (GST) fusion protein bound to a glutathione-sepharose4B column (GE Healthcare Life Sciences) according to the manufacturer's instructions.

Proteins and antibodies

A 100 kDa C-terminal recombinant TNX protein, containing six FNIII repeats and a fibrinogen domain, encoded by a 2.7 kb TNX sequence has previously been described by Tee et al. [19, 23]. MBP–FNIII27–28, MBP–FNIII28–29, MBP–FNIII29, MBP–FNIII29–30, MBP–FNIII30–31, MBP–FbgX and FNIII29–30 were obtained as described in the previous section.

Human Collagen type I from Chemicon International (Chemicon International, Temecula, CA, USA), human collagen type III and V from Rockland Inc (Tebu-bio, Heerhugowaard, NL). Bovine collagen type I (acid soluble) was obtained from BD biosciences (BD Biosciences, Alphen aan den Rijn, NL). Recombinant bovine tropoelastin (bTE) was a generous gift from Dr. R. Mecham (Washington University, St. Louis, MO, USA) [10]. Human recombinant fibrillin domains, Tb2-cbEGF11, Tb3-cbFGF11, cbEGF11–14, cbEGF22–23, cbEGF28–30, tb6-cbEGF32, cbEGF32–36, tb7-cbEGF37, were generously donated by Dr. P.A. Handford (Oxford University, Oxford, UK) [7, 9, 11, 17, 24, 25]. BSA and gelatin were obtained from Sigma–Aldrich (Sigma–Aldrich Chemie B.V., Zwijndrecht, NL). BSA was used as a negative control. MBP was obtained from New England Biolabs (Westburg B.V.) and used as a negative control.

We used monoclonal antibodies specific for MBP (Westburg B.V) and a previously described guinea pig-anti-TNX serum [22] for detection of untagged 100 kDa TNX and MBP-TNX-domains in our solid-phase assays. Pre-immunization serum was used as a

Table 1 TNX domains and primers

TNX domains	Forward primer	Reverse primer
FNIII27–28	5′-GGAATTCGAGCTACCTCCCCAC-3′	5′-CTCGTCGACTCACTGACCAGCAGGAGC-3′
FNIII28–29	5′-CTGAATTCCCTGAAGAGCCCCGC-3′	5′-TGGGTCGACTCAGCGGGCGGTTCCCTG-3′
FNIII29	5′-TCAGAATTCTCAAGGCCCCGCCTG-3′	5′-TGGGTCGACTCAGCGGGCGGTTCCCTG-3′
FNIII29–30	5′-TCAGAATTCTCAAGGCCCCGCCTG-3′	5′-GAAGTCGACTCAAGGCTCACTCTCCTC-3′
FNIII30–31	5′-ACCGAATTCACCCTCAGCCCAGTT-3′	5′-GTGTCGACTCAGATGCTGGCTGGGG-3′
FbgX	5′-TCTGAATTCACGGGTGGGCTGCGG-3′	5′-GGGTCGACAGAGAGGTGGGCAGCA-3′

The *Eco*RI and *Sal*I restriction sites are underlined in the primer sequences. Each *Sal*I site is preceded by a stop codon (TCA), except for the fibrinogen domain, which already contains a stop codon at the 3′ end of the sequence

negative control [22] FNIII29–30 of TNX was detected with a new affinity purified polyclonal rabbit antiserum, raised against a MBP–FNIII29–30 antigen.

Collagen fibrillogenesis assays

Native bovine type I collagen (BD Biosciences, Alphen aan den Rijn, NL) 2.9 mg/ml in 0.012 N HCl, as provided by the manufacturer, was dissolved in PBS. MBP, BSA, MBP–FNIII29, FNIII29–30 and 100 kDa TNX were added to samples in cuvettes after which the final volume was adjusted to 1 ml of 0.4 mg/ml collagen type I with PBS and incubated at 30°C. Turbidity change was measured by monitoring the change in absorbance at 400 nm in a UV-160A Shimadzu spectrophotometer (Shimadzu Benelux, Den Bosch, NL) at fixed intervals. Data points represent the mean of triplicate measurements.

Binding assays

Ninety-six well microtiter plates (Greiner Bio-One B.V., Alphen aan den Rijn, NL) were coated overnight at 4°C with ECM components diluted in PBS. All further incubation steps were performed at 37°C. After each incubation step wells were washed with PBS containing 0.05% Tween-20 (T-PBS). Wells were saturated with 1% BSA in T-PBS for 2 h and then incubated with recombinant TNX domains for 1 h. This was followed by incubation with antibodies against the recombinant TNX fragments for 1 h. Thereafter, wells were incubated with biotinylated anti guinea pig (Vector Laboratories Inc., Burlingame, CA, USA), biotinylated anti rabbit (Vector Laboratories Inc.) or anti mouse IgG (vectastain kit, Brunschwig Chemie, Amsterdam, NL) for 1 h followed by a 45 min incubation with an avidin–biotin–horse radish peroxidase mixture (vectastain kit, Brunschwig Chemie). Bound peroxidase was detected with *o*-phenylenediamine dihydrochlorid (Perbio Science Nederland B.V., Etten-Leur, NL) and the absorbance read at 490 nm. All antibodies and TNX proteins were diluted in T-PBS containing 0.1% BSA. PBS was substituted by tris buffered saline (TBS) + 5 mM Ca_2Cl_2 in solid phase assays in which binding of TNX to fibrillin-1 domains was investigated for proper folding/stability of the fibrillin-1 domains [7, 21]. Assays were performed at least twice. BSA, MBP and pre immunization guinea pig serum were used as negative controls or baseline correction.

As an alternative to the binding assay in ELISA format we investigated binding of MBP–FNIII29 to collagen fibrils generated during the fibrillogenesis assay. Briefly, various concentrations of MBP–FNIII29 were incubated overnight at 30°C in the presence of 0.1% BSA or collagen type I (0.4 mg/ml) + 0.1% BSA. Thereafter, the insoluble collagen fibrils were pelleted by centrifugation. The concentration of MBP–FNIII29 in the supernatant was determined using an assay similar to a previous described one [22] in which, instead of guinea pig anti TNX antiserum, fusion protein was detected with monoclonal antibodies specific for MBP (Westburg B.V.).

SDS-PAGE analysis

Proteins were loaded onto 12% Bis–Tris gels (Invitrogen) gel electrophoresis was carried out using the NuPAGE system according to the manufacturer's instructions (Invitrogen). To analyze protein purity gels were stained using coomassie brilliant blue R250 (Brunschwig).

Results

Binding of C-terminal 100 kDa TNX to extracellular matrix components

We postulated that TNX might interact with components of elastic fibers or collagens directly because of the disturbed properties of collagens and elastic fibers in TNX deficient patients. As a first approach to identify extracellular ligands of TNX, we performed solid phase assays to test binding of a recombinant C-terminal 100 kDa TNX fragment [19, 23] (soluble phase) to ECM molecules (immobilized substrates). Figure 1 a shows that TNX binds dose dependently to human collagens type I, III and V. Binding to BSA, which served as a negative control, was absent. Figure 1b compares the relative values of recombinant C-terminal 100 kDa TNX binding to human fibrillar collagens, at the highest concentration of fusion protein compared to the control values of BSA. Figure 2 a shows the interaction of TNX with bovine collagen type I, bovine tropoelastin and denatured collagen type I (gelatin). TNX did not bind to denatured bovine collagen (gelatin). Figure 2b compares the relative values of recombinant C-terminal 100 kDa TNX binding to bovine tropoelastin, collagen type I and gelatin, at the highest concentration of fusion protein compared to the control values of BSA. Half maximal saturation, a measure for the affinity of the interaction, was reached at a concentration of soluble 100 kDa TNX of 1.8×10^{-8} M for human collagen type I and 4.0×10^{-8} M for bovine collagen type I. Half maximal saturation was reached at

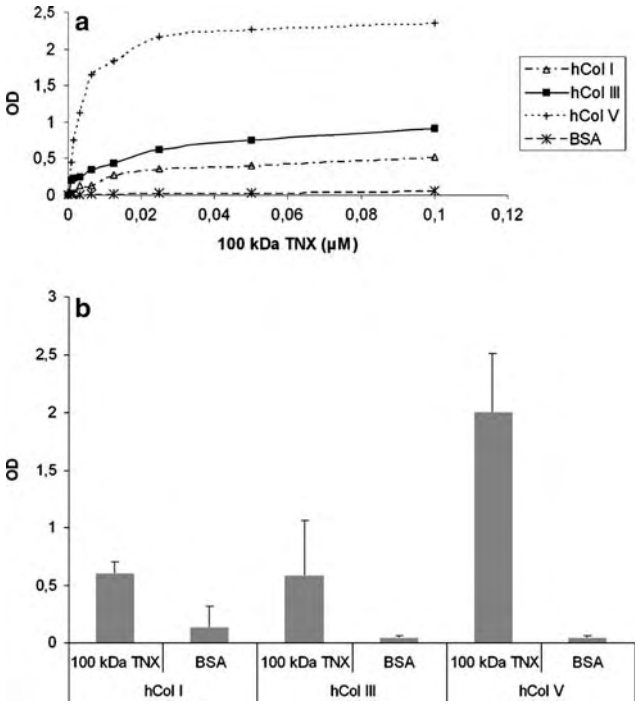

Fig. 1 Binding of recombinant C-terminal 100 kDa TNX to human collagen type I, III and V. **a** TNX binds dose dependently to human collagens type I, III and V. Binding to BSA, which served as a negative control, was absent. **b** Comparisons of binding of recombinant C-terminal 100 kDa TNX and BSA to collagens type I, III, and V at the highest concentration used (10 μM)

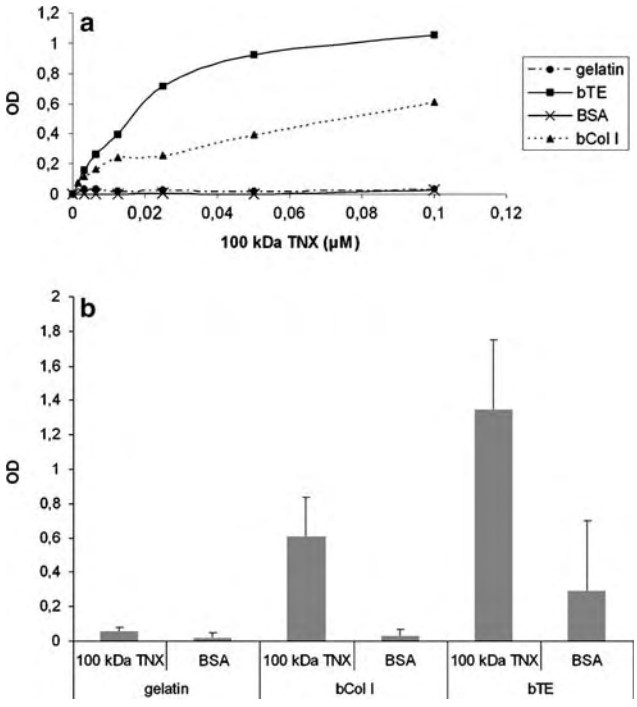

Fig. 2 Binding of recombinant C-terminal 100 kDa TNX to bovine collagen type I and bTE. **a** TNX binds dose dependently to bTE and bovine collagen type I. No binding to denatured bovine collagen type I (gelatin) was observed (the gelatin signal coincides with the BSA baseline signal). **b** Comparison of binding of recombinant C-terminal 100 kDa TNX and BSA to collagens type I, III and V at the highest concentration used (10 μM)

1.1×10^{-8} M for human collagen type III, 0.8×10^{-8} M for human collagen type V and 1.8×10^{-8} M for tropoelastin. We did not observe binding to several domains of the elastic fiber protein fibrillin-1 (data not shown).

Binding of specific C-terminal TNX fragments to extracellular matrix components

To identify the sequences in TNX responsible for binding to the ECM components we subcloned and expressed a number of fragments from the C-terminal 100 kDa TNX protein. Figure 3 gives a schematic overview of these fragments, and shows the purity of the fusion proteins used in this study. The domains studied here were produced as MBP-fusion proteins and included overlapping tandems of FNIII repeats and the FbgX domain.

All recombinant proteins containing the FNIII29 repeat showed dose dependent binding to collagen type I, III and V. As an example the binding curves for collagen type V are shown in Fig. 4a. Only FNIII29, FNIII28–29 and FNIII29–30 showed strong binding, whereas no binding was observed for repeats FNIII27–28, FNIII30–31 and the FbgX domain which yielded a flat line as for the MBP and BSA control. For reasons of clarity the curves for FNIII27–28, FNIII30–31, FbgX and BSA are not included in Fig. 4a because they coincide with MBP. Figure 4b compares the relative values of FNIII29 and FNIII27–28 binding to fibrillar collagens, at the highest concentration of fusion protein compared to the control values of MBP.

Figure 5a depicts binding of TNX fragments to recombinant bTE. All fusion proteins containing FNIII29 were found to bind to TE, but in addition we found interaction with the FbgX domain, which was not the case for collagens. Recombinant MBP shows some non-specific binding to bTE but this is clearly less than FNIII29 and FbgX containing recombinant proteins. This non-specific binding was also observed for BSA, FNIII27–28 and FNIII30–31. The lines from these proteins coincide with the line of the MBP control, therefore they were omitted from Fig. 5a for reasons of clarity. Figure 5b compares the relative values of FNIII29, FNIII27–28 and FbgX binding to recombinant TE, at the highest concentration of fusion protein compared to the control values of MBP.

We used TNX domains fused to MBP because this allows simple high yield purification and—importantly—it allows comparison and easy detection of bound fusion proteins by a single anti-MBP antibody.

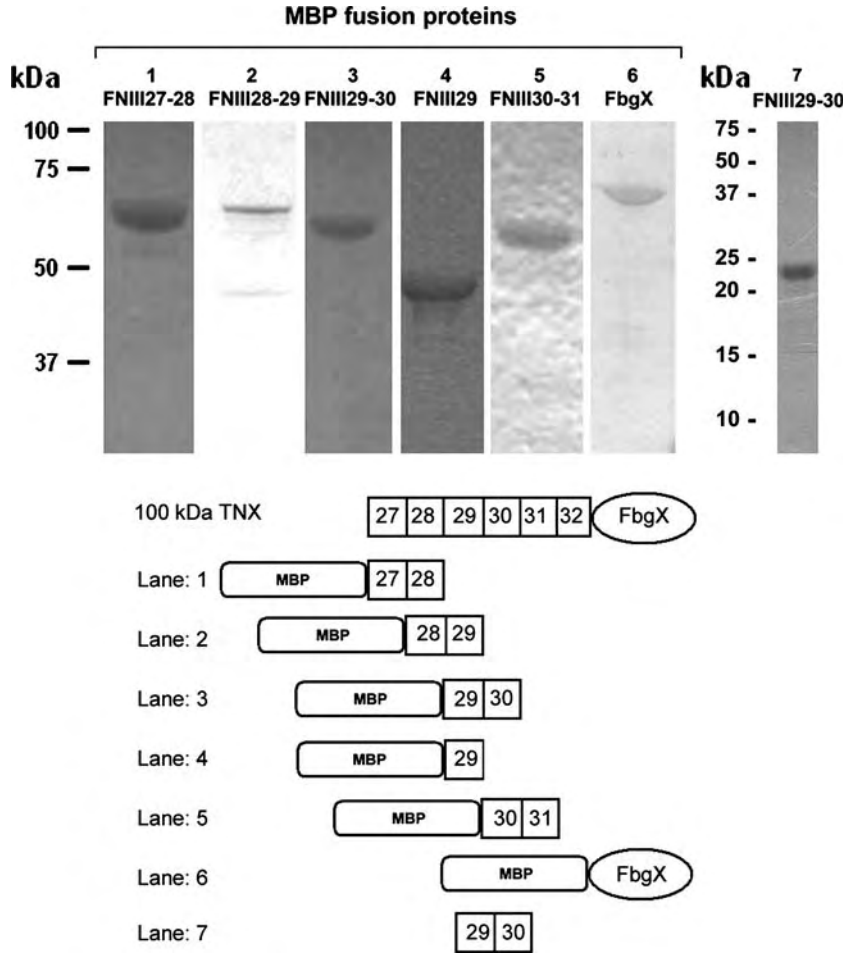

Fig. 3 Recombinant TNX proteins used in this study. **a** Coomassie staining of recombinant proteins, *lanes 1–5* MBP–FNIII repeats, *lane 6* MBP–FbgX domain, *lane 7* FNIII29–30 repeat without MBP fusion tag. **b** Schematic overview of recombinant proteins

MBP alone was used as a control throughout the studies described above. In order to check if MBP fused to TNX domains would cause artificial binding of fusion proteins to ECM molecules we decided to test binding of a recombinant TNX fragment without MBP. Unfortunately, it was not possible to produce FNIII29 as a single repeat protein without fusion protein tag in either the pMal protein fusion or GST gene fusion system. We therefore produced a recombinant FNIII29–30 repeat devoid of fusion tag and raised an antibody against FNIII29–30. Figure 6 shows that pure recombinant FNIII29–30 essentially has the same binding properties towards fibrillar collagens and TE as the MBP-fusion protein, indicating that the interaction site resides in the TNX moiety (FNIII29) of the fusion proteins.

Stimulation of fibrillogenesis by FNIII29

To extend the observed binding properties of TNX FNIII repeats at the functional level, we investigated whether the collagen binding FNIII29 repeat of human TNX could modulate collagen fibrillogenesis. Using a turbidity assay (see Fig. 7a) we found an increase in the rate of fibril formation and a shortening of the lag phase in the presence of the FNIII29 repeat of TNX compared to the control proteins (BSA (not shown) and MBP) The fibrillogenesis rate in the lateral growth phase, characterized by fibril- and aggregate formation [8, 26], was significantly increased ($P < 0.001$) when 48 µg/ml MBP–FNIII29 was added. At a concentration of 24 µg/ml, MBP–FNIII29 does not significantly influence the lateral growth phase, although it shortens the lag phase, characterized by linear growth of microfibrils and early fibril formation [8, 26], compared to controls. After 24 h all samples reached a similar maximal OD (data not shown). FNIII29–30 had only a minimal effect on collagen fibrillogenesis compared to MBP–FNIII29 and C-terminal 100 kDa TNX showed no significant effect on either the lag- or lateral growth phase of collagen fibrillogenesis (data not shown).

The fibrillogenesis assay also provided us with an alternative method to investigate binding of TNX fragments to ECM molecules. To investigate the binding of MBP–FNIII29 to the collagen fibrils formed during the assay, we measured the amount of MBP–FNIII29 that

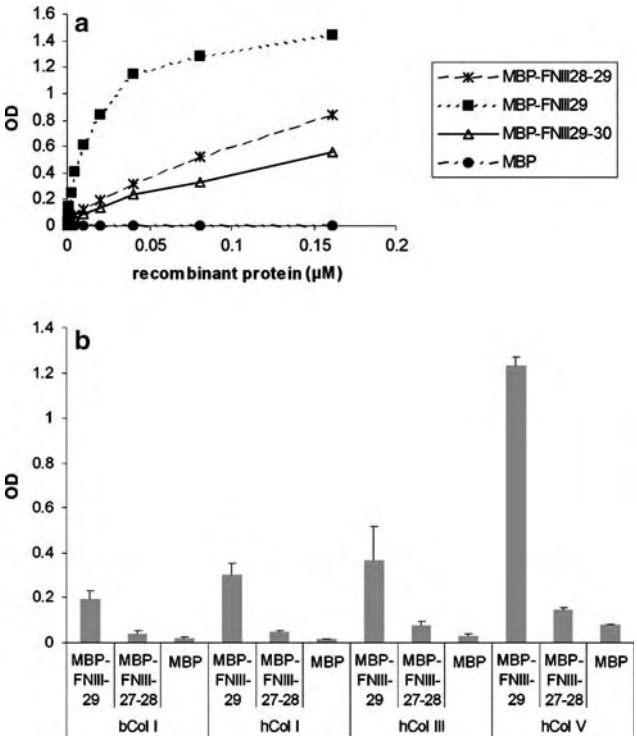

Fig. 4 Binding of TNX FNIII repeats to collagen type I, III an V. **a** Binding curves of recombinant TNX proteins containing FNIII29 show dose dependent binding to fibrillar collagens as shown here for human collagen type V. **b** Comparison of binding of MBP–FNIII29, MBP-FNIII27–28 and MBP to collagens type I, III and V at the highest concentration used (16 µM)

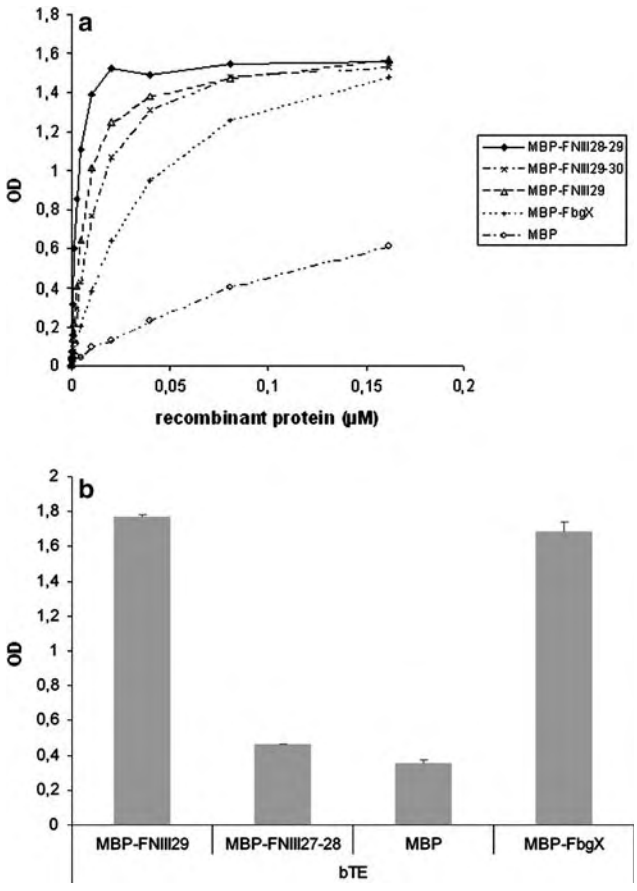

Fig. 5 Binding of TNX FNIII repeats and FbgX domain to TE. **a** Recombinant TNX fragments containing FNIII29 and the FbgX domain bind dose dependently to recombinant TE. The other investigated FNIII repeats of TNX do not show significant binding to bTE (not shown here). MBP alone shows non-specific binding which is significantly lower than the TNX containing fusion proteins. **b** Comparison of binding of MBP-FNIII29, MBP–FNIII27–28, MBP–FbgX and MBP to recombinant TE at the highest concentration used (16 µM)

remained in the supernatant after pelleting of the insoluble collagen fibrils. As shown in Fig. 7b MBP–FNIII29 was depleted from the soluble phase, indicating pull-down by the formation of collagen fibrils.

Discussion

We established a number of novel in vitro binding properties of human TNX that reside in the 100 kDa C-terminal portion. The binding properties of this fragment could be largely ascribed to the FbgX domain (tropoelastin binding) and the FNIII29 repeat, which was found to bind strongly to tropoelastin and collagen types I, III and V. Previous studies by others, using bovine and murine TNX have found binding to decorin [4] and collagen type I [18]. In the latter study, deletion of the EGF-like repeats or the FbgX domain did not abolish collagen binding, suggesting that binding of murine TNX resides somewhere in the FNIII repeats.

The binding to elastin was particularly interesting, as abnormal elastic fiber morphology is a characteristic feature of EDS patients with a complete TNX deficiency. We found binding of tropoelastin both to FNIII29 and FbgX. In contrast to FNIII29 the FbgX domain only binds to TE and not to other tested ECM proteins. The functional significance of this finding requires further investigation, but this interaction could be involved both in maturation or stability of the elastic fiber.

Dermal collagen deposition is reduced in TNX deficient patients, and their skin and other connective tissues is fragile as witnessed by easy bruising [22, 28]. The skin strength in TNX deficient mice is markedly reduced, although the significance and magnitude of the reduction of collagen deposition is debated [3, 15, 18]. In mice, the variation in collagen fibril diameter appears to be increased [15, 18]. Speculatively, the assembly or stability of collagen fibrils could be disturbed in TNX deficient patients. We found that the FNIII29 domain of human TNX is able to accelerate

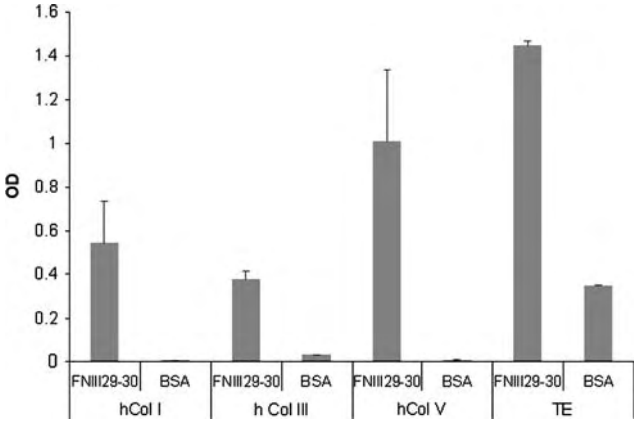

Fig. 6 Binding of FNIII29–30 to ECM proteins. Recombinant FNIII29–30 (without fusion tag) binds to collagen types I, III and V and to TE essentially in the same manner as the MBP fusion proteins containing FNIII29. BSA is used as a control for background staining (7.5 μg/ml)

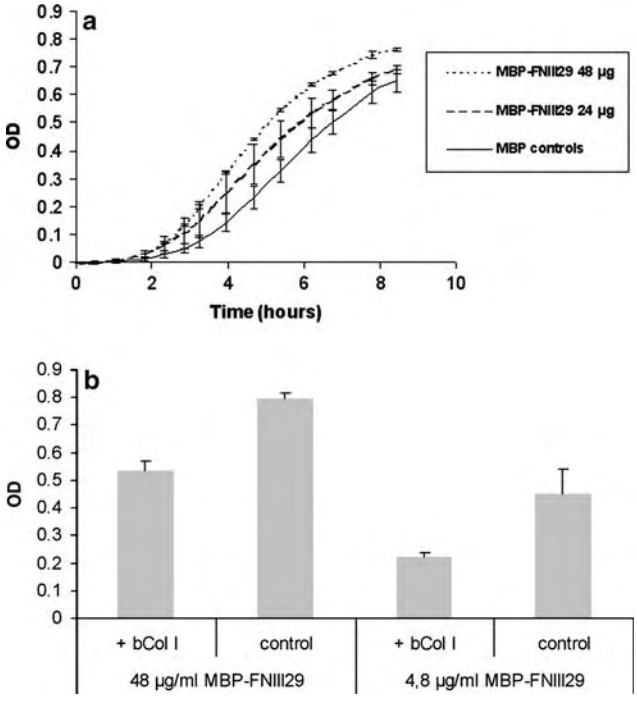

Fig. 7 TNX FNIII29 affects collagen fibrillogenesis. **a** TNX FNIII29 has a dose dependent effect on the fibrillogenesis rate of bovine collagen type I in a turbidimetric assay. At a concentration of 48 μg/ml MBP–FNIII29 the fibrillogenesis rate in the lateral growth phase is significantly increased. At a concentration of 24 μg/ml MBP–FNIII29 does not significantly influence the lateral growth phase, although at both 24 and 48 μg/ml the lag phase is shortened. MBP and BSA served as a negative control. The curves of BSA and 4.8 μg/ml MBP–FNIII29 overlapped with the MBP curve and have been omitted for reasons of clarity. **b** Comparison of TNX FNIII29 levels in the supernatant of pelleted insoluble collagen fibrils compared to controls. Differences of TNX FNIII29 concentration in the supernatant reflect the amount of TNX FNIII29 bound to the pelleted insoluble collagen fibrils

the collagen fibril formation in vitro. In contrast, however, we failed to detect a significant effect of the 100 kDa TNX fragment on fibrillogenesis. This might possibly be due to conformational changes caused by folding of the 100 kDa TNX in solution that precludes an effect on fibrillogenesis, although the 100 kDa fragment binds to collagen type I. Alternatively, the observed effect of the TNX FNIII29 repeat on fibrillogenesis could be artificial, because it is not known whether it is accessible to collagen in the native 450 kDa protein. Minamitani et al. found that a short isoform of murine TNX could accelerate collagen fibrillogenesis in an assay similar to the one we used [18]. Interestingly, they found that deletion of the EGF repeats or fibrinogen domain did not have an effect on binding of TNX to collagen although collagen fibrillogenesis kinetics were affected by deletion of these domains. Possibly conformational changes could account for this affect. Furthermore, we observed binding of the TNX FNIII29 repeat to the insoluble collagen fibrils formed during in vitro fibrillogenesis. This is in agreement with the observed binding properties of this domain in our solid phase assay in ELISA format. For fibrillar collagens type III and V we observed that preincubation of TNX FNIII29 with these collagens reduced the measured amount of TNX compared to controls in a previously described TNX ELISA [22] (data not shown). These findings are in accordance with the results from our solid phase binding assays. Clearly, the functional consequences of the interaction of TNX domains require further investigation. Ideally, the complete human 450 kDa [1] or adrenal specific 74 kDa [23] TNX form with correct glycosylation should be produced or purified, to provide definitive answers with respect to molecular interactions and effects on fibrillogenesis. On the other hand, the molecular diversity of TNX is far bigger than anticipated. We have found that various fragments of TNX, ranging from 70 to 450 kDa are present in human serum (unpublished results). Whether these represent alternative splice forms or posttranslationally processed fragments is unknown. All of these TNX forms contain the FNIII29 repeat and it is possible that these shorter forms adopt a conformation in which FNIII29 is exposed to exert binding to ECM molecules and causes functional effects.

In conclusion, our study shows that domains of TNX directly interact with a number of ECM molecules that form a major part of the affected structures in the dermis of TNX deficient patients. Our data could serve as a starting point to investigate the function of individual domains in the context of the physiological TNX

molecules, like the 450 kDa tissue form or the various serum forms. Further investigation of the role of TNX in extracellular matrix assembly and stability will increase our knowledge of connective tissue biology and will offer a molecular explanation for the phenotype of TNX deficient patients.

Acknowledgments The authors are grateful to Dr P. Handford, Dr N. Grebenchtchikov and Dr R. Mecham for providing biological reagents used in this study.

References

1. Bristow J, Tee MK, Gitelman SE, Mellon SH, Miller WL (1993) Tenascin-X: a novel extracellular matrix protein encoded by the human XB gene overlapping P450c21B. J Cell Biol 122:265–278
2. Burch GH, Gong Y, Liu W, Dettman RW, Curry CJ, Smith L, Miller WL, Bristow J (1997) Tenascin-X deficiency is associated with Ehlers–Danlos syndrome (see comments). Nat Genet 17:104–108
3. Egging DF, van Vlijmen I, Starcher B, Gijsen Y, Zweers MC, Blankevoort L, Bristow J, Schalkwijk J (2006) Dermal connective tissue development in mice: an essential role for tenascin-X. Cell Tissue Res 323:465–474
4. Elefteriou F, Exposito J, Garrone R, Lethias C (2001) Binding of tenascin-X to decorin. FEBS Lett 495:44–47
5. Elefteriou F, Exposito JY, Garrone R, Lethias C (1997) Characterization of the bovine tenascin-X. J Biol Chem 272:22866–22874
6. Ikuta T, Sogawa N, Ariga H, Ikemura T, Matsumoto K (1998) Structural analysis of mouse tenascin-X: evolutionary aspects of reduplication of FNIII repeats in the tenascin gene family. Gene 217:1–13
7. Jensen SA, Corbett AR, Knott V, Redfield C, Handford PA (2005) Ca2+ -dependent interface formation in fibrillin-1. J Biol Chem 280:14076–14084
8. Kadler KE, Holmes DF, Trotter JA, Chapman JA (1996) Collagen fibril formation. Biochem J 316(Pt1):1–11
9. Kettle S, Yuan X, Grundy G, Knott V, Downing AK, Handford PA (1999) Defective calcium binding to fibrillin-1: consequence of an N2144S change for fibrillin-1 structure and function. J Mol Biol 285:1277–1287
10. Kozel BA, Wachi H, Davis EC, Mecham RP (2003) Domains in tropoelastin that mediate elastin deposition in vitro and in vivo. J Biol Chem 278:18491–18498
11. Lee SS, Knott V, Jovanovic J, Harlos K, Grimes JM, Choulier L, Mardon HJ, Stuart DI, Handford PA (2004) Structure of the integrin binding fragment from fibrillin-1 gives new insights into microfibril organization. Structure (Camb) 12:717–729
12. Lethias C, Descollonges Y, Boutillon MM, Garrone R (1996) Flexilin: a new extracellular matrix glycoprotein localized on collagen fibrils. Matrix Biol 15:11–19
13. Lethias C, Elefteriou F, Parsiegla G, Exposito JY, Garrone R (2001) Identification and characterization of a conformational heparin-binding site involving two fibronectin type iii modules of bovine tenascin-X. J Biol Chem 276:16432–16438
14. Lindor NM, Bristow J (2005) Tenascin-X deficiency in autosomal recessive Ehlers–Danlos syndrome. Am J Med Genet A 135(1):75–80
15. Mao JR, Taylor G, Dean WB, Wagner DR, Afzal V, Lotz JC, Rubin EM, Bristow J (2002) Tenascin-X deficiency mimics Ehlers–Danlos syndrome in mice through alteration of collagen deposition. Nat Genet 30:421–425
16. Matsumoto K, Saga Y, Ikemura T, Sakakura T, Chiquet ER (1994) The distribution of tenascin-X is distinct and often reciprocal to that of tenascin-C. J Cell Biol 125:483–493
17. McGettrick AJ, Knott V, Willis A, Handford PA (2000) Molecular effects of calcium binding mutations in Marfan syndrome depend on domain context. Hum Mol Genet 9:1987–1994
18. Minamitani T, Ikuta T, Saito Y, Takebe G, Sato M, Sawa H, Nishimura T, Nakamura F, Takahashi K, Ariga H, Matsumoto K (2004) Modulation of collagen fibrillogenesis by tenascin-X and type VI collagen. Exp Cell Res 298:305–315
19. Morel Y, Bristow J, Gitelman SE, Miller WL (1989) Transcript encoded on the opposite strand of the human steroid 21-hydroxylase/complement component C4 gene locus. Proc Natl Acad Sci USA 86:6582–6586
20. Peeters ACTM, Kucharekova M, Timmermans J, van den Berkmortel FWPJ, Boers GH, Novakova IRO, Egging D, den Heijer M, Schalkwijk J (2004) A clinical and cardiovascular survey of Ehlers–Danlos syndrome patients with complete deficiency of tenascin-X. Neth J Med 62:23–25
21. Reinhardt DP, Mechling DE, Boswell BA, Keene DR, Sakai LY, Bachinger HP (1997) Calcium determines the shape of fibrillin. J Biol Chem 272:7368–7373
22. Schalkwijk J, Zweers MC, Steijlen PM, Dean WB, Taylor G, Van Vlijmen IM, van Haren B, Miller WL, Bristow J (2001) A recessive form of the Ehlers–Danlos syndrome caused by tenascin-X deficiency. N Engl J Med 345:1167–1175
23. Tee MK, Thomson AA, Bristow J, Miller WL (1995) Sequences promoting the transcription of the human XA gene overlapping P450c21A correctly predict the presence of a novel, adrenal-specific, truncated form of tenascin-X. Genomics 28:171–178
24. Whiteman P, Downing AK, Handford PA (1998) NMR analysis of cbEGF domains gives new insights into the structural consequences of a P1148A substitution in fibrillin-1. Protein Eng 11:957–959
25. Whiteman P, Smallridge RS, Knott V, Cordle JJ, Downing AK, Handford PA (2001) A G1127S change in calcium-binding epidermal growth factor-like domain 13 of human fibrillin-1 causes short range conformational effects. J Biol Chem 276:17156–17162
26. Williams BR, Gelman RA, Poppke DC, Piez KA (1978) Collagen fibril formation. Optimal in vitro conditions and preliminary kinetic results. J Biol Chem 253:6578–6585
27. Zweers MC, Bristow J, Steijlen PM, Dean WB, Hamel BC, Otero M, Kucharekova M, Boezeman JB, Schalkwijk J (2003) Haploinsufficiency of TNXB is associated with hypermobility type of Ehlers–Danlos syndrome. Am J Hum Genet 73:214–217
28. Zweers MC, Vlijmen-Willems IM, Van Kuppevelt TH, Mecham RP, Steijlen PM, Bristow J, Schalkwijk J (2004) Deficiency of tenascin-X causes abnormalities in dermal elastic fiber morphology. J Invest Dermatol 122:885–891

CHAPTER 6

IDENTIFICATION OF INTERACTION SITES BETWEEN COLLAGEN TYPE XII AND TENASCIN-X

This chapter under preparation for submission:
Egging DF & Veit G, Zwolanek D, Schalkwijk J, Koch M. Wound healing in tenascin-X deficient mice suggests that tenascin-X is involved in matrix maturation rather than matrix deposition. Under preparation for submission to JBC.

IDENTIFICATION OF INTERACTION SITES BETWEEN COLLAGEN TYPE XII AND TENASCIN-X

[+a]David F. Egging & [+b]Guido Veit, [b]Daniela Zwolanek, *[a]Joost Schalkwijk, [b,c]Manuel Koch

[a]Department of Dermatology, Nijmegen Centre for Molecular Life Sciences, Radboud University Nijmegen Medical Centre, P.O. Box 9101, 6500 HB, Nijmegen, the Netherlands
[b]Center for Biochemistry, Medical faculty, University of Cologne, Cologne, Germany
[c]Department of Dermatology and Center for Molecular Medicine Cologne , Medical faculty, University of Cologne, Cologne, Germany
*corresponding author. E-mail address: j.schalkwijk@derma.umcn.nl. P.O. Box 9101, 6500 HB, Nijmegen, the Netherlands
[+]these authors share first co-authorship

Keywords: tenascin-X, collagen XII, interaction sites, Ehlers-Danlos syndrome

ABSTRACT
Tenascin-X (TNX) is a large extracellular matrix protein expressed in a variety of tissues including skin, joints and blood vessels. Deficiency of TNX causes a recessive form of Ehlers-Danlos syndrome characterized by joint hypermobility, skin fragility and hyperextensible skin. Recently we have demonstrated that TNX binds to collagen type XII, a fibril associated collagen that co-localizes with TNX in a number of tissues. In this report we identify domains in TNX and collagen type XII responsible for this interaction.

INTRODUCTION
TNX is a large 450 kDa extracellular matrix (ECM) glycoprotein composed of EGF like-repeats, fibronectin type III (FNIII) repeats and a C-terminal fibrinogen domain (FbgX). TNX is expressed in several tissues such as skin, muscle and blood vessels [1-4]. Complete deficiency of TNX in humans leads to a recessive form of Ehlers Danlos syndrome and TNX haploinsufficiency is a cause of hypermobility type Ehlers Danlos syndrome. The skin of TNX deficient patients is markedly lax with poor recoil properties and shows easy bruising [5-9]. Recently we have demonstrated an interaction between TNX and collagen type XII [10]. Collagen type XII is a fibril associated collagen composed of two short collagen domains, which are flanked and interrupted by three non-collagenous domains (NC). The NC3 domain is the largest domain containing several von Willebrand factor type A domains (vWA), FNIII repeats and a thrombospondin N-terminal like domain (TSPN). Alternative splicing in the NC3 and NC1 domain results in four different collagen XII isotypes [10]. Collagen type XII is thought to act as a linker between collagen fibrils, although, until recently the mechanism by which this is accomplished was incompletely understood. In a previous report we demonstrated co-localization of collagen type XII and TNX in skin and muscle. Furthermore we showed binding of TNX to collagen type XII. In this report we identify sites in both collagen type XII and TNX responsible for the interaction between these proteins.

MATERIALS AND METHODS

Proteins and antibodies
TNX recombinant proteins were obtained as previously described [11;12] Briefly, sequences encoding for TNX domains were cloned into pMal-c2X (Westburg B.V., Leusden, NL) and pET28(a)+ plasmids (Brunschwig Chemie B.V., Amsterdam, NL). Sequences were verified by dideoxy sequencing with a 3730 DNA analyzer (Applied Biosystems, Nieuwekerk a/d IJssel, NL). The following TNX fragments were obtained from E.coli BL21 cells (Invitrogen, Breda, NL) as maltose binding protein (MBP) fusion proteins: MBP-FNIII27-28, MBP-FNIII28-29, MBP-FNIII29, MBP-FNIII29-30, MBP-FNIII30-31, MBP-FbgX. FNIII27-32 was obtained as 6xHIS tagged recombinant protein (HIS-FNIII27-32 from E.coli TOP10F' cells (Invitrogen, Breda, NL) according to the manufacturer's instructions. A 100 kDa C-terminal recombinant TNX protein,

containing six FNIII repeats (FNIII27-32) and the fibrinogen domain, encoded by a 2.7 kb TNX sequence has previously been described by Tee et al. [13;14]. Antibodies against human TNX were obtained as previously described [11;12].

For cloning of full-length collagen XIIA and B (short isoform) and collagen XII fragments, primers were designed according to GenBank™ accession number NM_007730. RT-PCR on total RNA of mouse E15.5 was performed as previously described by us [15]. The following fragments were amplified separately by RT-PCR with specific primers and ligated into a modified pBK II vector and sequenced: the 3rd vWA (von Willibrand factor A) domain to the 13th FNIII domain (primers: M854, M894, termed N-XIIB), 14th FNIII domain to 4th vWA domain (primers: P143, P144; termed middle fragment), TSPN domain to NC1 domain (primers: P3, P8; termed C-XIIB) (see table 1 for a list of PCR primers). For eukaryotic expression the N-XIIB and C-XIIB fragments alone were ligated into a modified pCEB-Pu vector. To assemble collagen type XIIB the N-XIIB and C-XIIB fragments were ligated together into a modified pCEB-Pu vector and the middle fragment was inserted through the internal restriction sites Bsp EI and Nde I. For the full-length collagen type XIIA the N-XIIB fragment from the 1st vWA domain to the 8th FNIII domain was amplified as described above (primers: P145, P146) and introduced into the collagen XIIB construct by using the internal restriction site Nsi I. The collagen type XII TSPN domain was amplified using the primer pair P3 - P581, the collagen type XII FNIII6-8 domains were amplified with the primer pair M920 - M921, and both were cloned into a modified pET vector for bacterial expression.

The cDNAs of full length Col XIIA and B and the C-XIIB and N-XIIB fragments ligated into the pCEB-Pu vector containing a His_8 tag were used to transfect 293-EBNA cells (Invitrogen) using FuGENE 6 reagent (Roche, Mannheim, DE) according to the manufacturer's instructions. Stable transfected cells were selected with puromycin (1.25 µg/ml). The highest protein-producing clones were expanded. For large-scale protein production the cells were cultivated in serum free DMEM/F12 with Glutamax™ (Gibco, Karlsruhe, DE) supplemented with 250 µM L-ascorbic acid and 450 µM L-ascorbic acid 2-phosphate. For each construct three litres of conditioned media were collected, filtrated and supplemented with 1 mM Pefablock (Merck, Darmstadt, DE), 10% Na_2HPO_4 and 0,2% Tween-20 (Sigma, Munich, DE). The supernatant was applied onto a Ni 6 Fast Flow column (GE Healthcare, Munich, DE). The recombinant protein was eluted by stepwise increasing concentrations of imidazole (5-250 mM) in TBS (20 mM Tris-HCl, 150 mM NaCl, pH 8.0) and dialysed against TBS. Bacterial expression in BL21 cells and purification was performed as described previously [10].

BSA and (Sigma-Aldrich Chemie B.V., Zwijndrecht, NL) MBP (Westburg B.V., Leusden, NL) were used as a negative control. Monoclonal antibodies specific for MBP (Westburg B.V., Leusden, NL) and previously described TNX and collagen type XII antibodies [10-12] were used for detection of TNX and collagen type XII in our solid-phase assays.

Solid phase binding assays

Ninety-six well microtiter plates (Greiner Bio-One B.V., Alphen aan den Rijn, NL) were coated overnight at 4°C with collagen type XII or TNX diluted in PBS. All further incubation steps were performed at 37°C. Wells were washed with PBS containing 0.05% Tween-20 (T-PBS) after each incubation step. After coating wells were saturated with 1% BSA in T-PBS for 2 h.

Binding of TNX domains (soluble phase) to collagen type XII and recombinant collagen type XII fragments (solid phase) was performed essentially as previously described for other ECM components [11]. Briefly wells were incubated with recombinant TNX domains for 1 h. After incubation with 100 kDa TNX wells were incubated with rabbit antibodies against HIS-TNX-FNIII27-32. Incubation with TNX MBP fusion proteins was followed by incubation with a mouse monoclonal antibody against MBP for 1 h. Thereafter, wells were incubated with

biotinylated anti rabbit (Vector Laboratories Inc., Burlingame, CA) or biotinylated anti mouse IgG (vectastain kit, Brunschwig Chemie, Amsterdam, NL) respectively for 1h followed by a 45 min incubation with an avidin-biotin-horse radish peroxidase mixture (vectastain kit, Brunschwig Chemie, Amsterdam, NL). Bound peroxidase was detected with o-phenylenediamine dihydrochlorid (Perbio Science Nederland B.V.**,** Etten-Leur, NL) and the absorbance read at 490 nm. All antibodies and TNX proteins were diluted in T-PBS containing 0.1% BSA. BSA was used as negative control, MBP for baseline correction.

Binding of collagen type XII (soluble phase) to TNX domains (solid phase) was performed essentially as described above. Briefly wells were incubated with collagen type XII and recombinant collagen type XII fragments for 1 h, followed by incubation with a previously described collagen XII antibody (KR33). Detection was performed with HRP linked anti-rabbit antibody (Cell Signalling, Berverly, US) and TMB substrate (Perbio Science Nederland B.V., Etten-Leur, NL). The reaction was stopped with 4 M H_2SO_4, absorbance was read at 450 nm. All antibodies and collagen type XII proteins were diluted in T-PBS containing 0.1% BSA. BSA was used as negative control.

Surface plasmon resonance spectroscopy

Surface plasmon resonance spectroscopy was performed using a BIAcore 2000 (BIAcore AB) system. For measurement of protein-protein interactions full-length collagen type XIIA or collagen type XII fragments were coupled in 25 mM sodium acetate, pH 4.5 with a flow rate of 5 µl/min to a CM5 chip. The chip was previously activated with N-hydroxysuccinimide and 1-ethyl-3-(3-dimethylaminopropyl) carbodi-imide hydrochloride. After coupling the required amount of protein (~ 1000 RU), unbound reactive groups were saturated with 1 M ethanolamine hydrochloride, pH 8.5. Experiments were carried out using serial dilutions (1000 nM, 500 nM, 250 nM, 125 nM, 62.5 nM and 31.25 nM) of the different TNX fragments diluted in running

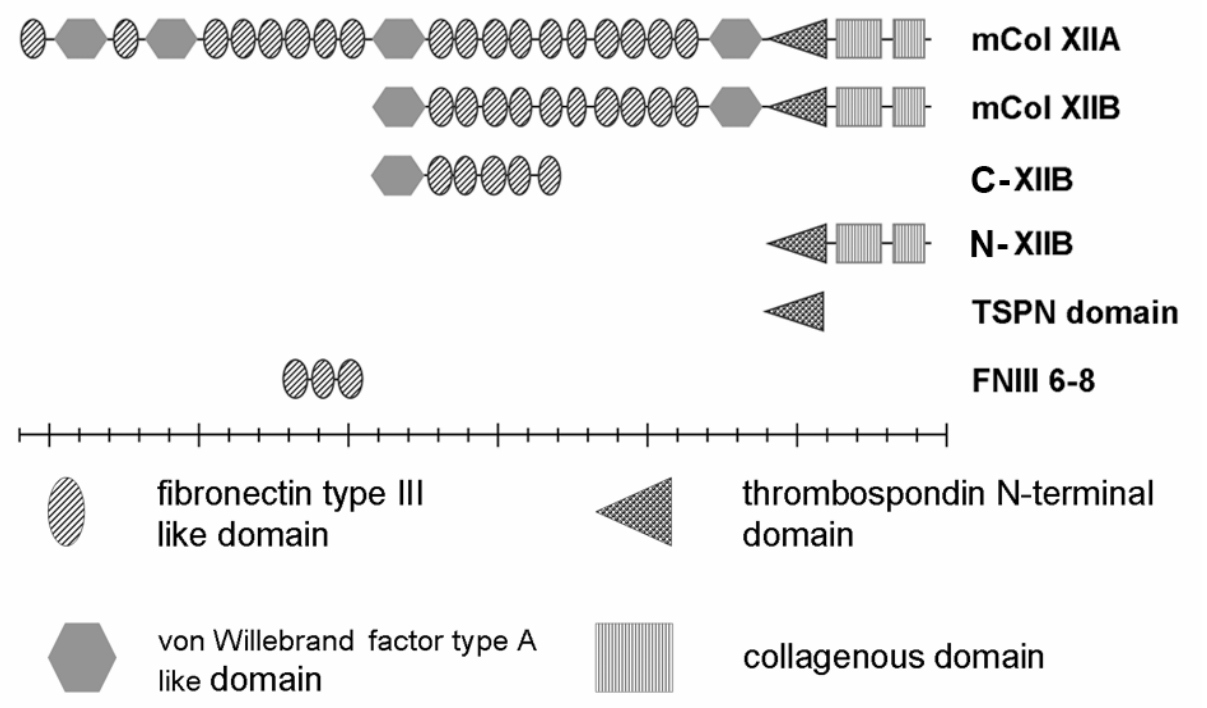

Figure 1: Schematic overview of collagen XII and recombinant collagen XII fragments.
Murine collagen XIIA (mCol XIIA), the short isoform of collagen type XII (mCol XIIB), recombinant collagen type XII fragments; C-XIIB, N-XIIB, thrombospondin N-terminal domain (TSPN) and FNIII6-8 are displayed schematically.

Table 1: List of PCR primers for collagen type XII constructs.

name	fw/rev	sequence
M854	fw	caagctagcgaagggatggattgtctcaccagag
M894	rev	caagcggccgcttaaccttctgtatagaccggaacc
M920	fw	aatgctagccttgaagaacgtggctcacc
M921	rev	tttggatccttaagaagatagaaatggtgtcac
P3	fw	aaagctagccaggatggctacacatcaccagg
P8	rev	ttgggatccttagccggaacctggatagccttgc
P143	fw	aaagctagcgcatatgacacaacccggc
P144	rev	caagcggccgcttaagatccggattccaaagagac
P145	fw	caagctagcgaagacccaccttccgacttg
P146	rev	ttgctcgagttacacatgcatagtggtggggcc
P581	rev	ttgggatccttagtctctactggtccacac

fw: forward primer; rev: reverse primer

buffer (20 mM hepes; 150 mM NaCl; 2 mM CaCl2; 0.005% Tween-20). The analyte was passed over the sensor chip with a constant flow rate of 30 µl/min for 120 sec, dissociation was measured over 300 sec. Fittings of the data, overlay plots and calculation of Kd values were perfomed with BIAevaluation software 3.2 estimating a 1:1 model.

SDS-PAGE analysis

Proteins were loaded onto 12% BIS-TRIS gels (Invitrogen, Breda, NL). Gel electrophoresis was carried out using the NuPAGE system according to the manufacturer's instructions (Invitrogen, Breda, NL). To analyze protein purity gels were stained using coomassie brilliant blue R250 (Brunschwig Chemie, Amsterdam, NL).

RESULTS

Binding of C-terminal 100 kDa TNX to collagen type XII

We previously showed interaction of the NC3 domain of collagen type XII to TNX [10]. As a first approach to identify the domain(s) in TNX responsible for binding to collagen XII we performed solid phase assays to test binding of a recombinant C-terminal 100 kDa TNX fragment [13;14] (soluble phase) to collagen type XII, recombinant collagen type XII fragments and BSA (immobilized substrates). The collagen type XII proteins are shown schematically in figure 1. The TNX proteins used in this study have been previously described [11-14]. Figure 2 shows that C-terminal 100 kDa TNX binds dose dependently to collagen XIIA, the short isoform of collagen type XII (XIIB) and the C-XIIB fragment. Binding to BSA, which served as a negative control, the N-XIIB fragment and FNIII6-8 of collagen type XII was absent.

Identification of the domain in TNX that interacts with collagen type XII

To identify the sequences in TNX responsible for binding to collagen XII we subcloned and expressed a number of fragments from the C-terminal 100 kDa TNX protein as previously described [11;12]. All TNX recombinant proteins containing the FNIII29 repeat showed

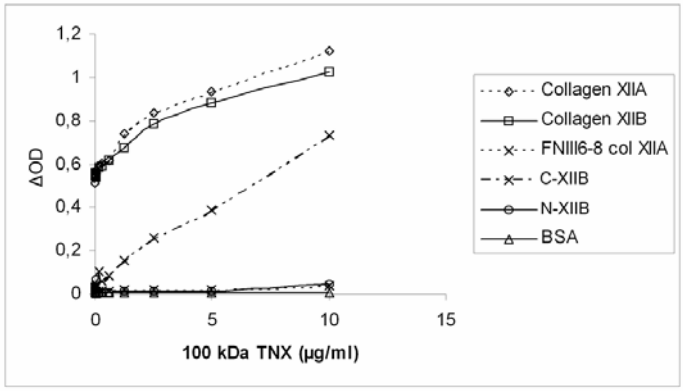

Figure 2: Binding of recombinant C-terminal 100 kDa TNX to full length -and fragments of collagen type XII. TNX binds dose dependently to full length (XIIA) -and the short isoform (XIIB) of collagen type XII. Binding to the C-XIIB fragment is observed, although saturation is not reached. Binding to BSA (solid phase), which served as a negative control, was absent. Proteins in the solid phase are marked in the legend.

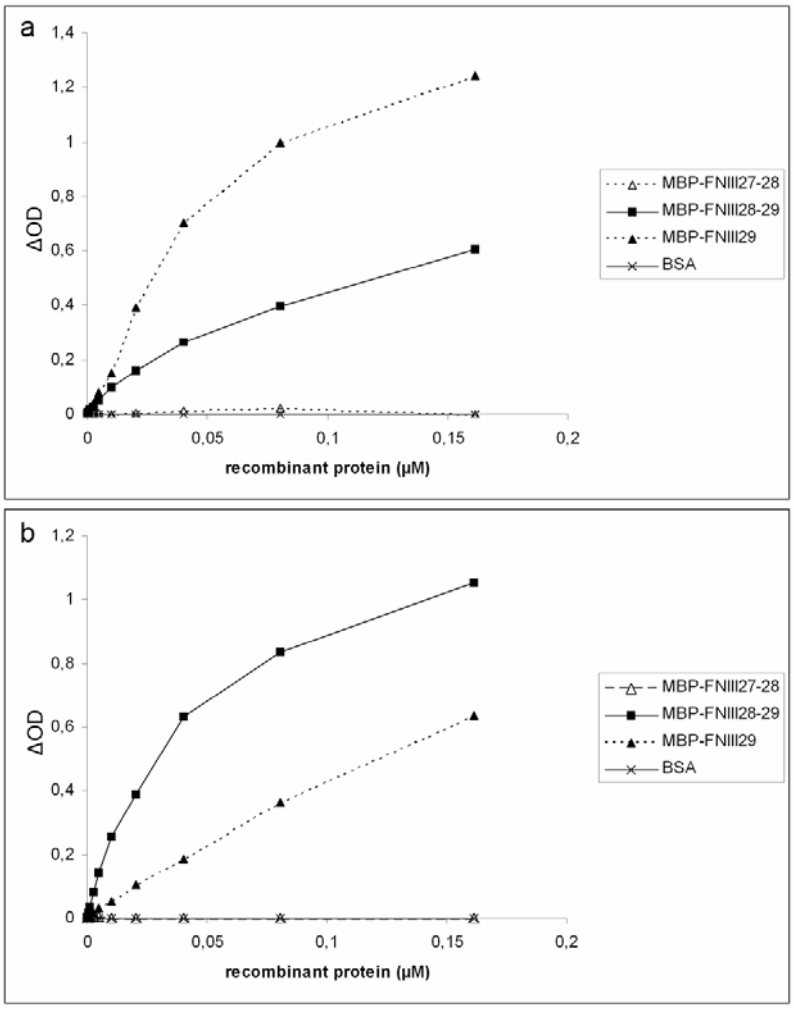

Figure 3: Binding of recombinant proteins containing TNX FNIII29 to collagen type XII.
(a) Recombinant TNX proteins containing FNIII 29 bind dose dependently to full length collagen type XII. Data for MBPFNIII29-30, FNIII30-31 and MBP-FbgX are not shown for reasons of clarity. No binding is observed for TNX recombinant proteins that lack FNIII29 for BSA. Proteins in the soluble phase are marked in the legend. (b) Recombinant TNX proteins containing FNIII 29 bind dose dependently to the C-XIIB fragment, a C-terminal fragment of collagen type XII. Data for MBPFNIII29-30, FNIII30-31 and MBP-FbgX are not shown for reasons of clarity. No binding is observed for TNX recombinant proteins that lack FNIII29 and for BSA. Proteins in the soluble phase are marked in the legend.

dose dependent binding to collagen type XII (fig. 3a, shown for collagen type XIIA) and C-XIIB fragment (fig. 3b). No binding was observed for repeats FNIII27-28, FNIII30-31, the FbgX domain as was also the case for BSA. For reasons of clarity only the data for MBP- FNIII27-28, FNIII28-29 and FNIII29 of TNX and BSA are shown. To verify the results, interaction of collagen type XIIA and XIIB (soluble phase) to HIS-FNIII27-32 (solid phase) and MBP-FNIII29 (solid phase) was investigated. Binding of collagen type XIIA and XIIB to these recombinant TNX fragments was found (data not shown), confirming the previous results.

To validate the results, surface plasmon resonance spectroscopy was performed and the associations and dissociations of the obtained binding curves were analyzed in a Langmuir 1:1 binding model (fig. 4). The apparent Kd values for MBP-FNIII29 as soluble partner were 8.3 x 10^{-9} M for collagen type XIIA and 1.3 x 10^{-8} M for C-XIIB fragment. These are comparable to the Kd values for HIS-FNIII27-32 as soluble partner; 6.5 x 10^{-9} M for collagen type XIIA and 8.8 x 10^{-9} M for C-XIIB fragment. The Kd value for C-terminal 100 kDa TNX as soluble partner for collagen type XIIA is 4.8 x 10^{-9} M (data not shown). MBP-FNIII27-28 and MBP (not shown) were used as negative controls and no binding to collagen type XII or the C-XIIB fragment was observed in either case. Furthermore, no binding of TNX recombinant proteins to N-XIIB was found (data not shown).

Identification of the domain in collagen type XII that interacts with FNIII repeat 29 of TNX

We previously showed interaction of the NC3 domain of collagen type XII to TNX [10]. We showed binding of the C-XIIB fragment, consisting of TSPN, NC1, NC2 and collageneous domains, to FNIII29 of TNX.

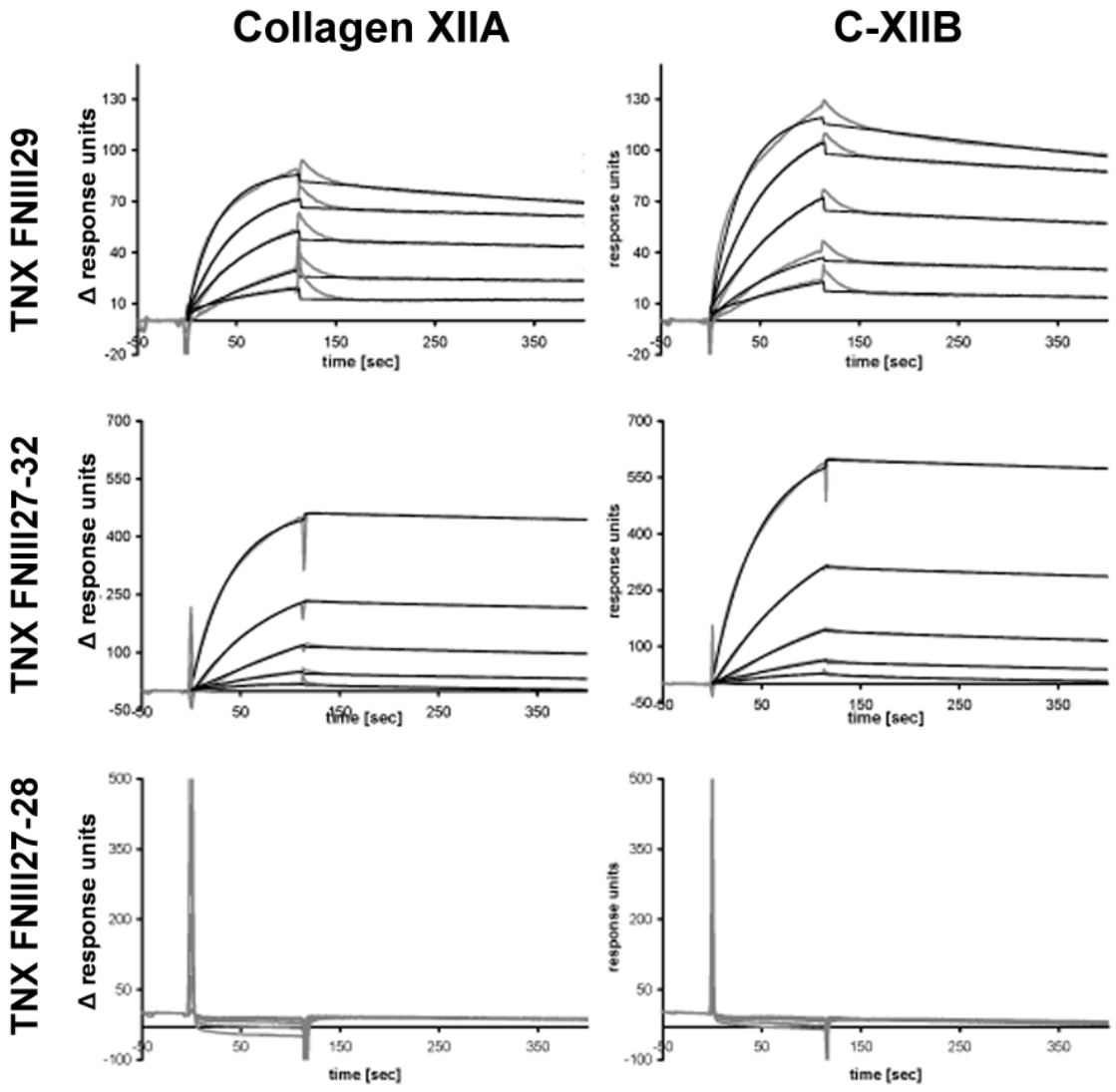

Figure 4: Surface plasmon resonance spectroscopy confirms binding of FNIII 29 to collagen type XII. MBP-FNIII29 and HIS-FNIII27-32 bind to collagen type XIIA and the C-XIIB fragment. MBP-FNIII27-28 and MBP (not shown) were used as negative controls and no binding to collagen type XII or the C-XIIB fragment was observed in either case. TNX recombinant proteins were used as soluble analytes and the amount of interacting analyte (1000, 500, 250, 125, 62.5 nM) was monitored by measuring the variation of the plasmon resonance angle as a function of time and expressed in terms of response units. The background signal has been subtracted from each curve; the curves are shown in ascending order depending on the analyte concentration used. Fitting and overlay plots were performed with BIAevaluation software version 3.2. The continuous black lines represent the fitted curves.

The TSPN domain is part of the NC3 domain, suggesting this domain is responsible for the binding to FNIII29 of TNX. The TSPN of collagen type XII was expressed as recombinant protein and binding to FNIII29 was investigated using surface plasmon resonance spectroscopy. The TSPN domain alone was able to bind to the FNIII29 repeat of TNX as shown in figure 5. The Kd value for the TSPN domain is 6.3 x 10^{-9} M for HIS-FNIII27-32 as soluble partner and 8.5 x 10^{-9} M for MBP-FNIII29 as soluble partner. Furthermore, collagenase treatment of collagen type XIIA/B did not result in a decrease of binding to FNIII29 of TNX (data not shown) as had also been previously shown for full length TNX [10].

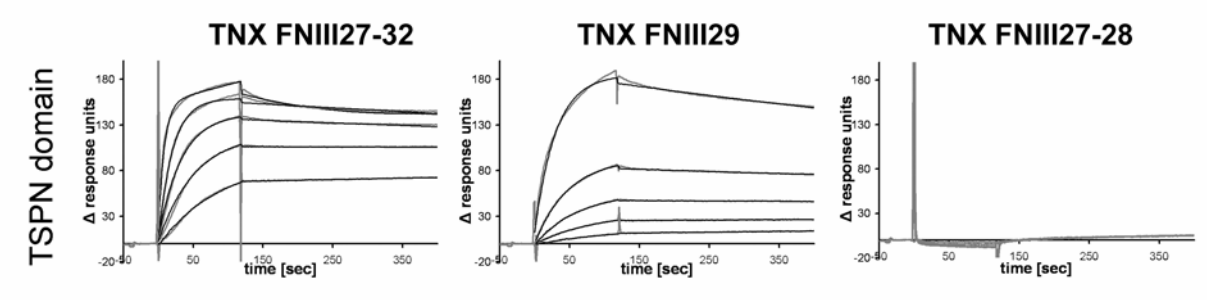

Figure 5: Binding of the TSPN domain of collagen type XII to FNIII29 of TNX.
Binding of the TSPN domain of collagen type XII to MBP-FNIII29 and HIS-FNIII27-32 of TNX is shown by surface plasmon resonance spectroscopy. MBP-FNIII27-28 was used as negative control and no binding to the TSPN domain of collagen type XII was detected. TNX recombinant proteins were used as soluble analytes and the amount of interacting analyte (1000, 500, 250, 125, 62.5 nM) was monitored by measuring the variation of the plasmon resonance angle as a function of time and expressed in terms of response units. The background signal has been subtracted from each curve; the curves are shown in ascending order depending on the analyte concentration used. Fitting and overlay plots were performed with BIAevaluation software version 3.2. The continuous black lines represent the fitted curves.

DISCUSSION

We identified domains in TNX and collagen type XII which are responsible for the interaction between these two proteins. In a previous study we linked the interaction for collagen type XII with TNX to the large NC3 domain of collagen type XII with the use of collagenase treated collagen type XII [10]. The NC3 domain contains, amongst vWA domains and FNIII repeats, a TSPN domain. In this study we demonstrated that the TSPN domain of collagen type XII is able to bind to the FNIII29 of TNX. We previously identified binding of elastin and collagen types I, III and V to FNIII29 of TNX [11]. Although collagen type V harbors a TSPN domain, collagen type I, III and elastin lack such a domain. This suggest that there could be multiple interaction sites in FNIII29 of TNX or that FNIII29 has more general binding properties allowing it to interact with a number of amino acid moieties or structural conformations. Further investigation into the domain structure of FNIII29 of TNX including generation of mutant FNIII29 recombinant proteins could provide answers to these questions.

The existence of multiple collagen type XII – TNX interaction sites cannot be excluded by this study. However, the discovery of an interaction between the TSPN domain of collagen type XII and FNIII29 of TNX provides novel biochemical evidence for collagen type XII and TNX as interaction partners through the binding sites in these two domains. Further investigations into the role of TNX and collagen type XII in extracellular matrix stability will increase our knowledge of connective tissue biology. Currently the genetic causes for the Ehlers-Danlos syndrome are known in approximately 50% of the cases. Our data could act as a starting point for the identification of novel genetic cause for the Ehlers-Danlos syndrome. Collagen type XII, considering the interaction with TNX, is a likely candidate gene for this disease.

REFERENCES

[1] Bristow,J., Tee,M.K., Gitelman,S.E., Mellon,S.H., & Miller,W.L. (1993) Tenascin-X: a novel extracellular matrix protein encoded by the human XB gene overlapping P450c21B. *J. Cell Biol.* **122,** 265-278.

[2] Lethias,C., Descollonges,Y., Boutillon,M.M., & Garrone,R. (1996) Flexilin: a new extracellular matrix glycoprotein localized on collagen fibrils. *Matrix Biol.* **15,** 11-19.

[3] Elefteriou,F., Exposito,J.Y., Garrone,R., & Lethias,C. (1997) Characterization of the bovine tenascin-X. *J. Biol. Chem.* **272,** 22866-22874.

[4] Ikuta,T., Sogawa,N., Ariga,H., Ikemura,T., & Matsumoto,K. (1998) Structural analysis of mouse tenascin-X: evolutionary aspects of reduplication of FNIII repeats in the tenascin gene family. *Gene* **217,** 1-13.

[5] Burch,G.H., Gong,Y., Liu,W., Dettman,R.W., Curry,C.J., Smith,L., Miller,W.L., & Bristow,J. (1997) Tenascin-X deficiency is associated with Ehlers-Danlos syndrome [see comments]. *Nat. Genet.* **17,** 104-108.

[6] Schalkwijk,J., Zweers,M.C., Steijlen,P.M., Dean,W.B., Taylor,G., Van Vlijmen,I.M., van Haren,B., Miller,W.L., & Bristow,J. (2001) A recessive form of the Ehlers-Danlos syndrome caused by tenascin-X deficiency. *N. Engl. J. Med.* **345,** 1167-1175.

[7] Zweers,M.C., Bristow,J., Steijlen,P.M., Dean,W.B., Hamel,B.C., Otero,M., Kucharekova,M., Boezeman,J.B., & Schalkwijk,J. (2003) Haploinsufficiency of TNXB is associated with hypermobility type of Ehlers-Danlos syndrome. *Am. J. Hum. Genet.* **73,** 214-217.

[8] Peeters,A.C.T.M., Kucharekova,M., Timmermans,J., van den Berkmortel,F.W.P.J., Boers,G.H., Novakova,I.R.O., Egging,D., den Heijer,M., & Schalkwijk,J. (2004) A clinical and cardiovascular survey of Ehlers-Danlos syndrome patients with complete deficiency of tenascin-X. *Neth. J. Med.* **62,** 23-25.

[9] Lindor,N.M. & Bristow,J. (2005) Tenascin-X deficiency in autosomal recessive Ehlers-Danlos syndrome. *Am. J. Med. Genet. A* **135,** 75-80.

[10] Veit,G., Hansen,U., Keene,D.R., Bruckner,P., Chiquet-Ehrismann,R., Chiquet,M., & Koch,M. (2006) Collagen XII Interacts with Avian Tenascin-X through Its NC3 Domain. *J. Biol. Chem.* **281,** 27461-27470.

[11] Egging,D., van den,B.F., Taylor,G., Bristow,J., & Schalkwijk,J. (2006) Interactions of human tenascin-X domains with dermal extracellular matrix molecules. *Arch. Dermatol. Res.* **298,** 389-396.

[12] Egging,D.F., Peeters,A.C., Grebenchtchikov,N., Geurts-Moespot,A., Sweep,C.G., den,H.M., & Schalkwijk,J. (2007) Identification and characterization of multiple species of tenascin-X in human serum. *FEBS J.* **274,** 1280-1289.

[13] Morel,Y., Bristow,J., Gitelman,S.E., & Miller,W.L. (1989) Transcript encoded on the opposite strand of the human steroid 21-hydroxylase/complement component C4 gene locus. *Proc. Natl. Acad. Sci. U. S. A* **86,** 6582-6586.

[14] Tee,M.K., Thomson,A.A., Bristow,J., & Miller,W.L. (1995) Sequences promoting the transcription of the human XA gene overlapping P450c21A correctly predict the presence of a novel, adrenal-specific, truncated form of tenascin-X. *Genomics* **28,** 171-178.

[15] Koch,M., Olson,P.F., Albus,A., Jin,W., Hunter,D.D., Brunken,W.J., Burgeson,R.E., & Champliaud,M.F. (1999) Characterization and expression of the laminin gamma3 chain: a novel, non-basement membrane-associated, laminin chain. *J. Cell Biol.* **145,** 605-618.

CHAPTER 7

Identification and characterization of multiple species of tenascin-X in human serum

This chapter has been previously published:
Egging DF, Peeters AC, Grebenchtchikov N, Geurts-Moespot A, Sweep CG, den Heijer M, Schalkwijk J. Identification and characterization of multiple species of tenascin-X in human serum. FEBS J. 2007 Mar;274(5):1280-9. Reprinted with permission.

the FEBS Journal

Identification and characterization of multiple species of tenascin-X in human serum

D. F. Egging[1], A. C. T. M. Peeters[2], N. Grebenchtchikov[3], A. Geurts-Moespot[3], C. G. J. Sweep[3], M. den Heijer[2] and J. Schalkwijk[1]

1 Department of Dermatology, Nijmegen Centre for Molecular Life Sciences, Radboud University Nijmegen Medical Centre, the Netherlands
2 Department of Endocrinology, Radboud University Nijmegen Medical Centre, the Netherlands
3 Department of Chemical Endocrinology, Radboud University Nijmegen Medical Centre, the Netherlands

Keywords
collagen; Ehlers–Danlos syndrome; elastin; serum; tenascin-X

Correspondence
J. Schalkwijk, Department of Dermatology, Nijmegen Centre for Molecular Life Sciences, Radboud University Nijmegen Medical Centre, PO Box 9101, 6500 HB, Nijmegen, the Netherlands
Fax: +31 24 354 1184
Tel: +31 24 3613 272
E-mail: j.schalkwijk@derma.umcn.nl

(Received 23 November 2006, revised 21 December 2006, accepted 29 December 2006)

doi:10.1111/j.1742-4658.2007.05671.x

We analysed the diversity of tenascin-X (TNX) species in serum and studied parameters that could affect determination of TNX levels in serum. Using western blot analysis we identified at least seven distinct TNX species, ranging from 75 kDa to the presumably full-length 450 kDa form. Purification of serum TNX followed by sequence analysis positively identified two major TNX species of 75 and 140 kDa. We found that serum TNX binds to tropoelastin but not to fibrillar collagens. We conclude that serum TNX is composed of distinct molecular species that retain functional activity.

Tenascin-X (TNX) is a large 450 kDa extracellular matrix (ECM) glycoprotein composed of epidermal growth factor (EGF)-like repeats, fibronectin type III (FNIII) repeats and a C-terminal fibrinogen domain (FbgX) [1–4]. A 140 kDa fragment of TNX has been identified in human serum [5]. TNX abnormalities are associated with several pathological conditions [5–9]. Complete TNX deficiency in humans leads to a recessive form of Ehlers–Danlos syndrome (EDS) and TNX haploinsufficiency is associated with hypermobility type EDS [5–7]. The skin of TNX-deficient patients reveals abnormal elastic fibres and reduced collagen density [5,8]. TNX-deficient patients show easy bruising and some exhibit cardiovascular abnormalities, such as mitral valve insufficiency. There are, however, no indications for generalized cardiovascular abnormalities [5,10,11].

The level of TNX in serum likely reflects the level of synthesis and or breakdown at the tissue level because individuals heterozygous for TNX have greatly decreased levels of serum TNX (~ 50–60% of the mean level seen in control subjects) [5,7]. Abdominal aortic aneurysm is associated with high serum levels of TNX, whereas TNX in abdominal aortic aneurysm tissue appears reduced [9]. Matsumoto *et al.* [12] recently identified a 200 kDa mouse serum TNX species probably generated by proteolytic cleavage. The biochemical properties of human serum TNX have not been investigated in detail to date. In this study, we identified multiple TNX species and found that serum TNX

Abbreviations
ECM, extracellular matrix; EDS, Ehlers–Danlos syndrome; EGF, epidermal growth factor; FNIII, fibronectin type III; HIS, poly(histidine); MBP, maltose-binding protein; TNX, tenascin-X.

retains biological activity as it is able to bind to tropoelastin.

Results

Multiple TNX species in human serum

We have previously shown that polyclonal antibodies raised against a C-terminal 100-kDa fragment of TNX recognize a fragment of TNX in serum of ~140 kDa [5]. As a first approach to characterize serum TNX we generated antibodies against nonoverlapping FNIII repeats starting at the N-terminus of the C-terminal 100-kDa portion of TNX, as shown in Fig. 1A. Using our new set of antisera, we found several different TNX species in human serum (Fig. 1B). The combined lanes 1 and 3 of Fig. 1B reveal at least seven distinct TNX species recognized by the respective antisera. Serum from TNX-deficient patients, which is a convenient control, is negative, indicating the specificity of the antisera. Little or no cross-reaction between antibodies specific for FNIII27–28 and FNIII29–30 antigen and FNIII29–30 with FNIII27–28 antigen could be detected (Fig. 1C). The molecular masses of these seven species vary between 75 kDa and a high molecular mass form, which by extrapolation may be identical to the full-length 450 kDa tissue form. A polyclonal antibody raised against FNIII29–30 recognizes a TNX species migrating at ~75 kDa, which is not recognized by a polyclonal antibody raised against FNIII27–28 of TNX. This suggests that the N-terminus of the 75 kDa

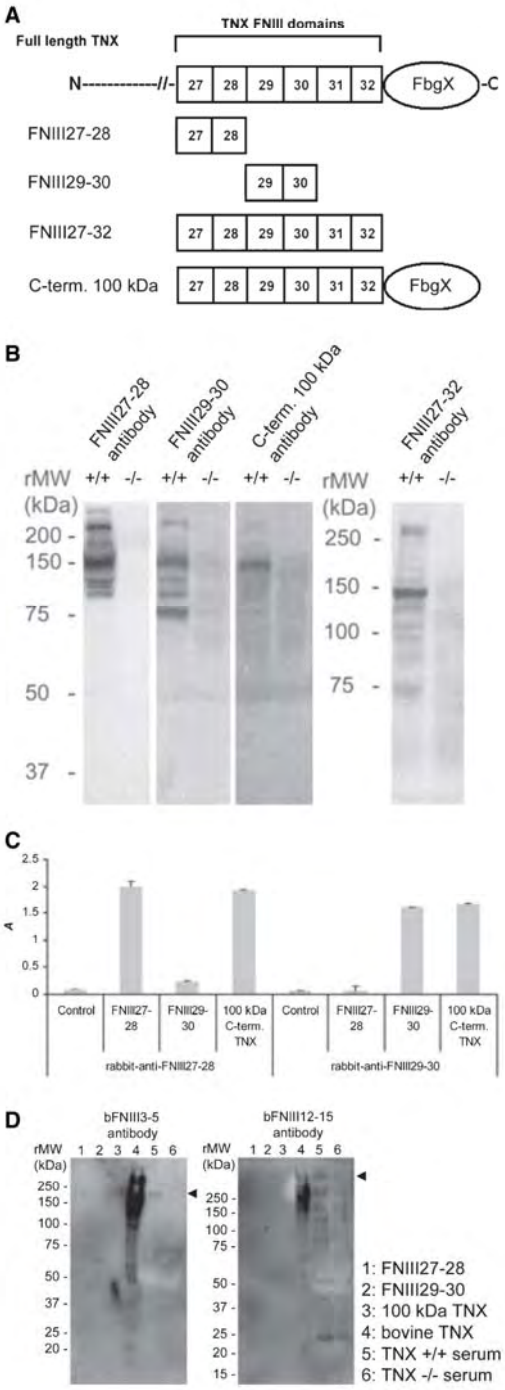

Fig. 1. Identification and characterization of TNX species in serum. (A) The antigens to which the TNX antibodies have been generated are shown schematically. (B) Several species of TNX can be identified by the different antibodies in normal human serum (lanes+/+), serum from TNX-deficient patients is used as a negative control (lanes −/−). Not all bands show equal signal strength if antibodies against FNIII27–28, 29–30 and 27–32 are compared, however, with antibodies against FNIII29–30 and 27–32 a band migrating at ~75 kDa can be distinguished. This 75 kDa band is not recognized by the FNIII27–28 antibody. The background of the antibody against C-terminal 100 kDa TNX is relatively high, making analysis difficult. (C) We investigated the cross-reactivity of FNIII27–28 and FNIII29–30 antibodies against FNIII27–28, FNIII29–30 and 100 kDa C-terminal TNX. Both antibodies showed little to no significant cross-reactivity to each other's antigens, however, they both recognized 100 kDa C-terminal TNX as strongly as their own antigens. (D) A mAb directed against FNIII3-5 of bovine TNX detected an N-terminal-located TNX species in normal human serum, of ~200 kDa (lane 5 of the first blot, indicated by an arrowhead). This species was absent in serum from a TNX-deficient patient (lane 6). This N-terminal TNX species was not recognized by a mAb directed against FNIII12–15 of bovine TNX. The FNIII12-15 antibody detected a high molecular TNX species (lane 5 of right blot, indicated by an arrowhead), which by extrapolation could be full-length 450 kDa TNX. Other bands are difficult to interpret due to similar bands in serum from TNX-deficient patients (lane 5–6 of the right blot). mAbs against bovine TNX do not cross-react with C-terminal human FNIII TNX repeats (lanes 1–3). Bovine TNX was used as a positive control, some degradation products can be observed (lane 4).

TNX fragment is located somewhere in the C-terminus of FNIII repeat 28 or in the N-terminus of repeat 29. The 75 kDa species is also recognized, although with less affinity, by a polyclonal antibody raised against FNIII27–32. Other (> 75 kDa) TNX species in serum are also recognized by these antibodies (Fig. 1B). The polyclonal antibody raised against 100 kDa TNX suffers from a high background signal, making it difficult to distinguish TNX species other than the 140 kDa species that we have described previously. In our previous study the 140 kDa form migrated just below a 148 kDa marker band. Here we find, depending on the gel type used, a molecular mass of ~150 kDa (Fig. 1B, lanes 1, 3 and 5) or slightly under 150 kDa (Fig. 1B, lane 7). We refer to this species as the 140–150 kDa serum form. An N-terminal-located TNX serum species of ~200 kDa was detected using an antibody directed against FNIII3–5 of bovine TNX (Fig. 1D). This N-terminal TNX species was not recognized by an antibody directed against FNIII12–15 of bovine TNX (Fig. 1D). A high molecular mass species was detected by the FNIII12–15 antibody, other bands are difficult to interpret due to similar bands in serum from TNX-deficient patients. C-Terminal FNIII repeats 27–32 were not recognized by either antibody. Bovine TNX was used as a positive control, and some degradation products could be observed.

The number of TNX species appeared to be the same in 30 healthy individuals that we examined. Because TNX may play a role in abdominal aortic aneurysms, we examined serum TNX species in 20 patients; in one abdominal aortic aneurysm patient we found a TNX species of a different molecular mass, as shown in Fig. 2.

The 75 kDa serum TNX species has the approximate molecular mass of the 74-kDa C-terminal adrenal-specific truncated TNX protein (XB-S) [13]. We investigated serum from two patients with a bilateral adrenalectomy and found that the 75 kDa band for TNX was present on western blot (data not shown). This indicates that the 75 kDa species found in blood is not the XB-S form derived from the adrenal glands.

Amino acid sequences of TNX species in human serum

Having identified at least seven distinct TNX species, we subsequently tried to isolate serum TNX for further characterization. Serum TNX was purified by affinity chromatography and blotted onto a poly(vinylidene difluoride) membrane. Only two TNX species were sufficiently abundant to be distinguished using Coomassie Brilliant Blue staining, migrating at ~140–150 and

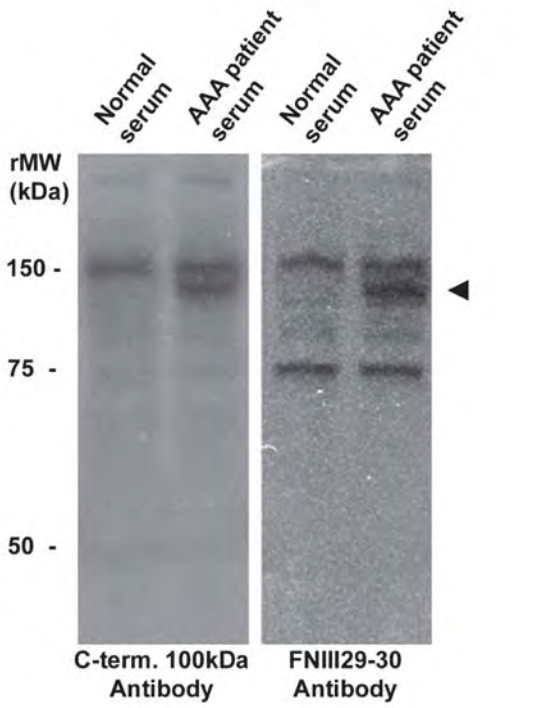

Fig. 2. Alternative TNX species in one abdominal aortic aneurysm patient. The number of TNX species appears to be the same in most individuals (examined in 30 healthy individuals). One abdominal aorta aneurysm patient of a group of 20 showed a TNX species of a different molecular mass as indicated by the arrow.

75 kDa (Fig. 3). Sequence coverage by MS/MS of the 75 kDa TNX species revealed peptide sequences that align with the C-terminal part of TNX (accession number NM_019105; Fig. 4A). The exact N-terminus could not be determined by N-terminal sequencing (Edman type), however, the covered amino acid sequence by MS/MS suggested a molecular mass of at least 70 kDa (without glycosylation), which is in line with the estimated molecular mass on SDS/PAGE. Sequence coverage by MS/MS of the 140–150 kDa TNX species revealed peptide sequences that align mostly with the C-terminal part of TNX. Because of the high degree of similarity between FNIII repeats, three peptide sequences can be aligned on multiple positions in the TNX sequence (Fig. 4B). Furthermore, the exact N-terminus could not be determined by N-terminal sequencing (Edman type), making it difficult to assess the exact molecular mass.

Factors influencing serum TNX levels

Serum TNX levels, as determined by ELISA, have been used as a surrogate marker to correlate tissue

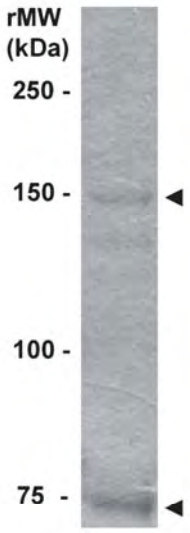

Fig. 3. Isolation of TNX from serum. The predominant species in TNX appear to be 140–150 and 75 kDa (indicated by arrows) after isolation from human serum using a HIS–FNIII27–32-coupled affinity column, as shown by Coomassie Brilliant Blue staining.

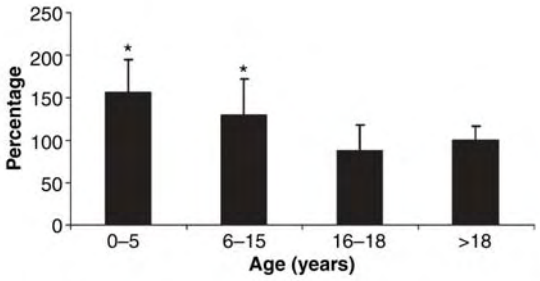

Fig. 5. TNX levels measured in serum from children compared with adults. TNX levels of children were calculated as percentages compared with adults. The mean TNX concentration in serum from children aged < 16 years is lower than that of adults ($*P < 0.05$, Duncan's *post hoc* test, $N = 18$ for 1–5 years, $N = 20$ for 5–16 years, $N = 8$ for 16–18 years and $N = 10$ for > 18 years of age).

TNX expression to pathology in several diseases. In the previous section, we showed that serum TNX is more heterogeneous than previously anticipated. As a next step, we investigated several parameters that may affect the apparent concentration of TNX in serum, such as age, gender, circadian cycle, fasting/nonfasting and the use of plasma versus serum. None of these factors, with the exception of age, was found to have a significant effect on TNX levels determined by ELISA (data not shown). Figure 5 shows a moderate but significant effect of age on mean serum TNX levels, with adults having significantly lower TNX levels than children. We used an ANOVA followed by posthoc testing, analysed using our previously described sandwich ELISA [5], similar results were obtained by an ELISA using chicken anti-(TNX FNIII29–30) and rabbit anti-(TNX FNIII29-30) (data not shown).

Another factor, when performing population-based studies on serum samples is the stability of the analyte. Although freeze–thaw cycles appear to have little effect on TNX concentration, prolonged storage at −20 °C results in an apparent decrease in TNX levels as determined by ELISA. TNX concentrations appear to be stable when stored at −80 °C. We analysed a number of samples from serum stored over longer periods and fresh serum and found no evidence of the appearance of additional bands after storage (data not shown).

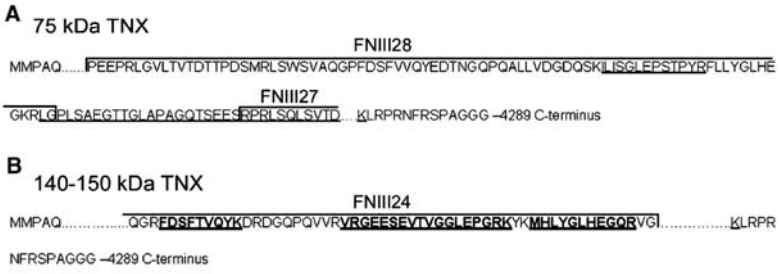

Fig. 4. Amino acid sequence coverage of the 75 and 140–150 kDa species. Amino acid sequences found after trypsinization and analysis by MS/MS are underlined. Peptides found by MS/MS for the 75 kDa TNX species cover 42% of the amino acid sequence between the most N-terminal peptide (amino acid 3654) and C-terminal peptide (amino acid 4276) and 64% for the 140–150 kDa TNX species (between amino acid 3238 and 4276) (not shown). (A) The covered peptide amino acid sequences by MS/MS suggest a molecular mass (MW) of at least 70 kDa (without glycosylation) for the 75 kDa species. The most N-terminal peptide amino acid sequence is located near the C-terminus of FNIII28 starting at amino acid 3654. The amino acid sequences for FNIII28 and FNIII29 are designated by horizontal brackets. (B) Sequence coverage by MS/MS of the 140–150 kDa TNX species revealed peptide amino acid sequences which align mostly with the C-terminal part of TNX. Because of the homology between FNIII repeats three peptide sequences can be aligned on multiple positions in the TNX sequence, the most C-terminal occurrences are marked in bold (the amino acid sequence for FNIII24 is designated by horizontal brackets).

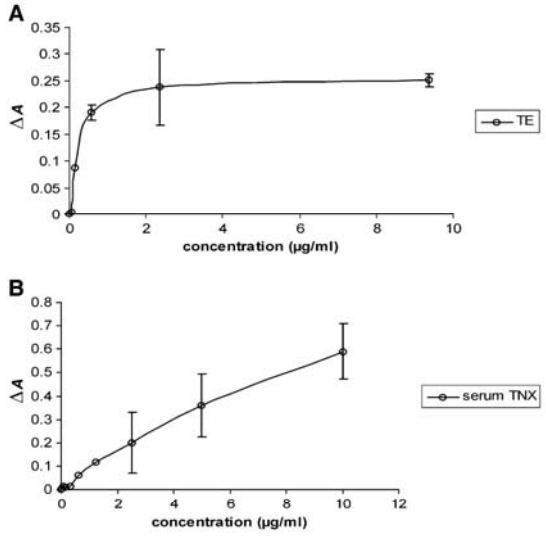

Fig. 6. Binding of TNX to tropoelastin. (A) Tropoelastin (soluble phase) binds dose dependently to TNX isolated from serum (solid phase). (B) TNX (soluble phase) isolated from serum binds to tropoelastin (solid phase), although saturation was not reached in the concentration range analysed. We failed to detect binding of serum TNX to collagen types I, III and V, fibronectin, laminin and nonsense protein (BSA) (data not shown).

Functional properties of serum TNX

TNX deficiency causes connective tissue disease, and it is speculated that TNX regulates the assembly or stability of the ECM. Previous studies have shown that TNX can bind to various ECM molecules [14–21]. We investigated if human serum TNX could interact with components of elastic fibres, fibrillar collagens or matrix glycoproteins. To identify extracellular ligands of TNX, we performed solid-phase assays to test the binding of TNX purified from serum (soluble phase) to ECM molecules (immobilized substrates). Figure 6A shows that bovine tropoelastin (soluble phase) binds dose dependently to serum TNX (solid phase); Fig. 6B shows binding of serum TNX as soluble binding partner to TE (solid phase). We did not detect any significant binding to human collagen type I, III and V; binding to human fibronectin, laminin or irrelevant protein (BSA) was also absent (data not shown). Similarly, we did not find any effect of serum TNX on collagen fibrillogenesis, using an *in vitro* assay based on turbidimetry [18] (data not shown).

Discussion

We previously identified a 140–150 kDa species of TNX in human serum and used serum TNX levels to assess the relationship between TNX expression and disease [5,7,9,11]. Serum TNX measurement was used to detect heterozygosity for TNX null alleles and we found that high levels of serum TNX are a risk factor for abdominal aortic aneurysm [5,9]. Here we demonstrate that multiple species of TNX exist in serum, using newly developed antibodies against FNIII27–28 and 29–30 of TNX. A polyclonal antibody against the complete C-terminal 100 kDa portion of TNX showed only one clear band at ~140–150 kDa in our previous study [5], although repeats FNIII27–28 and 29–30 are also present in 100 kDa TNX. Several factors can explain this apparent discrepancy; the background signal is quite high in the polyclonal serum against C-terminal 100 kDa TNX, making most bands indistinguishable. Furthermore, the serum samples in our previous study were enriched for high molecular mass proteins by ammonium sulfate precipitation, which may have distorted the result. In this study we analysed full serum and were able to vaguely distinguish a 75 kDa TNX species using the polyclonal antiserum against C-terminal 100 kDa TNX. The 75 kDa TNX species was clearly distinguishable with the polyclonal antiserum against FNIII29–30 of TNX and the signal for the bands corresponding to the 75 and 140–150 kDa species are approximately of equal strength. Most likely, the FNIII29–30 repeats of TNX are not as immunogenic as other FNIII repeats because our newly developed polyclonal antibody against FNIII27–32 has a higher affinity for the 140–150 kDa species compared with the 75 kDa TNX species.

Sequence coverage by MS/MS of the affinity-purified 140–150 and 75 kDa TNX species suggests they are C-terminal fragments of TNX. The exact N-terminus of both TNX species could not be determined in two separate runs using N-terminal sequencing (Edman type). Both runs were complete blanks, instead of multiple possible sequences as is the case in rugged N-terminal ends, suggesting blocked N-termini. The 75 kDa species is not recognized by a polyclonal antibody against FNIII27–28, but is recognized by a polyclonal antibody against FNIII29–30. This is in line with the sequence obtained using MS/MS, which shows the most N-terminal part of the sequence for the 75 kDa TNX species starting in the C-terminal part of FNIII28. Polyclonal antibodies against both FNIII27–28 and FNIII29–30 recognize the 140–150 kDa species. This is in line with the sequence obtained by MS/MS, which covers all these domains. Most peptide sequences were found covering the last 115 kDa. Because of the large sequence similarity between FNIII repeats, some peptide sequences can be aligned at several different positions within the TNX sequence. Unique peptide

sequences, only aligning once within the TNX sequence, were found in the last C-terminal 115 kDa. These findings suggest that the 140–150 kDa TNX species is a C-terminal fragment of full-length 450 kDa TNX comprising the fibrinogen-like domain. Whether the TNX species in serum are products of proteolytic cleavage or alternative splicing is not clear. It is attractive to speculate that the 75 kDa species found in human serum is the same as the adrenal specific XB-S short isoform [13]. The 75 kDa species however, is found in serum from patients with bilateral adrenalectomy making it unlikely that the 75 kDa species in serum is derived from the adrenal glands. It could be that XB-S is expressed in other tissues which were not examined in the original study by Tee *et al.* [13]. An N-terminal-located TNX serum species of ~200 kDa was detected using an antibody directed against FNIII3–5 of bovine TNX. This N-terminal TNX species was not recognized by an antibody directed against FNIII12–15 of bovine TNX. The antibody against bovine FNIII3–5 did not recognize the high molecular mass species visible in Fig. 1B, which is presumably the full-length 450 kDa species. We speculate that limited affinity of the anti-(bovine TNX) sera for human TNX and the amount of this species in serum could have precluded possible detection.

Because serum TNX may reflect TNX turnover in tissue, it is of interest to examine the diversity of TNX species in healthy individuals and abdominal aortic aneurysm patients. Western blot analysis of 30 healthy individuals showed a fairly similar pattern of TNX species, with the major bands migrating at 75 and 140–150 kDa. In only one patient with aortic aneurysm did we find a distinct pattern of TNX species. We conclude, however, that no consistently distinct pattern of TNX species exists in serum from these patients. We showed that several parameters are important when quantification of TNX serum levels is required, such as donor age and sample storage. These parameters should be taken into consideration when studying correlations of pathological conditions and TNX levels in serum.

Full-length TNX is present in connective tissue in which it presumably regulates the deposition and maintenance of structural ECM molecules such as elastin and fibrillar collagens. Abnormalities of TNX are associated with several pathological conditions in which collagen and elastic fibre abnormalities are observed [5–9,22]. This study indicates that serum TNX can still bind to tropoelastin. Our finding suggests that the domains relevant for binding to tropoelastin and regulation of elastic fibre assembly or stability could reside in the 75 and 140–150 kDa C-terminal species. The failure of serum TNX to bind to collagen types I, III and V [18,20,21] is surprising because we previously mapped binding of these proteins to the FNIII29 of TNX in a study of C-terminal TNX domains [20]. The recombinant TNX domains in our previous study were produced in prokaryotic cells [20], therefore glycosylation may influence binding of native TNX forms. However, Minamitani *et al.* showed that glycosylated mouse TNX binds to collagen type I via the FNIII repeats [18]. Binding of TNX to collagens appears quite complex, and Lethias *et al.* demonstrated that deletion of the EGF repeats, fibrinogen domain or both resulted in a loss of binding to collagen type I, contradicting the results by Minamitani *et al.* [18,21]. Furthermore, Minamitani *et al.* showed that deletion of either the EGF repeats or fibrinogen domain negatively influenced the effect of TNX on collagen fibrillogenesis, whereas they showed that deletion of these domains did not influence binding to collagen type I [18]. We showed that the FNIII29 of human TNX has an effect on collagen fibrillogenesis, however, this effect was absent in 100 kDa C-terminal TNX. By contrast, 100 kDa C-terminal TNX was still able to bind to bind to collagen type I [20]. Taking all the data into account, it is feasible that conformational changes imposed on these shorter TNX species could influence binding of TNX to collagen types I, III and V. In addition, binding of TNX to collagen fibres could also be regulated through other ECM molecules [15,19]. In conclusion, our data provide novel information on serum TNX that could be useful in future studies on the physiological role of this intriguing extracellular matrix molecule, and its role in human pathology.

Experimental procedures

Recombinant TNX protein production and purification

TNX FNIII repeats 27–28, 29–30 and 27–32 were amplified by PCR with the primers listed in Table 1 using a previously described 2.7 kb human TNX cDNA as a template [23].

PCR products were ligated into the pCR2.1TOPO vector (Invitrogen, Breda, the Netherlands) according to the manufacturer's instructions for easy digestion with restriction enzymes. The pCR2.1 TOPO vectors with inserts were digested with *Eco*RI and *Sal*I and regions coding for FNIII27–28 and FNIII29–30 were cloned into the *Eco*RI/*Sal*I site of the pMal-c2X plasmid (Westburg B.V., Leusden, the Netherlands). The region coding for FNIII27–32 was inserted into the *Eco*RI/*Sal*I site of the pET28(a)+

Table 1. TNX domains and primers. The *Eco*RI and *Sal*I site are underlined in each primer sequence. Each *Sal*I site is preceded by a stop codon (TCA).

TNX domains	Forward primer (5′- to 3′)	Reverse primer (5′- to 3′)
FNIII27-28	GGAATTCGAGCTACCTCCCCAC	CTCGTCGACTCACTGACCAGCAGGAGC
FNIII29-30	TCAGAATTCTCAAGGCCCCGCCTG	GAAGTCGACTCAAGGCTCACTCTCCTC
FNIII27-32	GGAATTCGAGCTACCTCCCCAC	CAGGTCGACTCAGGTGAAAGAGGTGGA

plasmid (Brunschwig Chemie B.V., Amsterdam, the Netherlands). The sequence of the TNX domains was verified by dideoxy sequencing with a 3730 DNA analyser (Applied Biosystems, Nieuwekerk a/d IJssel, the Netherlands).

TNX FNIII27–28 and 29–30 were expressed as maltose-binding protein (MBP) fusion proteins in *Escherichia coli* TOP10F′ cells (Invitrogen). TNX FNIII27–32 was expressed as a poly(histidine) (HIS) fusion protein in *E. coli* TOP10F′ cells. TNX FNIII27–32 was extracted from the cell pellet using SDS extraction steps. MBP-tagged fusion proteins were purified over amylose resin columns (Westburg). HIS-tagged FNIII27–32 was purified over a Ni-NTA resin column (Invitrogen). All expression and purification steps were performed according to the manufacturer's instructions. All fusion proteins were analysed for purity using SDS/PAGE.

ECM components for protein interactions

Human collagen type I was from Chemicon International (Temecula, CA), and human collagen types III and V were from Rockland Inc. (Tebu-bio, Heerhugowaard, the Netherlands). Bovine collagen type I (acid soluble) was obtained from BD Biosciences (Alphen aan den Rijn, the Netherlands). Recombinant bovine tropoelastin (bTE) was a generous gift from Dr R. Mecham (Washington University, St Louis, MO) [24]. Human laminin was obtained from Gibco (Life Technologies, Breda, the Netherlands). BSA and human fibronectin were obtained from Sigma-Aldrich (Zwijndrecht, the Netherlands). BSA was used as a negative control.

Production of anti-TNX sera

Purified MBP–TNX FNIII27–28 and 29–30 protein was used to immunize rabbits and chickens. Aliquots containing 10 μg of protein in 500 μL of NaCl/P_i were mixed with an equal volume of Freund's complete adjuvant for the first injection and Freund's incomplete adjuvant for boosters. All injections in chickens and booster injections in rabbits were administered subcutaneously, whereas the first injection in rabbits was in the popliteal gland. Injections were repeated 12 times for both chickens and rabbits at 2-week intervals. The experimental design was approved by the animal use committee of the Radboud University Nijmen. Polyclonal antibodies against MBP–TNX FNIII27–28 and 29–30, isolated from chicken egg yolks and citrate plasma from rabbits, were purified by affinity chromatography on HIS–TNX FNIII27–32 coupled AffiGel®15 columns (Bio-Rad Laboratories B.V., Veenendaal, the Netherlands) according to previously described procedures [25,26].

Purified HIS–TNX FNIII27–32 protein was used for immunization of a rabbit. Aliquots of 500 μg HIS–TNX FNIII27–32 in 500 μL of NaCl/P_i were mixed with an equal volume of Freund's complete adjuvant for the first injection and Freund's incomplete adjuvant for boosters. Three injections were administered subcutaneously at 3-week intervals. Polyclonal antibodies against HIS–TNX FNIII27–32, isolated from serum, were purified by affinity chromatography on HIS–TNX FNIII27–32 couples to CNBr-activated Sepharose 4B column (GE Healthcare Life Sciences, Diegem, Belgium). Filtered (0.2 μm sterile filter; Schleider & Schuell, Dassel, Germany) 1 : 5 NaCl/P_i-diluted serum was loaded onto the column. The column was washed with 200 column volumes of NaCl/P_i and eluted with 0.1 M glycine–HCl (pH 2.7). Protein-containing fractions were pH neutralized with 1 M Tris/HCl (pH 9.5).

Affinity-purified rabbit and guinea-pig antibodies raised against a C-terminal 100 kDa fragment of TNX used in this study have been described previously [5,6]. Bovine TNX and monoclonal antibodies against FNIII3–5 and FNIII12–15 of bovine TNX were generously provided by Dr C. Lethias (Institut de Biologie et Chimie des Protéines, Lyon, France).

TNX ELISA

TNX concentrations were measured in a sandwich ELISA described previously [5] or in a new ELISA incorporating four different antibodies [25]. Briefly, the new assay format incorporated four different antibodies: duck anti-(chicken IgY) sera; chicken anti-(TNX FNIII27–28) or anti-(FNIII29–30) sera; rabbit anti-(TNX FNIII27–28) or anti-(FNIII29–30) sera; and goat anti-(rabbit IgG) labelled with biotin. Microtitre plates (96-well Nunc Maxisorb™ flat-bottomed plates, eBioscience, San Diego, CA) were coated with duck anti-(chicken IgY) (3.2 $mg \cdot L^{-1}$ in 50 $mmol \cdot L^{-1}$ $NaHCO_3/Na_2CO_3$, pH 9.6) overnight at 4 °C. All further incubation steps were performed at 37 °C. After each incubation step, wells were washed with NaCl/P_i containing 0.05% Tween-20 (T-NaCl/P_i). Wells were saturated with 1% BSA in T-NaCl/P_i for 2 h and then incubated with chicken anti-TNX sera for 2 h. This was followed by

incubation with the calibrator (His–TNX FNIII27–32), serum samples and reference samples for 2 h. Thereafter, wells were subsequently incubated with rabbit anti-TNX and biotinylated anti-rabbit IgG (Vector Laboratories Inc., Burlingame, CA). Thereafter, wells were incubated with the streptavidin/β-galactosidase conjugate (Roche Diagnostics Nederland B.V., Almere, the Netherlands) for 2 h followed by incubation with 4-methylumbelliferyl-β-D-galactopyranoside conjugate (Sigma-Aldrich) in substrate buffer (100 mmol·L^{-1} KH_2PO_4/K_2HPO_4 and 1 mmol·L^{-1} $MgCl_2$, pH 7.4) for 1 h. The reaction was stopped by the addition of 50 mmol·L^{-1} $NaHCO_3/Na_2CO_3$ (pH 10.5), and fluorescence was measured with a fluorometric plate reader (Fluoroskan; MTX Laboratory Systems Inc., Vienna, VA) using 355 nm excitation and 460 nm emission filters. All antibodies, sera and TNX proteins were diluted in T-NaCl/P_i containing 1% BSA.

Cross-reactivity of antibodies with antigens

Cross-reactivity was tested using a solid phase assay. Recombinant TNX was coated onto microtitre plates (96-well Nunc Maxisorb^{TM} flat-bottomed plates; eBioscience) overnight at 4 °C. All further incubation steps were performed at 37 °C. Wells were saturated with T-NaCl/P_i containing 1% BSA and subsequently incubated with rabbit anti-(TNX FNIII27–28) or anti-(TNX FNIII29–30) sera. Detection was performed with horseradish peroxidase-linked anti-rabbit IgG (Cell Signalling, Berverly, MA) and TMB substrate (Perbio Science Nederland B.V., Etten-Leur, the Netherlands). The reaction was stopped with 4 M H_2SO_4, absorbance was read at 450 nm.

Protein-binding assays

Protein interactions were measured in a solid phase assay with ECM components bound to a microtitre plate (solid phase) followed by incubation with serum TNX (soluble phase). Ninety-six-well microtitre plates (Greiner Bio-One B.V., Alphen aan den Rijn, the Netherlands) were coated overnight at 4 °C with ECM components, or with BSA as a control, diluted in NaCl/P_i. All further incubation steps were performed at 37 °C. After each incubation step, wells were washed with T–NaCl/P_i. Wells were saturated with 1% BSA in T-NaCl/P_i for 2 h and then incubated with serum TNX for 1 h. This was followed by incubation with rabbit anti-(TNX FNIII29–30) serum for 1 h. Thereafter, wells were incubated with biotinylated anti-rabbit IgG (Vector Laboratories) for 1 h followed by a 45 min incubation with an avidin–biotin–horseradish peroxidase mixture (vectastain kit; Brunschwig Chemie, Amsterdam, the Netherlands). Bound peroxidase was detected with *o*-phenylenediamine dihydrochloride (Perbio Science) and the absorbance read at 490 nm. All antibodies and TNX proteins were diluted in T-NaCl/P_i containing 0.1% BSA.

Binding of TE to serum TNX was performed as described above. Briefly, serum TNX was coated onto microtitre plates (96-well Nunc Maxisorb^{TM} flat-bottomed plates; eBioscience) overnight at 4 °C. All further incubation steps were performed at 37 °C. Wells were saturated with T-NaCl/P_i containing 1% BSA and subsequently incubated with various concentrations of TE. This was followed by incubation with a rabbit anti-TE serum (cat. no. 324756; Merck Biosciences, Nottingham, UK). Detection was performed with horseradish peroxidase-linked anti-rabbit IgG (Cell Signaling) and TMB substrate (Perbio Science). The reaction was stopped with 4 M H_2SO_4, absorbance was read at 450 nm.

Human serum and plasma collection and storage

We collected blood samples from 27 healthy volunteers (13 males and 14 females, median age 33 years, range 25–51 years). Nonfasting blood samples were drawn from an anticubital vein in 9 mL EDTA- and 9 mL dry vacuum glass tubes (BD Vacutainer Systems, Plymouth, UK). The EDTA tubes were placed on ice immediately and the dry tubes were kept at room temperature. Both tubes were centrifuged at 3500 ***g*** for 10 min within 30 min (Hettich Zentrifugen, type 4319 centrifuge, swing-out rotor 001559). Plasma and serum samples were stored at −20 °C (< 2 months). We also collected samples at 00:00 and 17:00 from five persons. From these same five persons we also collected a 09:00 fasting plasma and serum sample. Serum from previously described obligate TNX deficient- and heterozygous patients [5,7,8,22] and serum from matched healthy individuals stored at −20 °C was used to validate the specificity of the ELISA. An additional 217 samples from healthy individuals or patients with aortic aneurysm, stored at −20 °C or −80 °C were used for analyses of age, storage conditions or western blot analysis. In all experiments controls were matched for age and storage condition of samples. Informed consent was obtained from patients and volunteers, and the local ethics committee approved all study protocols.

SDS/PAGE and western blot

Proteins were loaded onto 12% Bis-Tris gels (Invitrogen) and gel electrophoresis was carried out using the NuPAGE system according to the manufacturer's instructions (Invitrogen). Gels were stained using Coomassie Brilliant Blue R250 (Brunschwig Chemie) to analyse protein purity.

Immunologic detection of proteins by western blot was performed essentially as described previously [5], with the exception that serum was not ammonium sulfate precipitated. Serum samples were diluted 20-fold and loaded onto 12% Bis-Tris gels (Invitrogen). The rabbit polyclonal antibodies against TNX FNIII27–28, 29–30 and 27–32 were used to detect TNX fragments in a 100-fold dilution, whereas rabbit polyclonal antibody against C-terminal 100 kDa TNX was used in a 1000-fold dilution. The

secondary antibodies (conjugated to biotin) against rabbit (Brunschwig Chemie) and antibiotin antibodies (conjugated to horseradish peroxidase) (Sigma-Aldrich) were diluted 1000-fold followed by detection with the chemiluminescent substrate lumiGLO (Cell Signaling).

Isolation of serum TNX

TNX species were purified from serum from healthy individuals using affinity chromatography on a column with polyclonal antibodies against HIS–TNX FNIII27–32 coupled to CNBr-activated Sepharose 4B (GE Healthcare Life Sciences). Briefly, filtered (0.2 μm sterile filter; Schleider & Schuell) 1 : 5 NaCl/P_i-diluted serum was loaded onto the column. The column was washed with 500 column volumes NaCl/P_i and TNX species were eluted with 0.1 M glycine–HCl (pH 2.7). Protein containing fractions were neutralized with 1 M Tris/HCl (pH 9.5).

Protein sequencing

Affinity-purified serum TNX was blotted onto a poly(vinylidene difluoride) membrane (Sigma-Aldrich) and stained using Coomassie Brilliant Blue R250 (Brunschwig Chemie) to reveal protein bands. Bands were excised and analysed by N-terminal sequencing (Edman type) or MS/MS. Sequence coverage of the isolated TNX fragments was analysed by MS/MS. Briefly, isolated TNX fragments were redissolved and digested with trypsin into small peptides. The amino sequence of the peptides was determined by a mass spectrophotometer composed of a linear ion trap mass spectrometer (LTQ) and a Fourier Transform Ion Cyclotron Resonance (FT-ICR) mass spectrometer (FTMS) (Thermo Electron Breda, NL).

Acknowledgements

We are grateful to Wendy Pluk of the proteomics facility of the Radboud University Medical Centre for her assistance in the MS/MS measurements. Tom Broekelmann and Bob Mecham of the Department of Cell Biology and Physiology of the Washington University School of Medicine are acknowledged for performing N-terminal sequencing and providing recombinant tropoelastin. Claire Lethias of the Institut de Biologie et Chimie des Protéines is acknowledged for providing bovine TNX and antibodies.

References

1 Bristow J, Tee MK, Gitelman SE, Mellon SH & Miller WL (1993) Tenascin-X: a novel extracellular matrix protein encoded by the human XB gene overlapping P450c21B. *J Cell Biol* **122**, 265–278.

2 Lethias C, Descollonges Y, Boutillon MM & Garrone R (1996) Flexilin: a new extracellular matrix glycoprotein localized on collagen fibrils. *Matrix Biol* **15**, 11–19.

3 Elefteriou F, Exposito JY, Garrone R & Lethias C (1997) Characterization of the bovine tenascin-X. *J Biol Chem* **272**, 22866–22874.

4 Ikuta T, Sogawa N, Ariga H, Ikemura T & Matsumoto K (1998) Structural analysis of mouse tenascin-X: evolutionary aspects of reduplication of FNIII repeats in the tenascin gene family. *Gene* **217**, 1–13.

5 Schalkwijk J, Zweers MC, Steijlen PM, Dean WB, Taylor G, Van Vlijmen IM, van Haren B, Miller WL & Bristow J (2001) A recessive form of the Ehlers–Danlos syndrome caused by tenascin-X deficiency. *N Engl J Med* **345**, 1167–1175.

6 Burch GH, Gong Y, Liu W, Dettman RW, Curry CJ, Smith L, Miller WL & Bristow J (1997) Tenascin-X deficiency is associated with Ehlers–Danlos syndrome. *Nat Genet* **17**, 104–108.

7 Zweers MC, Bristow J, Steijlen PM, Dean WB, Hamel BC, Otero M, Kucharekova M, Boezeman JB & Schalkwijk J (2003) Haploinsufficiency of TNXB is associated with hypermobility type of Ehlers–Danlos syndrome. *Am J Hum Genet* **73**, 214–217.

8 Zweers MC, Vlijmen-Willems IM, Van Kuppevelt TH, Mecham RP, Steijlen PM, Bristow J & Schalkwijk J (2004) Deficiency of tenascin-X causes abnormalities in dermal elastic fiber morphology. *J Invest Dermatol* **122**, 885–891.

9 Zweers MC, Peeters AC, Graafsma S, Kranendonk S, van Vlijmen I, den Heijer M & Schalkwijk J (2006) Abdominal aortic aneurysm is associated with high serum levels of tenascin-X and decreased aneurysmal tissue tenascin-X. *Circulation* **113**, 1702–1707.

10 Peeters ACTM, Kucharekova M, Timmermans J, van den Berkmortel FWPJ, Boers GH, Novakova IRO, Egging D, den Heijer M & Schalkwijk J (2004) A clinical and cardiovascular survey of Ehlers–Danlos syndrome patients with complete deficiency of tenascin-X. *Neth J Med* **62**, 23–25.

11 Lindor NM & Bristow J (2005) Tenascin-X deficiency in autosomal recessive Ehlers–Danlos syndrome. *Am J Med Genet A* **135**, 75–80.

12 Matsumoto K, Kinoshita T, Hirose T & Ariga H (2006) Characterization of mouse serum tenascin-X. *DNA Cell Biol* **25**, 448–456.

13 Tee MK, Thomson AA, Bristow J & Miller WL (1995) Sequences promoting the transcription of the human XA gene overlapping P450c21A correctly predict the presence of a novel, adrenal-specific, truncated form of tenascin-X. *Genomics* **28**, 171–178.

14 Elefteriou F, Exposito JY, Garrone R & Lethias C (1999) Cell adhesion to tenascin-X mapping of cell adhesion sites and identification of integrin receptors. *Eur J Biochem* **263**, 840–848.

15 Elefteriou F, Exposito J, Garrone R & Lethias C (2001) Binding of tenascin-X to decorin. *FEBS Lett* **495**, 44–47.
16 Lethias C, Elefteriou F, Parsiegla G, Exposito JY & Garrone R (2001) Identification and characterization of a conformational heparin-binding site involving two fibronectin type III modules of bovine tenascin-X. *J Biol Chem* **276**, 16432–16438.
17 Matsumoto K, Saga Y, Ikemura T, Sakakura T & Chiquet ER (1994) The distribution of tenascin-X is distinct and often reciprocal to that of tenascin-C. *J Cell Biol* **125**, 483–493.
18 Minamitani T, Ikuta T, Saito Y, Takebe G, Sato M, Sawa H, Nishimura T, Nakamura F, Takahashi K, Ariga H *et al.* (2004) Modulation of collagen fibrillogenesis by tenascin-X and type VI collagen. *Exp Cell Res* **298**, 305–315.
19 Veit G, Hansen U, Keene DR, Bruckner P, Chiquet-Ehrismann R, Chiquet M & Koch M (2006) Collagen XII interacts with avian tenascin-X through its NC3 domain. *J Biol Chem* **281**, 27461–27470.
20 Egging D, van den Berkmortel F, Taylor G, Bristow J & Schalkwijk J (2007) Interactions of human tenascin-X domains with dermal extracellular matrix molecules. *Arch Dermatol Res* **298**, 389–396.
21 Lethias C, Carisey A, Comte J, Cluzel C & Exposito JY (2006) A model of tenascin-X integration within the collagenous network. *FEBS Lett* **580**, 6281–6285.
22 Zweers MC, Dean WB, Van Kuppevelt TH, Bristow J & Schalkwijk J (2005) Elastic fiber abnormalities in hypermobility type Ehlers–Danlos syndrome patients with tenascin-X mutations. *Clin Genet* **67**, 330–334.
23 Morel Y, Bristow J, Gitelman SE & Miller WL (1989) Transcript encoded on the opposite strand of the human steroid 21-hydroxylase/complement component C4 gene locus. *Proc Natl Acad Sci USA* **86**, 6582–6586.
24 Kozel BA, Wachi H, Davis EC & Mecham RP (2003) Domains in tropoelastin that mediate elastin deposition *in vitro* and *in vivo*. *J Biol Chem* **278**, 18491–18498.
25 Grebenschikov N, Geurts-Moespot A, de Witte H, Heuvel J, Leake R, Sweep F & Benraad T (1997) A sensitive and robust assay for urokinase and tissue-type plasminogen activators (uPA and tPA) and their inhibitor type I (PAI-1) in breast tumor cytosols. *Int J Biol Markers* **12**, 6–14.
26 Grebenchtchikov N, Sweep CG, Geurts-Moespot A, Piffanelli A, Foekens JA & Benraad TJ (2002) An ELISA avoiding interference by heterophilic antibodies in the measurement of components of the plasminogen activation system in blood. *J Immunol Methods* **268**, 219–231.

Supplementary material

The following supplementary material is available online:

Fig. S1. Amino acid sequence coverage of the 75 and 140-150 kDa species. (Figure expanded from Fig. 4.)

This material is available as part of the online article from http://www.blackwell-synergy.com

Please note: Blackwell Publishing is not responsible for the content or functionality of any supplementary materials supplied by the authors. Any queries (other than missing material) should be directed to the corresponding author for the article.

a) 75 kDa TNX

MMPAQ.....DSTTAPLEKELPPHLGELTVAEETSSSLRLSWTVAQGPFDSFVVQYRDTDGQPRAVPVAADQRTVTVEDLEPGKK

FNIII28

YKFLLYGLLGGKRLGPVSALGMTAPEEDTPAPELAPEAPEPPEEPRLGVLTVTDTTPDSMRLSWSVAQGPFDSFVVQYEDTNGQ

FNIII28 FNIII29

PQALLVDGDQSKILISGLEPSTPYRFLLYGLHEGKRLGPLSAEGTTGLAPAGQTSEESRPRLSQLSVTDVTTSSLRLNWEAPPGA

FNIII29

FDSFLLRFGVPSPSTLEPHPRPLLQRELMVPGTRHSAVLRDLRSGTLYSLTLYGLRGPHKADSIQGTARTLSPVLESPRDLQFSEI

RETSAKVNWMPPPSRADSFKVSYQLADGGEPQSVQVDGQARTQKLQGLIPGARYEVTVVSVRGFEESEPLTGFLTTVPDGPTQ

LRALNLTEGFAVLHWKPPQNPVDTYDVQVTAPGAPPLQAETPGSAVDYPLHDLVLHTNYTATVRGLRGPNLTSPASITFTTGLEA

PRDLEAKEVTPRTALLTWTEPPVRPAGYLLSFHTPGGQNQEILLPGGITSHQLLGLFPSTSYNARLQAMWGQSLLPPVSTSFTTG

GLRIPFPRDCGEEMQNGAGASRTSTIFLNGNRERPLNVFCDMETDGGGWLVFQRRMDGQTDFWRDWEDYAHGFGNISGEFW

LGNEALHSLTQAGDYSMRVDLRAGDEAVFAQYDSFHVDSAAEYYRLHLEGYHGTAGDSMSYHSGSVFSARDRDPNSLLISCAV

SYRGAWWYRNCHYANLNGLYGSTVDHQGVSWYHWKGFEFSVPFTEMKLRPRNFRSPAGGG –4289 C-terminus

b) 140-150 kDa TNX

FNIII24

MMPAQ.....QGRFDSFTVQYKDRDGQPQVVRVRGEESEVTVGGLEPGRKYKMHLYGLHEGQRVGPVSTVGITAPLPTPLPVEP

RLGELAVAAVTSDSVGLSWTVAQGPFDSFLVQYRDAQGQPQAVPVSGDLRAVAVSGLDPARKYKFLLFGLQNGKRHGPVPVEA

RTAPDTKPSPRLGELTVTDATPDSVGLSWTVPEGEFDSFVVQYKDKDGRLQVVPVAANQREVTVQGLEPSRKYRFLLYGLSGR

KRLGPISADSTTAPLEKELPPHLGELTVAEETSSSLRLSWTVAQGPFDSFVVQYRDTDGQPRAVPVAADQRTVTVEDLEPGKKY

FNIII28

KFLLYGLLGGKRLGPVSALGMTAPEEDTPAPELAPEAPEPPEEPRLGVLTVTDTTPDSMRLSWSVAQGPFDSFVVQYEDTNGQP

QALLVDGDQSKILISGLEPSTPYRFLLYGLHEGKRLGPLSAEGTTGLAPAGQTSEESRPRLSQLSVTDVTTSSLRLNWEAPPGAF

DSFLLRFGVPSPSTLEPHPRPLLQRELMVPGTRHSAVLRDLRSGTLYSLTLYGLRGPHKADSIQGTARTLSPVLESPRDLQFSEIR

ETSAKVNWMPPPSRADSFKVSYQLADGGEPQSVQVDGQARTQKLQGLIPGARYEVTVVSVRGFEESEPLTGFLTTVPDGPTQL

RALNLTEGFAVLHWKPPQNPVDTYDVQVTAPGAPPLQAETPGSAVDYPLHDLVLHTNYTATVRGLRGPNLTSPASITFTTGLEAP

RDLEAKEVTPRTALLTWTEPPVRPAGYLLSFHTPGGQNQEILLPGGITSHQLLGLFPSTSYNARLQAMWGQSLLPPVSTSFTTGG

LRIPFPRDCGEEMQNGAGASRTSTIFLNGNRERPLNVFCDMETDGGGWLVFQRRMDGQTDFWRDWEDYAHGFGNISGEFWL

GNEALHSLTQAGDYSMRVDLRAGDEAVFAQYDSFHVDSAAEYYRLHLEGYHGTAGDSMSYHSGSVFSARDRDPNSLLISCAVS

YRGAWWYRNCHYANLNGLYGSTVDHQGVSWYHWKGFEFSVPFTEMKLRPRNFRSPAGGG –4289 C-terminus

Figure S1. Amino acid sequence coverage of the 75 and 140-150 kDa species.
Peptide amino acid sequences found after trypsinization and analysis by MS/MS are underlined (Figure expanded from Fig. 4). (a) The covered peptide amino acid sequences by MS/MS suggest a molecular weight (MW) of at least 70 kDa (without glycosylation) for the 75 kDa species. The most N-terminal peptide amino acid sequence is located near the C-terminus of FNIII28 (the amino acid sequences for FNIII28 and FNIII29 are designated by horizontal brackets) b). Sequence coverage by MS/MS of the 140-150 kDa TNX species revealed peptide amino acid sequences which align mostly with the C-terminal part of TNX. Due to the homology between FNIII repeats three peptide sequences can be aligned on multiple positions in the TNX sequence (the most C-terminal occurrences are marked bold, the amino acid sequences for FNIII24 and FNIII28 are designated by horizontal brackets).

CHAPTER 8

SUMMARY, DISCUSSION AND FUTURE PROSPECTS

SUMMARY, GENERAL DISCUSSION AND FUTURE PROSPECTS

INFLUENCE OF TENASCIN-X ON MATRIX DEVELOPMENT, MATURATION AND REMODELING

One of the objectives of the investigations described in this thesis was to study the role of tenascin-X (TNX) in the development, maturation and remodeling of the extracellular matrix (ECM). In 1997 Burch et al. described a reduced collagen density in the skin of the TNX deficient index patient [1]. Two groups independently generated TNX deficient mice in order to gain more insight into the function of TNX. Matsumoto et al. were the first to publish data on a TNX KO mouse model [2]. According to Matsumoto et al. TNX KO mice appeared healthy and had no gross abnormalities, however tumor invasion and metastasis appeared increased [2]. Mao et al. described a skin phenotype in the TNX KO mice. The skin of the TNX KO mice was markedly lax and fragile, supposedly induced by a disturbed collagen deposition [3]. Zweers et al. quantified the reduction in collagen density in a group of TNX deficient patients [4]. However, the collagen reduction in the skin of TNX KO mice is a matter of debate. Mao et al showed a reduction in density of collagen in skin and claimed similar results in tail and Achilles tendon. Mao et al. suggested that TNX is essential for collagen deposition into the ECM based on observations made in cultured dermal fibroblasts [3]. However, they incorrectly stated that TNX is not expressed in fetal rodent skin referring to a study by Burch et al. [5], where skin was not investigated and a study by Matsumoto et al., which did show expression of TNX in the dermis of E15.5 mice [6]. Mao et al. did not investigate TNX in fetal rodent development. In **chapter 2** we investigated the role of TNX in dermal development. We found that TNX KO skin is already significantly weaker compared to wild type (WT) mice at the earliest measurable time point (two weeks post partum). The difference in skin strength between TNX KO and WT is larger in adult mice compared to young mice. However, as outlined in **chapters 2 and 3** we found no difference in collagen distribution or density for total collagen or the fibrillar collagens type I, III and V nor in the amount of collagen as measured by hydroxyproline content. Independent studies by Minamitani et al. [7] and Matsumoto et al. [8] showed no difference in density or shape of collagen fibrils in sciatic nerves or dermis as evaluated by EM, although there appears to be an increase in size variation in dermal collagen fibrils [3;7]. Even more interestingly we found protein expression of fibrillar collagens type I, III and V to precede TNX both in dermal development as well as in matrix remodeling after skin injury (**chapters 2 and 3**). This suggests TNX is not involved in the initial deposition of collagen in the ECM of the dermis. This theory is supported by the observation that no obvious differences in density or localization of the fibrillar collagens in uterus between TNX KO and WT mice were found, in spite of constant remodeling of the connective tissue in the uterus during the menstrual cycle and during pregnancy (chapter 3). It must be noted that Mao et al. used littermates from a heterogeneous background in their studies, while our studies and those of the group of Matsumoto were performed on a more homogenous background (C57B6 mice), offering a possible explanation for the discrepancies in the studies. Another point of interest is the difference of TNX deficiency on collagen density in humans and mice. The relative collagen density in TNX deficient patients, quantified by Elastica-von-Gieson stained sections, appears reduced [4]. This is in contrast with observations made by us (**chapters 2 and 3**) and Minamitani et al. [7] in the dermis of mice. It seems unlikely that TNX, which is very similar in mouse and human, would have different functions in those species. However, due to species differences the effects of TNX deficiency could differ between the species. The TNX

KO mice appears to have a much milder phenotype compared to TNX deficient patients as they do not exhibit signs of hypermobility or lax ligaments (**chapter 2**), nor do they exhibit a high frequency of associated GU and rectal abnormalities (**chapter 3**) or other complications as observed in TNX deficient patients (**chapter 3**) [1;9;10].

Another alteration in the connective tissue of TNX deficient patients concerns the elastic fibers. The index patient showed abnormal elastic bodies beneath the dermal-epidermal junction [1]. Zweers et al. investigated this in a group of TNX deficient patients and observed that elastic fiber abnormalities are associated with TNX deficiency. Elastic fibers in these patients are shorter and contain fewer branches compared to age matched controls. EM revealed fragmented elastic fibers and aggregates of microfibrils and elastin [4]. Interestingly, elastic fiber abnormalities are found in the dermis of mice only after 3-6 months of age, suggesting a role for TNX in the stability or maintenance of elastic fibers. After 3-6 months there is an increase in elastin reactive material in the dermis of these mice as observed by immunostaining and elastin aggregates can be observed through EM. Also fibers in the TNX KO mice appear bigger compared to WT mice, though the shape appears normal. No elastic fiber abnormalities are found in the uterus and aorta of mice or in the mitral valve of a TNX deficient patient (**chapter 2 and 4**) [11] in spite of TNX expression in these tissues, suggesting the effects of TNX deficiency on elastic fibers are tissue specific.

Puzzling however, is the observation that despite the apparent lack of pronounced differences in collagen content and the late onset of elastic fiber abnormalities in the skin of TNX KO and WT mice the skin strength of the TNX KO mouse is markedly reduced compared to WT mice even at a young age (**chapters 2 and 3**) [3]. As soon as TNX protein expression starts, colocalisation with dermal fibrillar collagens I, III and V can be observed, suggesting TNX could play a role in matrix maturation or stability (**chapters 2 and 3**). Alternatively, TNX deficiency could lead to an upregulation of matrix degrading enzymes. It has been shown that lack of TNX in the dermis appears to facilitate tumor progression in mice and MeLiM swine [2;12;13], possibly due to an increase in matrix metalloproteinase (MMP) expression or adhesive defects in TNX null fibroblasts [2;13-15]. However, several questions regarding the interpretation of these studies remain. The expression is shown on mRNA level for most MMPs, only for MMP-2 an increase in active form is shown. Fibroblast cultures of TNX KO mice and WT mice show no differences in MMP activity, unless in the presence of a collagen lattice. A co-culture of fibroblasts with B16-BL6 melanoma cells even showed a decrease in the MMP activity in TNX KO fibroblasts compared to WT fibroblasts. Furthermore, data from TNX/TNC double KO mice are difficult to interpret since only the tumor size in TNX KO mice is increased, while tumors in the TNC KO and TNX/TNC double KO mice are equal to WT, yet survival in all tenascin KO mice is decreased. Interestingly, while an increase of pro-MMP-9 was shown in TNX KO mice, MMP-9 mRNA expression is increased in all tenascin KO mice. Most importantly however, no qualitative differences in collagen fibrils or the basement membrane are observed on the ultrastructural level in TNX KO mice [2;7;13-15]. Abnormalities in elastic fibers appear only in adult mice (as of 3-6 months) and are not yet appreciatable in young mice (<2 months). All investigated TNX deficient patients are well into adulthood and the collagen density and abnormal elastic fibers could not be investigated in young individuals. Although it cannot be excluded that a slow degradation of the ECM by an upregulation MMP could account for these changes it is more plausible that TNX itself could stabilize the matrix by interacting with various ECM components strengthening the ECM and making it less susceptible to breakdown. TNX could also play a role in the maturation and thus the quality of elastic fibers and collagen.

INTERACTIONS OF TNX WITH ECM COMPONENTS

In order to play a role in the stabilization or maturation of the ECM TNX must colocalize and interact with other ECM components. We have shown that TNX starts to colocalize with collagen types I, III and V and elastin in the dermis during development after the intial deposition of these proteins (**chapter 2**). In **chapter 5** we show binding to collagen types I, III and V and elastin and identify interaction sites in the C-terminus of TNX. We found binding of fibronectin type III repeat 29 (FNIII29) of human TNX to collagen types I, III, V and elastin. The fibrinogen domain of TNX showed binding to elastin and not to any other of the ECM components tested. Furthermore, in **chapter 6** we show binding of TNX to collagen type XII, a fibril associated collagen (FACIT) thought to link collagen fibrils together. We show that the TSPN-like domain in the non-collagenous region 3 of COLXII and the FNIII29 of TNX are able to interact with each other. It has become increasingly clear that TNX can interact with a large number of ECM components such as; heparin, decorin, elastin and collagen types I, III, V, XII, XIV (**chapter 5 and 6**) [6;7;16-19]. Furthermore, cells are able to adhere to TNX, suggesting a function for TNX as linker between cells and the ECM [20;21]. Here we propose a model, as depicted in figure 1, in which TNX acts as a linker between various components of the ECM and to cells, thus stabilizing the extracellular matrix.

TNX AS A COMPONENT OF SERUM

Previously, a 140 kDa TNX species was identified in human serum. The 140 kDa TNX serum species is recognized by an antibody directed against the C-terminus of TNX however, further details were not known [10]. A sandwich ELISA was developed by Schalkwijk et al. [10] to determine the relative concentration of TNX in serum for screening of TNX deficient patients and TNX heterozygosis [9;10;22]. The same ELISA was used by Zweers et al. to show that an elevated level of serum TNX is a risk indicator for abdominal aorta aneurysm. During the research on TNX in human serum we developed and validated TNX ELISAs, which incorporated avian antibodies to avoid the effects of heterophilic antibodies. The ELISAs could be used to investigate serum TNX concentrations in pathological conditions other than EDS. In **chapter 7** we investigated serum TNX using newly generated and existing antibodies against the C-and N-terminus of TNX and mass spectrometry. Interestingly we discovered multiple species of TNX in serum, some of which surprisingly were not discovered in previous studies. Furthermore we found that during storage of serum samples the measured serum TNX concentration would decrease. We also discovered a correlation between serum TNX levels and age, as it appears young children have elevated serum levels compared to adults. Recently Matsumoto et al. described serum forms of TNX in mice. They found one predominant species of 200 kDa and showed that a 200 kDa TNX species was formed from full length TNX after incubation with spleen homogenate at acidic pH. They speculated that other TNX species were proteolytic intermediate products derived from full length TNX [23]. No full human length TNX was available to study the proteolytic cleavage products of human TNX. Although a TNX species of approximately 200 kDa appears present in human serum, the two predominant human serum TNX species are approximately 75 kDa and 140-150 kDa. Unfortunately, the exact N-terminus of neither species could be established making it difficult to make any assumptions on cleavage sites. However, the 75 kDa form is very similar to the adrenal specific short TNX isoform (XB-S) [24]. Although the 75 kDa TNX species is still present in serum of patients with a double adrenal ectomy, it cannot be excluded that XB-S is expressed and excreted by cells other than adrenal gland cells since only adrenal, muscle, liver, brain, kidney and heart tissue were examined [24]. In conclusion we have shown that, there are multiple TNX species in serum and TNX concentration in serum is dependant on storage and patient age. There are two predominant C-terminal TNX species,

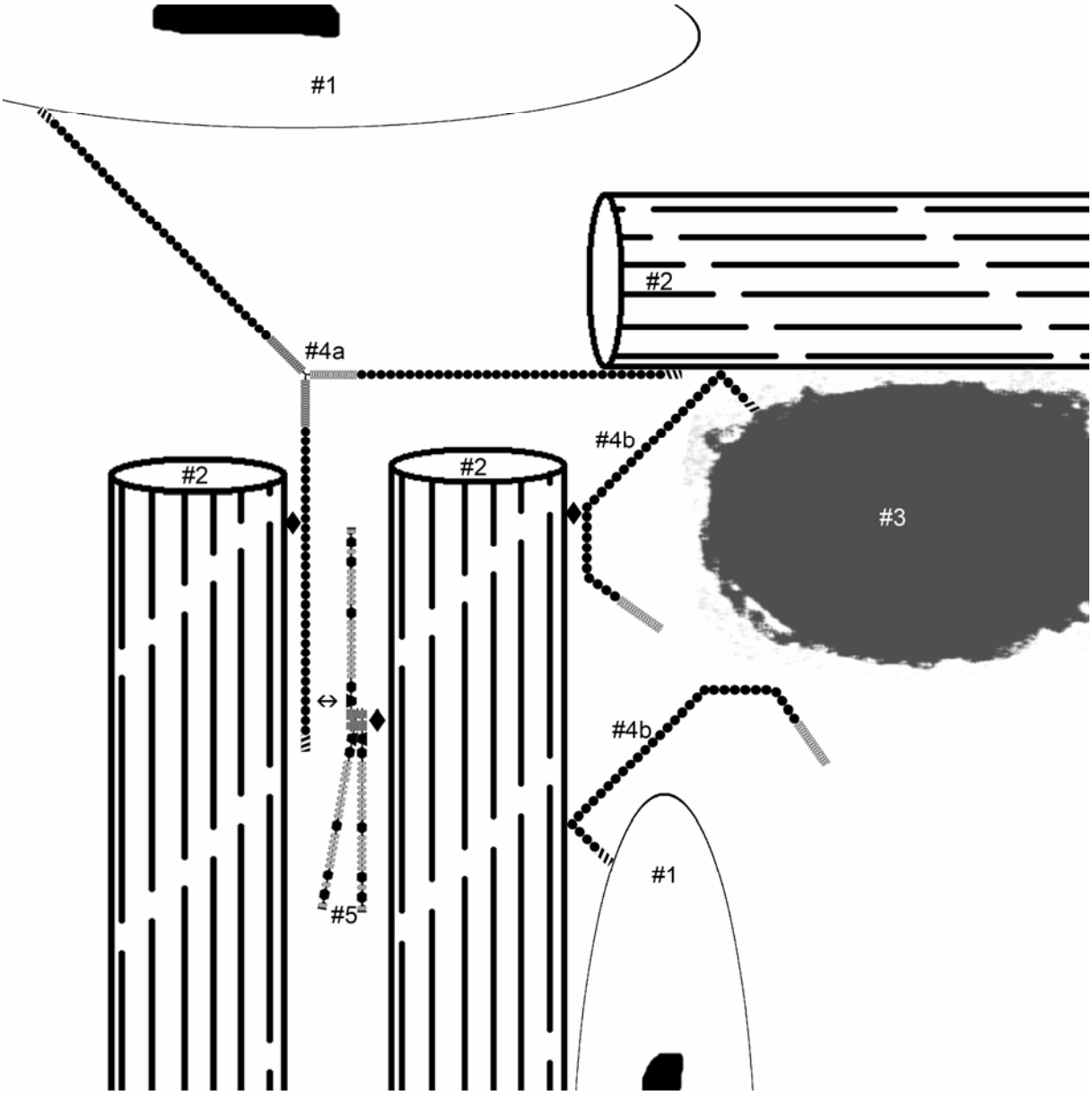

Figure 1: A model of stabilization of the ECM by TNX.
TNX links together various components of the ECM either as a trimer (#4a) or monomer (#4b). TNX can link collagen fibrils containing collagen I, III or V (#2) together directly, through decorin (♦) or FACIT collagens such as collagen XII (#5). Furthermore TNX could link collagen bundles to cells (#1) or elastic fibers (#3), thus acting as an "extracellular glue".

which are to have some biological activity as they are able to bind to tropoelastin (**chapter 7**).

CONCLUDING REMARKS AND FUTURE PROSPECTS

TNX was the first tenascin of which deficiency could be linked to a human pathological condition. The TNX KO mouse was the first tenascin KO mouse with an overt phenotype. During the course of this thesis it became apparent that there are several discrepancies between studies regarding the changes in tissue morphology associated with TNX deficiency. In this thesis we describe a major role for TNX as stabilizer of the ECM, acting as a linker between collagen fibrils, elastic fibers and cells.

We provide a basis for the research on serum TNX levels in pathological conditions, in which our observations should act as guidelines. Our observations on the interaction between

collagen type I, III, V and XII and elastin with TNX provides a basis for further research. Interestingly FNIII repeat number 29 of human TNX is able to bind to a large number of ECM molecules. This repeat differs from other FNIII repeats in TNX because it contains an additional, unique stretch of amino acids, as is shown in figure 2 for FNIII27 to 31. Murine FNIII26 of TNX and bovine FNIII27 of TNX match human FNIII29 of TNX and also contain this additional stretch of amino acids, suggesting a similar biological function. Mutational analysis of repeat FNIII29 should reveal more details on the amino acid sequence responsible for the interaction. This could result in development of FNIII29 derived peptides that could possibly be used as a research tool or as a therapeutic application in matrix biology and wound healing.

A second important starting point for future research is collagen type XII as a candidate gene for connective tissue diseases such as the Ehlers-Danlos syndrome. Taken together I conclude that the work described in this thesis will open up new avenues in basic and applied biology of TNX.

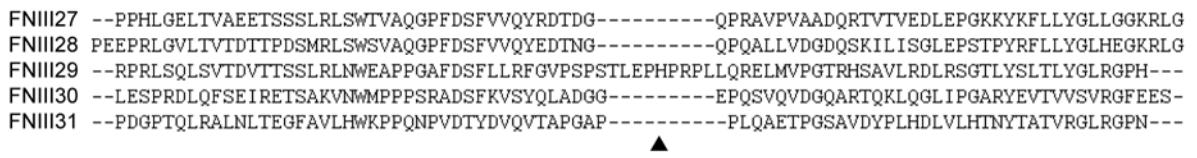

Figure 2: Alignment of human TNX FNIII repeats.
Alignment of FNIII29 of human TNX to FNIII repeats tested in chapters 5 and 6 (CLUSTAL W (1.83) multiple sequence alignment). An arrow indicates a unique stretch of extra amino acids, not found in other FNIII repeats in TNX.

REFERENCES

[1] Burch,G.H., Gong,Y., Liu,W., Dettman,R.W., Curry,C.J., Smith,L., Miller,W.L., & Bristow,J. (1997) Tenascin-X deficiency is associated with Ehlers-Danlos syndrome. *Nat. Genet.* **17,** 104-108.

[2] Matsumoto,K., Takayama,N., Ohnishi,J., Ohnishi,E., Shirayoshi,Y., Nakatsuji,N., & Ariga,H. (2001) Tumour invasion and metastasis are promoted in mice deficient in tenascin-X. *Genes Cells* **6,** 1101-1111.

[3] Mao,J.R., Taylor,G., Dean,W.B., Wagner,D.R., Afzal,V., Lotz,J.C., Rubin,E.M., & Bristow,J. (2002) Tenascin-X deficiency mimics Ehlers-Danlos syndrome in mice through alteration of collagen deposition. *Nat. Genet.* **30,** 421-425.

[4] Zweers,M.C., Vlijmen-Willems,I.M., Van Kuppevelt,T.H., Mecham,R.P., Steijlen,P.M., Bristow,J., & Schalkwijk,J. (2004) Deficiency of tenascin-x causes abnormalities in dermal elastic fiber morphology. *J. Invest Dermatol.* **122,** 885-891.

[5] Burch,G.H., Bedolli,M.A., McDonough,S., Rosenthal,S.M., & Bristow,J. (1995) Embryonic expression of tenascin-X suggests a role in limb, muscle, and heart development. *Dev. Dyn.* **203,** 491-504.

[6] Matsumoto,K., Saga,Y., Ikemura,T., Sakakura,T., & Chiquet,E.R. (1994) The distribution of tenascin-X is distinct and often reciprocal to that of tenascin-C. *J. Cell Biol.* **125,** 483-493.

[7] Minamitani,T., Ikuta,T., Saito,Y., Takebe,G., Sato,M., Sawa,H., Nishimura,T., Nakamura,F., Takahashi,K., Ariga,H., & Matsumoto,K. (2004) Modulation of collagen fibrillogenesis by tenascin-X and type VI collagen. *Exp. Cell Res.* **298,** 305-315.

[8] Matsumoto,K., Sawa,H., Sato,M., Orba,Y., Nagashima,K., & Ariga,H. (2002) Distribution of extracellular matrix tenascin-X in sciatic nerves. *Acta Neuropathol. (Berl)* **104,** 448-454.

[9] Lindor,N.M. & Bristow,J. (2005) Tenascin-X deficiency in autosomal recessive Ehlers-Danlos syndrome. *Am. J. Med. Genet. A* **135,** 75-80.

[10] Schalkwijk,J., Zweers,M.C., Steijlen,P.M., Dean,W.B., Taylor,G., Van Vlijmen,I.M., van Haren,B., Miller,W.L., & Bristow,J. (2001) A recessive form of the Ehlers-Danlos syndrome caused by tenascin-X deficiency. *N. Engl. J. Med.* **345,** 1167-1175.

[11] Peeters,A.C.T.M., Kucharekova,M., Timmermans,J., van den Berkmortel,F.W.P.J., Boers,G.H., Novakova,I.R.O., Egging,D., den Heijer,M., & Schalkwijk,J. (2004) A clinical and cardiovascular survey of Ehlers-Danlos

syndrome patients with complete deficiency of tenascin-X. *Neth. J. Med.* **62,** 23-25.

[12] Geffrotin,C., Horak,V., Crechet,F., Tricaud,Y., Lethias,C., Vincent-Naulleau,S., & Vielh,P. (2000) Opposite regulation of tenascin-C and tenascin-X in MeLiM swine heritable cutaneous malignant melanoma [In Process Citation]. *Biochim. Biophys. Acta* **1524,** 196-202.

[13] Matsumoto,K., Takahashi,K., Yoshiki,A., Kusakabe,M., & Ariga,H. (2002) Invasion of melanoma in double knockout mice lacking tenascin-X and tenascin-C. *Jpn. J. Cancer Res.* **93,** 968-975.

[14] Matsumoto,K., Minamitani,T., Orba,Y., Sato,M., Sawa,H., & Ariga,H. (2004) Induction of matrix metalloproteinase-2 by tenascin-X deficiency is mediated through the c-Jun N-terminal kinase and protein tyrosine kinase phosphorylation pathway. *Exp. Cell Res.* **297,** 404-414.

[15] Minamitani,T., Ariga,H., & Matsumoto,K. (2002) Adhesive defect in extracellular matrix tenascin-x-null fibroblasts: a possible mechanism of tumor invasion. *Biol. Pharm. Bull.* **25,** 1472-1475.

[16] Elefteriou,F., Exposito,J., Garrone,R., & Lethias,C. (2001) Binding of tenascin-X to decorin. *FEBS Lett.* **495,** 44-47.

[17] Lethias,C., Elefteriou,F., Parsiegla,G., Exposito,J.Y., & Garrone,R. (2001) Identification and characterization of a conformational heparin-binding site involving two fibronectin type iii modules of bovine tenascin-x. *J. Biol. Chem.* **276,** 16432-16438.

[18] Lethias,C., Carisey,A., Comte,J., Cluzel,C., & Exposito,J.Y. (2006) A model of tenascin-X integration within the collagenous network. *FEBS Lett.* **580,** 6281-6285.

[19] Veit,G., Hansen,U., Keene,D.R., Bruckner,P., Chiquet-Ehrismann,R., Chiquet,M., & Koch,M. (2006) Collagen XII Interacts with Avian Tenascin-X through Its NC3 Domain. *J. Biol. Chem.* **281,** 27461-27470.

[20] Elefteriou,F., Exposito,J.Y., Garrone,R., & Lethias,C. (1997) Characterization of the bovine tenascin-X. *J. Biol. Chem.* **272,** 22866-22874.

[21] Elefteriou,F., Exposito,J.Y., Garrone,R., & Lethias,C. (1999) Cell adhesion to tenascin-X mapping of cell adhesion sites and identification of integrin receptors. *Eur. J. Biochem.* **263,** 840-848.

[22] Zweers,M.C., Bristow,J., Steijlen,P.M., Dean,W.B., Hamel,B.C., Otero,M., Kucharekova,M., Boezeman,J.B., & Schalkwijk,J. (2003) Haploinsufficiency of TNXB is associated with hypermobility type of Ehlers-Danlos syndrome. *Am. J. Hum. Genet.* **73,** 214-217.

[23] Matsumoto,K., Kinoshita,T., Hirose,T., & Ariga,H. (2006) Characterization of mouse serum tenascin-X. *DNA Cell Biol.* **25,** 448-456.

[24] Tee,M.K., Thomson,A.A., Bristow,J., & Miller,W.L. (1995) Sequences promoting the transcription of the human XA gene overlapping P450c21A correctly predict the presence of a novel, adrenal-specific, truncated form of tenascin-X. *Genomics* **28,** 171-178.

NEDERLANDSE SAMENVATTING

De extracellulaire matrix is de materie tussen cellen en is essentieel voor de ontwikkeling, vorm en instandhouding van ons lichaam. De extracellulaire matrix bestaat voornamelijk uit collageen bundels, elastische vezels, glycoproteïnen (proteïnen = eiwitten) en proteoglycanen. Afwijkingen in de opbouw en samenstelling van de extracellulaire matrix kunnen leiden tot het ontstaan van diverse ziekten. Een van de bestanddelen van de extracellulaire matrix is het eiwit tenascine-X. In samenwerking met Amerikaanse wetenschappers is op de afdeling dermatologie van het Radboud ziekenhuis enkele jaren geleden aangetoond dat de afwezigheid van dit eiwit in een mens leidt tot een vorm van het Ehlers-Danlos syndroom. Deze erfelijke bindweefselaandoening uit zich in overbeweeglijke gewrichten en een sterk uitrekbare, fragiele huid. Wanneer de huid van deze mensen onder de microscoop wordt bekeken, hebben zij een verminderde dichtheid van collageen en er zijn misvormde elastische vezels in de lederhuid (= dermis). Om te begrijpen hoe afwezigheid van tenascine-X tot deze afwijkingen leidt, is het belangrijk om de veranderingen in de extracellulaire matrix te volgen. Deze studies zijn vanwege medisch-ethische en praktische redenen niet in mensen uitvoerbaar. Om toch onderzoek te kunnen doen hebben we gebruik gemaakt van een tenascine-X “knockout” muis model. Deze muizen zijn gemodificeerd zodat zij, net als de tenascine-X deficiënte patiënten, geen tenascin-X eiwit kunnen maken.

In **hoofdstuk 2** hebben we laten zien dat de huid van de tenascine-X “knockout” muis van jongs af aan al zwakker is dan die van een normale muis. Vreemd genoeg zijn er bij de tenascine-X “knockout” muizen geen aanwijzingen gevonden voor overbeweeglijke gewrichten, zoals bij de tenascine-X deficiënte patiënten wel het geval is (**hoofdstuk 2**). Ook lijken de afwijkingen van baarmoederweefsel van tenascine-X “knockout” muizen minder dan bij tenascine-X deficiënte patiënten (**hoofdstuk 4**). Over het algemeen lijken de tenascine-X “knockout” muizen minder complicaties te hebben dan de tenascine-X deficiënte patiënten. We kunnen dan ook stellen dat de tenascine-X deficiëntie bij de mens een grotere impact heeft dan bij de muis. Eerder was deze zwakkere huid al beschreven voor volwassen muizen door de Amerikaanse wetenschappers waarmee is samengewerkt. Zij dachten dat dit veroorzaakt werd door een verstoring van de collageen depositie in de huid. Uit onze studie bleek dit niet het geval te zijn, omdat de belangrijkste collageen eiwitten in de huid, type I, III en V, al vóór tenascine-X aanwezig lijken te zijn. Ook vonden wij geen verminderde dichtheid van collageen in de huid. Dit werd door middel van een andere methode door Japanse wetenschappers nogmaals bevestigd. Bij veranderingen in volwassen bindweefsel, zoals bij wondgenezing in de huid (**hoofdstuk 3**) en in de baarmoederwand tijdens zwangerschap (**hoofdstuk 4**), vonden we geen afwijkingen in collageen depositie. Bij wondgenezing waren de collageen eiwitten ook weer eerder aanwezig dan tenascine-X, wat bevestigt dat tenascin-X nooit bij de initiële depositie van het collageen betrokken kan zijn. Een interessante bevinding was dat het wondgebied in toenemende mate kracht kon weerstaan nadat tenascine-X in de extracellulaire matrix tot expressie kwam. De afwijkingen in elastische vezels, hoewel niet precies gelijk aan die in de mens, werden pas op latere leeftijd zichtbaar (**hoofdstuk 2 en 4**). Ook zijn de hoofdcomponenten van elastische vezels, zoals het eiwit elastine, al veel eerder aanwezig in de ontwikkeling van de extracellulaire matrix van de huid dan tenascine-X. Wel geldt dat tenascine-X eiwit, wanneer het eenmaal in de extracellulaire matrix tot expressie komt, op dezelfde plek zit (= co-lokalisatie) als verschillende collageen componenten en elastine.

Om te bestuderen of tenascine-X ook een fysieke interactie kan aangaan met de componenten van de extracellulaire matrix waar het mee co-lokaliseert zijn er verschillende bindingsstudies uitgevoerd. In **hoofdstuk 5** wordt de binding van het 29ste fibronectine domein in tenascine-X aan elastine en collageen type I, III en V aangetoond en de binding van het fibrinogeen domein in tenascine-X aan elastine beschreven. In **hoofdstuk 6** wordt de binding van tenascine-X aan collageen type XII onderzocht en zijn de domeinen die verantwoordelijk zijn voor deze interactie in beide eiwitten geïdentificeerd. Collageen type XII zit aan collageen bundels en kan in samenwerking met tenascine-X een verbinding vormen tussen collageen bundels. Tijdens en voor het schrijven van dit proefschrift hebben andere wetenschappers aangetoond dat tenascine-X ook aan andere componenten van de extracellulaire matrix en cellen kan binden. Al deze informatie en de bevindingen uit **hoofdstukken 2 tm 6** hebben geleid tot de theorie dat tenascine-X als een soort lijm een aantal belangrijke componenten van de extracellulaire matrix aan elkaar verbindt en zo de extracellulaire matrix stabiliteit geeft.

Niet alleen in de extracellulaire matrix van veel weefsels komt tenascine-X voor maar er is ook een fragment van 140 kDa aanwezig in het bloed van gezonde mensen. Over dit fragment was weinig bekend behalve dat het waarschijnlijk gedeeltelijk overeenkomstig was met het C-terminale deel (uiteinde) van het volledige tenascine-X (450 kDa). Om te bestuderen welk gedeelte van het volledige eiwit dit fragment nu precies was en welke parameters belangrijk waren bij de gemeten hoeveelheid van dit fragment in het bloed, zijn er verschillende nieuwe antilichamen tegen tenascine-X ontwikkeld (**hoofdstuk 7**). Uiteindelijk bleek dat er niet één maar veel meer fragmenten in bloed aanwezig waren. Ook bleek dat jonge kinderen een hogere waarde hadden dan volwassenen. Verder viel op dat bij opslag van het afgenomen bloed de gemeten waarde sterk terugliep, zelfs bij -20°C. Bij het correleren van ziektebeelden aan gemeten tenascine-X waarden in bloed, moet hier zeer zeker rekening mee worden gehouden. Na zuivering van tenascine-X fragmenten uit bloed met behulp van antilichamen tegen de C-terminus van tenascine-X, blijken twee fragmenten, van ~75 kDa en van ~140-150 kDa, het meest voor te komen. Deze fragmenten tonen nog biologische activiteit in de vorm van binding aan elastine.

De resultaten beschreven in dit proefschrift laten zien dat tenascine-X een belangrijke functie heeft in de stabiliteit van de extracellulaire matrix en dat het niet betrokken is bij de initiële depositie ervan. Onze bevindingen over tenascine-X in bloed kunnen als richtlijnen gelden bij onderzoek naar de betrokkenheid van dit eiwit in andere ziektebeelden. Ook het uitzoeken van de domeinen in tenascine-X die interacties met andere eiwitten kunnen aangaan, vormt een mooie basis voor onderzoek naar gebruik van deze domeinen als peptide bij bijvoorbeeld wondgenezing. Tenslotte is de interactie van tenascine-X met collageen type XII erg interessant. De genetische oorzaken van het Ehlers-Danlos syndroom zijn bij veel patiënten nog niet opgehelderd, mogelijk zou een afwijking in collageen type XII een gedeelte hiervan kunnen verklaren.

DANKWOORD

Misschien is het schrijven van het dankwoord nog wel een van de moeilijkste onderdelen van het proefschrift. Er zijn zoveel mensen om te bedanken en meestal verdienen ze meer dan de paar regels die in het dankwoord staan.

Joost Schalkwijk, bedankt voor alle ondersteuning tijdens het promotietraject. Je merkte nu al dat je AIO's meer gemeen hadden met je kinderen dan met jezelf. Vroeger wisselde je CD's uit met je AIO's, nu wisselen je AIO's computergames uit met je kinderen. Nog een paar jaar en je AIO's zijn jonger dan je kinderen. Op zich maakt dat niet uit, want je blijft gewoon een toffe peer.

Ivonne, bedankt voor alle hulp. Zonder jou was dit boekje zeker niet zo uitgebreid geworden als het nu is.

Aan mijn **(ex)kamer- & labgenoten**; **Desiree, Patrick J, Sandra, Marijke, Evert en Manon**, bedankt voor alle gezelligheid, ongein en waardevolle (waar toepasbaar) discussies.

Gys, de Nestor van de afdeling**,** bedankt voor alle tips en advies. Voor jou ligt nog steeds de mooie taak om alle "amateurs" erop te wijzen hoe je echte wetenschap bedrijft.

Alle (ex)labgenoten, Patrick Z, Diana, Tsing, Mieke, Arno, Wynand en AGNIO's en **AGIKO's** bedankt voor alle gezelligheid, sfeer en het doorstaan van mijn plagerijtjes.

De mensen van het dierenlab. Jullie kennis en hulp waren onmisbaar voor dit onderzoek, **Debby, ILona, Geert, Kai, Brenda, Helma, Jeroen, Nancy en Aglaja**, bedankt!

Marisol, bedankt voor alle keren dat jij bloed aftapte van mijn vrijwilligers als ik weer serum nodig had voor mijn onderzoek.

Alle studenten; meisjes en jongens hartelijk bedankt. Ook al hadden de meeste van jullie niks met mijn onderzoek te maken, vaak kon ik jullie wel strikken om wat coupes voor mij te snijden of een glaasje voor mij mee te kleuren.

Natuurlijk ook de mensen met wie ik heb samengewerkt bij de verschillende artikelen over TNX. **Anita**, **Marijke en Maartje** bedankt, zonder jullie bijdrage was o.a. het artikel over TNX in serum nooit tot stand gekomen. **Nicol**, veel succes met het laatste stukje TNX onderzoek in het St. Radboud. I would like to thank all **collaborators** for their contributions.

Alle **stafleden, dames van de balie, mensen van secretariaat, verpleging en anderen**. Bedankt voor de fijne sfeer op de afdeling!

Jobke en Judith, jullie wacht de schone taak om jullie oudste broer te ondersteunen als paranimf bij de verdediging van dit proefschrift.

Natuurlijk wil ik mijn **ouders** ook bedanken voor alle steun die ze mij hebben gegeven tijdens mijn studie. Ma, bedankt voor alle voedselpakketten die ik tijdens mijn studie biologie meekreeg als ik weer eens thuis was geweest. Pa jij ook bedankt voor het uitknippen van de advertentie voor "junior onderzoeker" bij de afdeling dermatologie in 2002. Anders had ik misschien nog steeds een McJob gehad.

Karen, jij zei mij eens dat "In de liefde is wat niet wordt uitgesproken belangrijker dan wat wordt gezegd". Ik hoop dat ik jou dat nog heel lang mag laten blijken. Bedankt voor al je steun tijdens mijn promotieonderzoek.

CURRICULUM VITAE

Op zondag 21 oktober 1979 werd David Franciscus Egging geboren in Arnhem. Op vijf jarige leeftijd vertrok hij met het gezin Egging naar Winschoten in Groningen om vervolgens na een jaar naar Borculo (Achterhoek) te verhuizen. Hij volgde het Atheneum in Lochem en haalde in de zomer van 1997 zijn diploma. Op 17 jarige leeftijd ging hij op kamers wonen in Nijmegen waar hij Biologie studeerde aan de universiteit van Nijmegen (KUN). Eind augustus 2001 studeerde hij af met als deelrichting de medische biologie. Begin 2002 vond hij een mooie promotieplek aan het academische ziekenhuis te Nijmegen bij de afdeling Dermatologie. Hier werd, onder leiding van Prof. Dr. J. Schalkwijk, door hem het in dit proefschrift beschreven onderzoek uitgevoerd. Hij werkt nu als onderzoeker biotechnologie bij Synthon BV.

LIST OF PUBLICATIONS

- Peeters AC, Kucharekova M, Timmermans J, van den Berkmortel FW, Boers GH, Novakova IR, Egging D, den Heijer M, Schalkwijk J. *A clinical and cardiovascular survey of Ehlers-Danlos syndrome patients with complete deficiency of tenascin-X*. Neth J Med. 2004 May;62(5):160-2.

- Bristow J, Carey W, Egging D, Schalkwijk J. *Tenascin-X, collagen, elastin, and the Ehlers-Danlos syndrome.* Am J Med Genet C Semin Med Genet. 2005 Nov 15;139(1):24-30.

- Egging et al. *Dermal connective tissue development in mice: an essential role for tenascin-X.* Cell Tissue Res. 2006 Mar;323(3):465-74.

- Egging et al. J. *Interactions of human tenascin-X domains with dermal extracellular matrix molecules.* Arch Dermatol Res. 2007 Jan;298(8):389-96.

- Egging et al. *Identification and characterization of multiple species of tenascin-X in human serum.* FEBS J. 2007 Mar;274(5):1280-9.

- Egging et al. *Wound healing in tenascin-X deficient mice suggests that tenascin-X is involved in matrix maturation rather than matrix deposition.* Connect Tissue Res. 2007;48(2):93-8.

- Egging et al. *Analysis of obstetric complications and uterine connective tissue in tenascin-X deficient humans and mice: a clinical and morphological study*. CTR, submitted.

- Egging et al. *Domain mapping of interaction sites between collagen type XII and tenascin-X.* In preparation.

COLOR ILLUSTRATIONS

CHAPTER 2

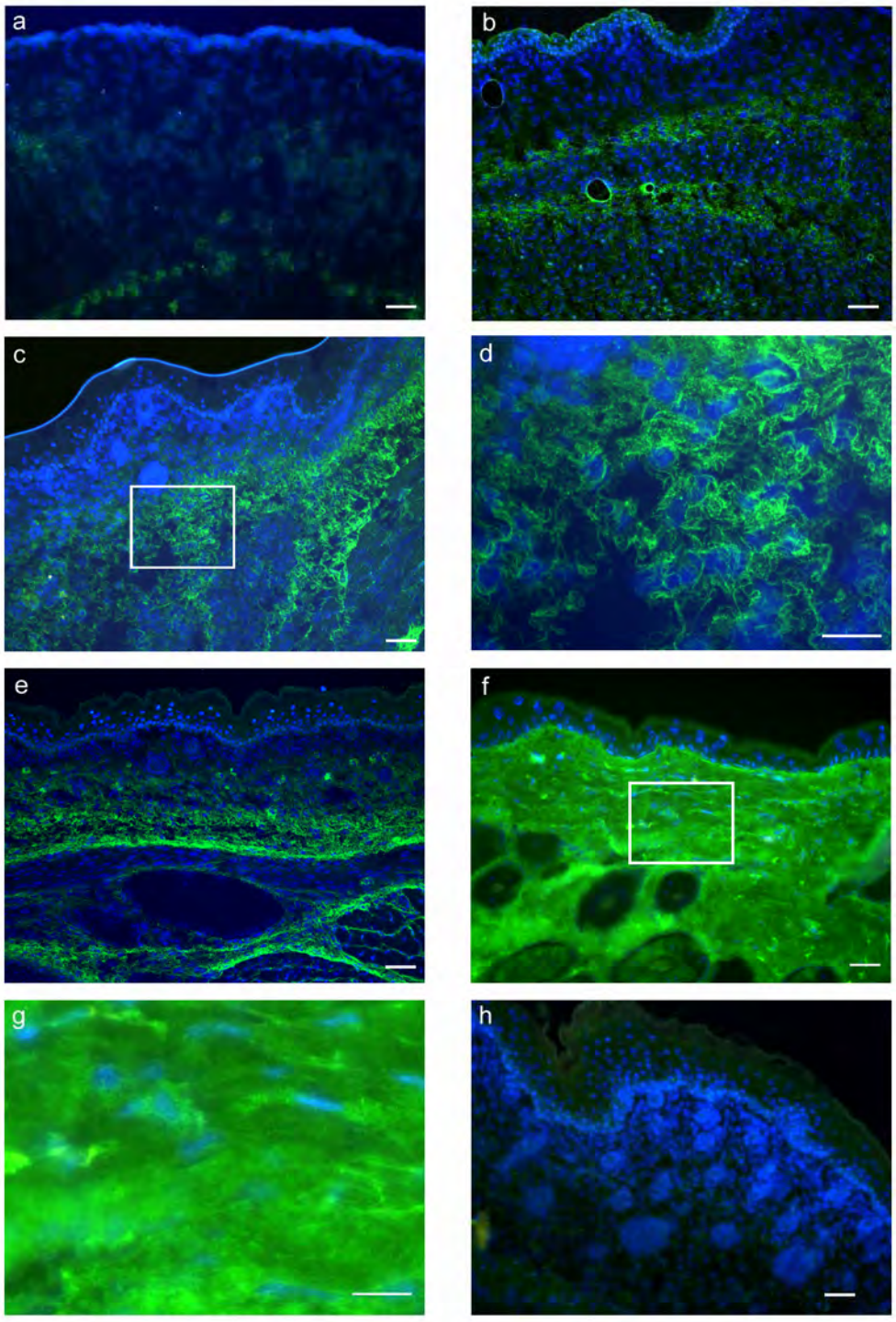

Figure 2: TNX immunofluorescent staining of the developing skin of wild-type mice.
(a) At stage E14, no significant signal in the prospective dermis is detected (blue nuclear staining with DAPI). (b) By stage E15, TNX expression (green) is visible in the developing reticular dermis and around the fascia of the carnosus muscle layer. (c, e) At E18 and in 1-day-old neonatal mice, respectively, expression of TNX has extended further into the dermis. (d) Higher magnification of the rectangle in (c); TNX is expressed in the fetal mouse in a distinct fibre-like pattern. (f) In adult mouse skin, TNX is observed throughout the dermis in a more homogeneous pattern. (g) Higher magnification of the rectangle in (f). (h) The specificity of the anti-TNX serum is demonstrated in TNX knockout mice skin (E18), which is devoid of signal. Bars 50 µm (a–c, e, f, h), 25 µm (d, g).

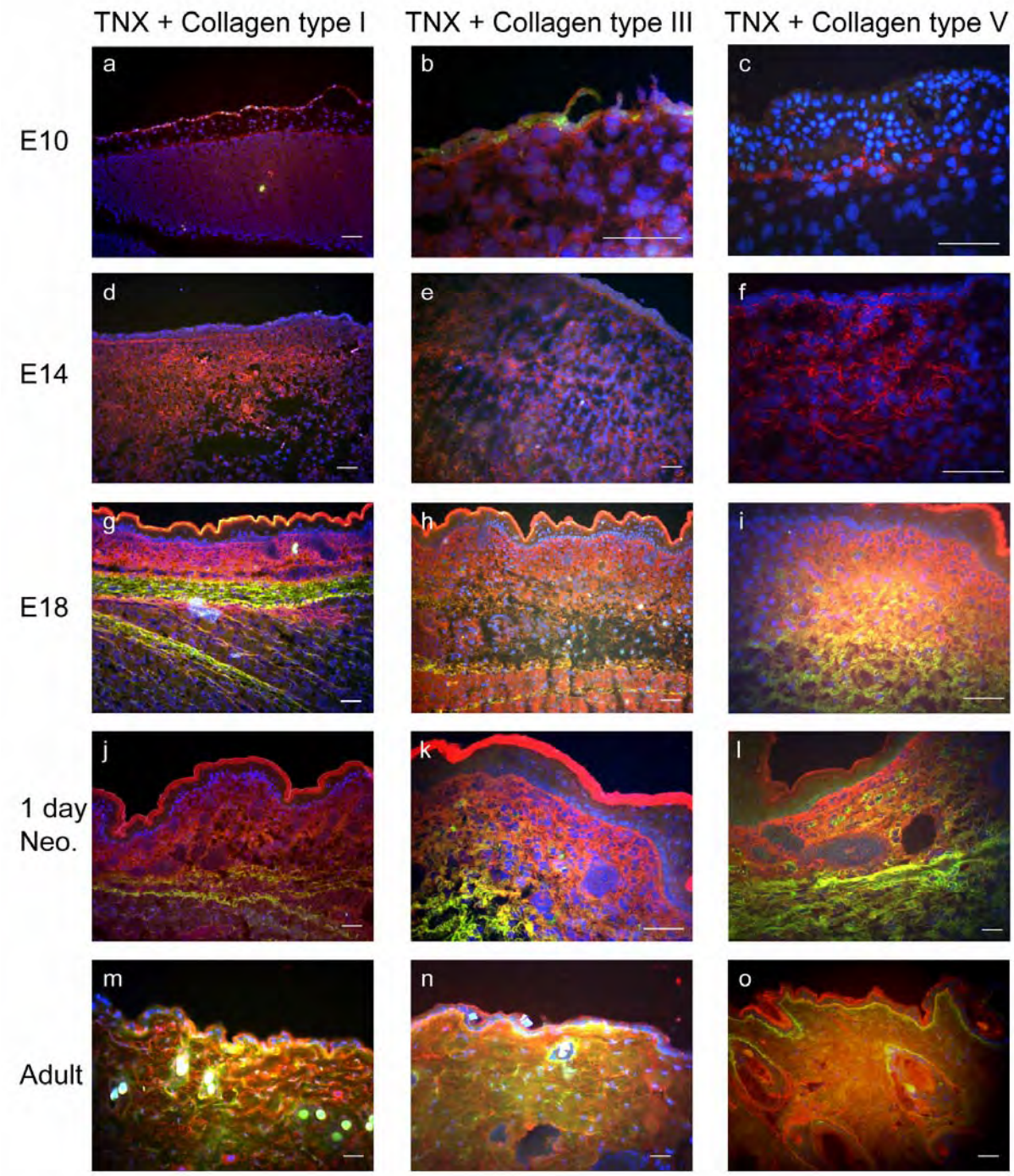

Figure 3: Merged micrographs showing immunofluorescent doublestaining for TNX (green) and collagens (red) type I (a, d, g, j,m), III (b, e, h, k, n), or V (c, f, i, l, o) in developing skin of wild-type mice.
Nuclei are stained blue with DAPI. The different types of collagen are expressed even at fetal stages E10 (a–c) and E14 (d–f) in the prospective dermis. At E18 (g–i) and 1-day-old neonatal (1 day Neo.) mice (j–l), TNX starts to colocalize with the various types of collagens (orange, yellow). In adult mice, TNX is expressed in the entire dermis and overlaps with collagens type I (m), III (n), and V (o). Non-specific staining of the stratum corneum was present in some sections. Bars 50 µm.

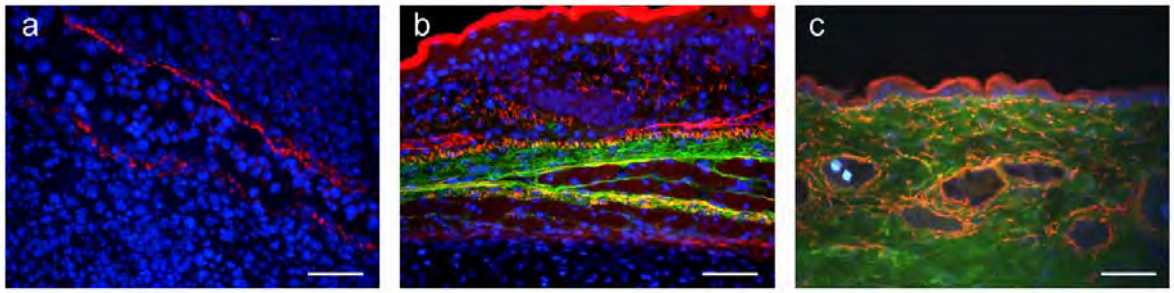

Figure 4: Merged micrographs of immunofluorescent double-staining for TNX (green) and tropoelastin (TE; red) in developing skin in wild-type mice.
TE is expressed in the undifferentiated mesenchyme at the earliest investigated stage, E10 (a). The signals for TE and TNX partially overlap (orange, yellow) in the developing mice skin around the fascia of the carnosus muscle at E18 (b). In adult mice (c), the entire dermis is stained positively for TNX with overlapping signal for TE (orange, yellow). Bars 50 µm.

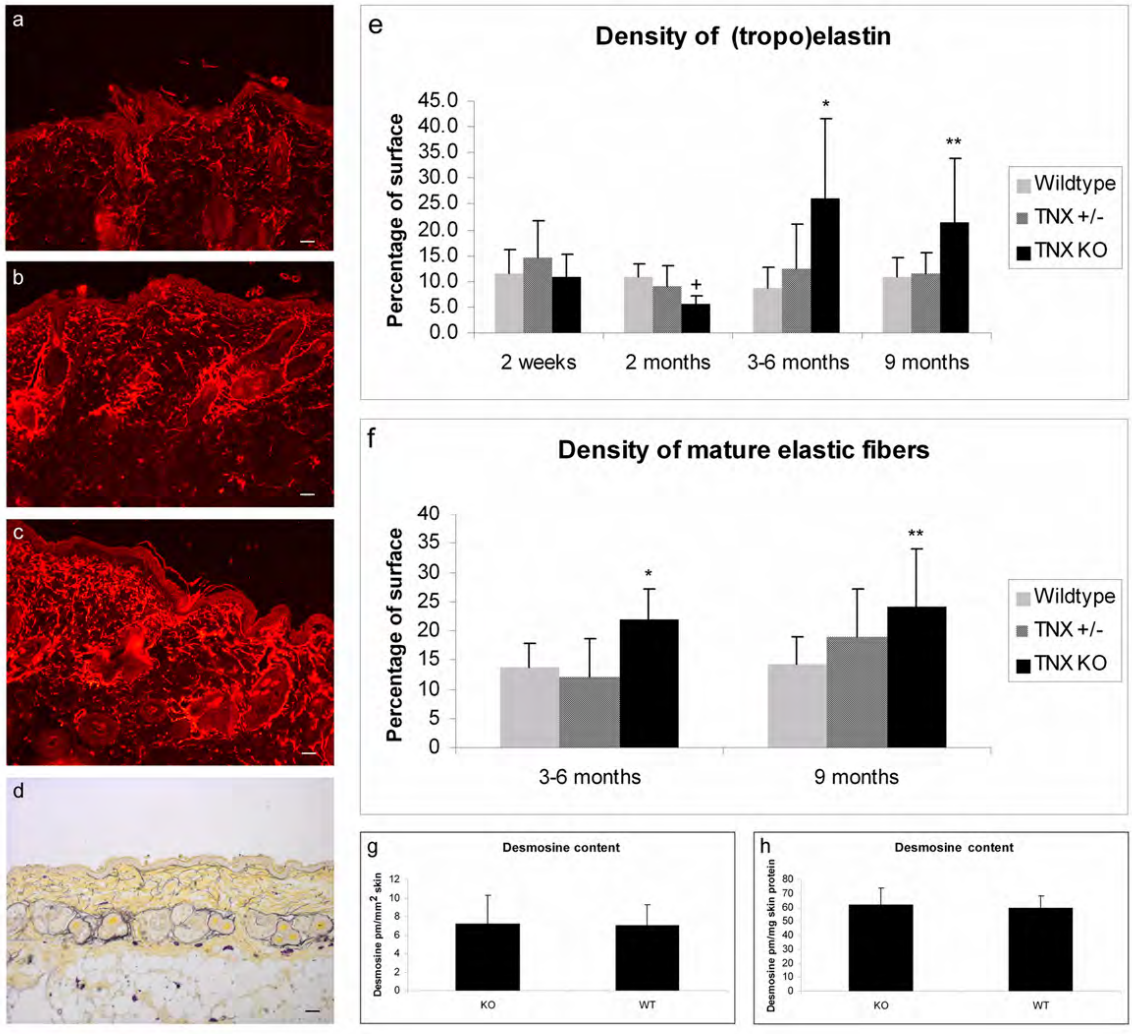

Figure 5: Analysis of elastin and elastic fibers. Immunostaining for TE on paraffin sections of 9-month-old mice (a–c).
At 3–6 months, TNX knockout mice (c) show a higher density of TE in their dermis than do wild-type (a) and heterozygous (b) mice (represented graphically in e). The density of mature elastic fibers made visible by modified Hart's staining in TNX knockout skin (not shown) compared with wild-type mice (d) is increased (f). No differences in desmosine content expressed per milligram protein (h) or per mm2 (g) skin were found between the different phenotypes in adult mice. *P<0.01, **P<0.05, + not significant. For all comparisons, n=12 for each genotype for mice at 3–6 months, n=6 (or more) for mice at 2 weeks and 9 months. For 2-month-old mice, n=8 for heterozygous mice, n=4 for TNX knockout mice and n=3 for wild-type mice (KO knockout, WT wild-type, +/− heterozygous).

CHAPTER 3

Figure 1: Widened scar in TNX deficient patient.
An example of a widened scar with irregular boundaries, indicated by arrows, on the arm of a TNX-deficient patient. This is found in some of our TNX-deficient patients, but not in all patients. Atrophic scars (cigarette paper-like skin) were never observed in these patients.

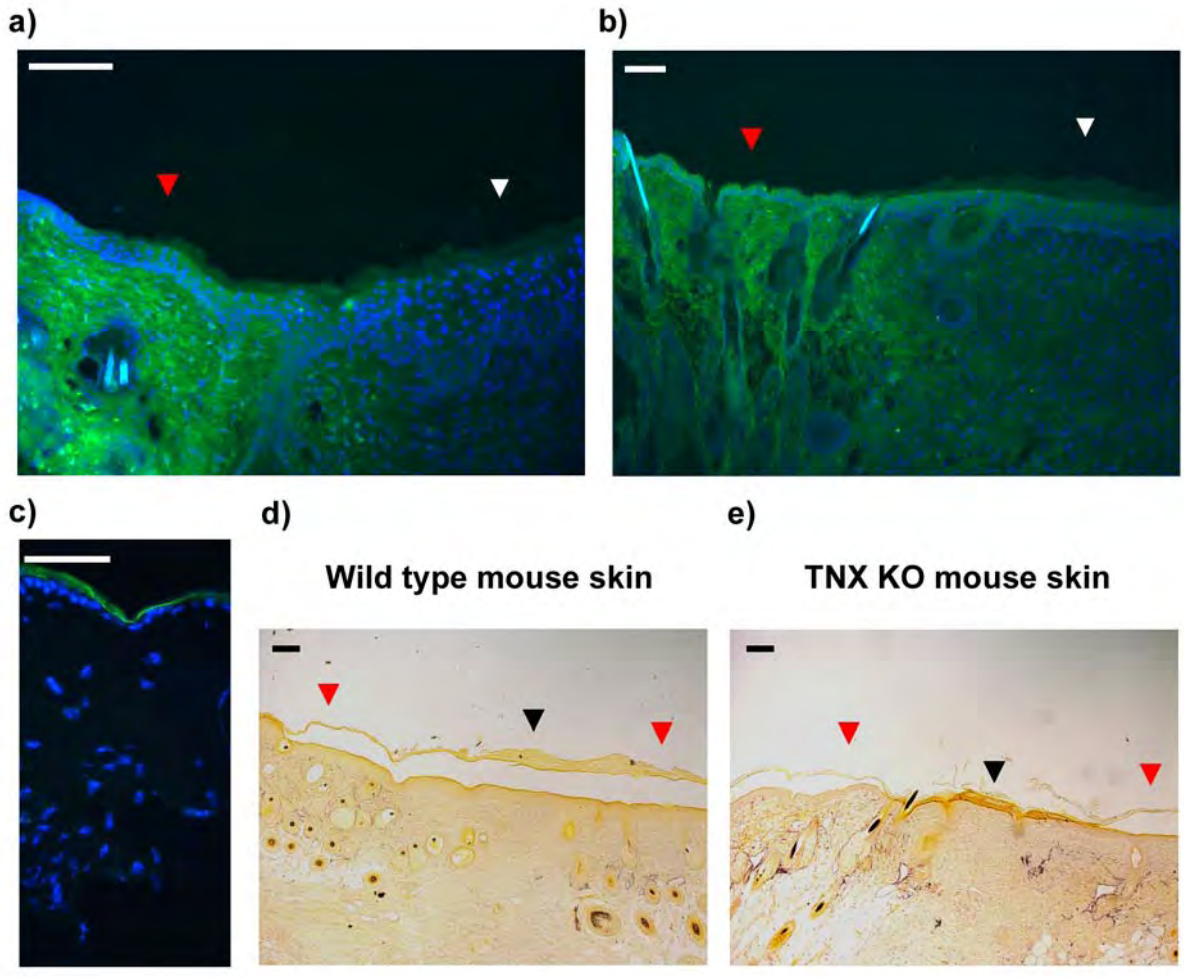

Figure 3: Low expression of TNX and absence of elastic fibers in wound tissue.
White arrows indicate the wound area in sections (a) and (b). Red arrows indicate uninjured skin. TNX expression is very low/not present in a 7-day-old wound area of WT skin (a). TNX expression (green) can be observed in a 14-day-old wound area of WT skin but it is far less strong than in the adjacent normal skin (b). The specificity of the anti-TNX antibody is demonstrated in TNX KO skin, which is devoid of signal (c). Note that staining of the stratum corneum is nonspecific (a–c). No elastic fibers can be detected in a 14-day-old wound area as shown by modified Hart's staining for WT skin (d) and TNX KO skin. Black arrows indicate the wound area, white. Bars in (a), (b), (d), and (e) are 100 μm and 50 μm in (c).

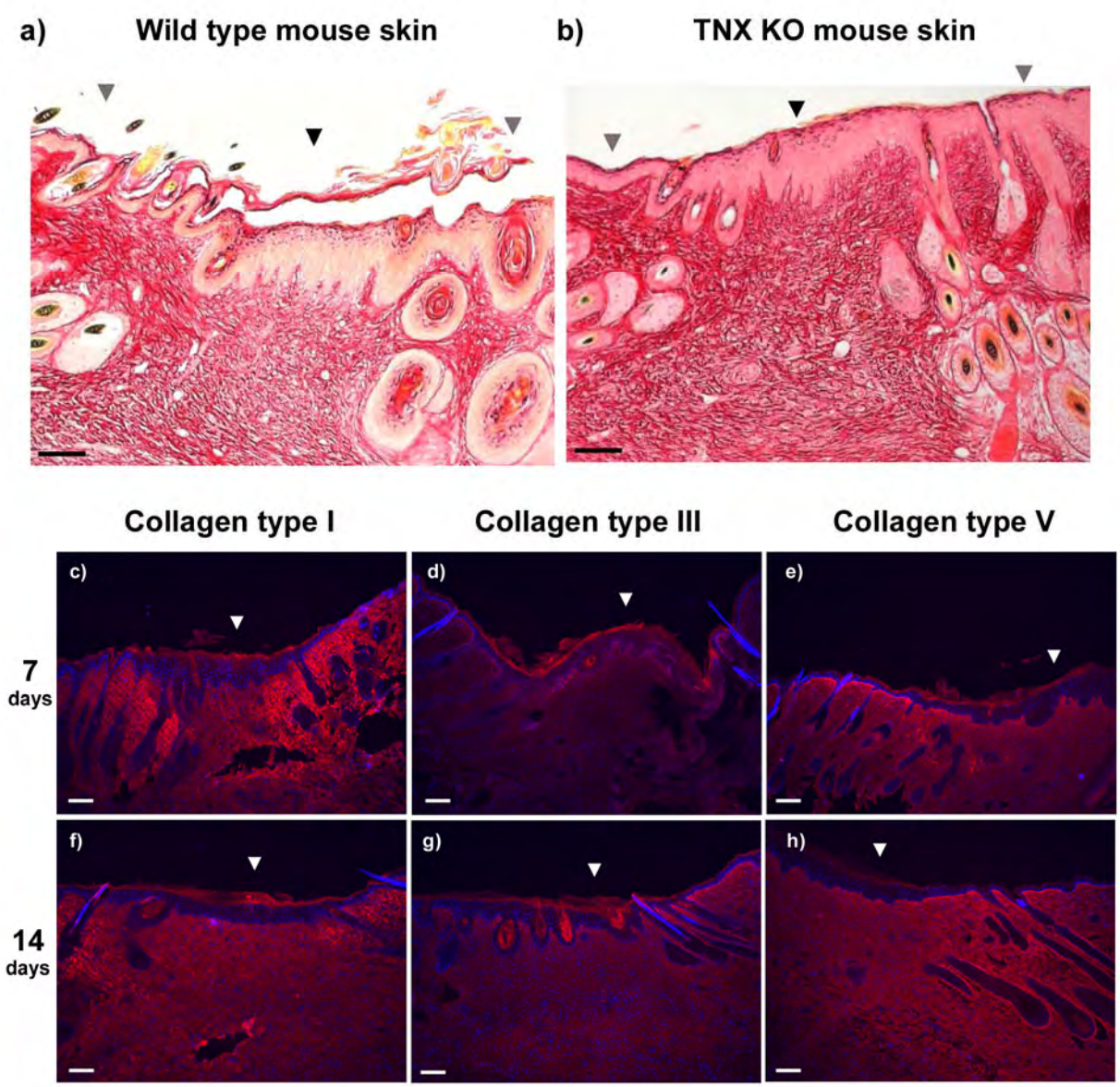

Figure 2: Collagen distribution in the wound area.
In (a) and (b) collagen is stained red/pink by Sirius red staining. The wound area is indicated by black arrows. The collagen fibrils in the dermis under the wound area are packed less tight compared with uninjured skin (indicated by grey arrows). No obvious differences in collagen density in the wound area between WT (a) and TNX KO (b) mice were noted as is shown for a 14-day-old wound area. Immunofluorescent staining (red) of collagen type I (c, f), III (d, g) and V (e, h) are abundantly expressed in a 7-day (c–e) and 14-day (f–h) wound area (as shown for WT skin). The area under white arrows indicates the wounded skin. Hair follicles are absent in the wound area but present in uninjured skin. Positive staining of the outer layer of the epidermis (stratum corneum) is nonspecific. Bars in (a, b) are 25 μm, bars in (c-h) are 100 μm.

CHAPTER 4

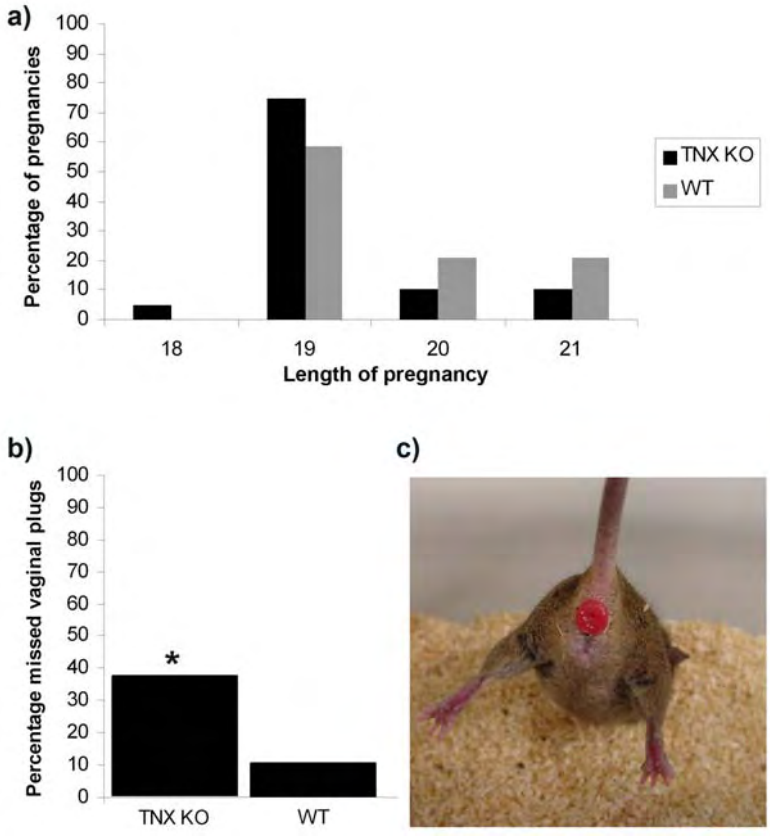

Figure 1: TNX KO mice abnormalities.
(a) Although the difference in the length of pregnancy between TNX KO and WT mice is found non-significant by Fisher exact test, a decreasing trend in the length of pregnancy of TNX KO mouse compared to WT mice can be observed. Vaginal plugs, which are present after mating, are much more difficult to asses in TNX KO mice than in WT mice. This results in a significant increase of pregnancies in which the insemination date was unknown as shown in panel (b). In this study no uterine prolapses have been observed, however, some TNX KO mice suffer from a rectal prolapse as shown in panel (c). Rectal prolapses are also observed in TNX-deficient patients, although the incidence in TNX KO mouse appears low. (* $p<0.025$, chi square test).

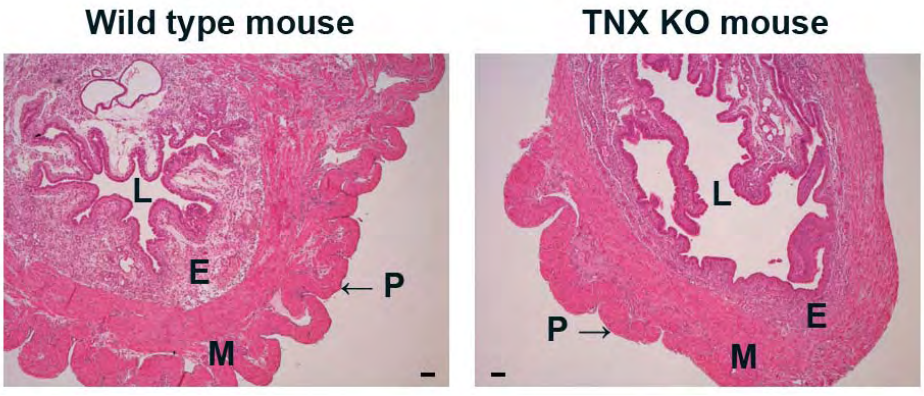

Figure 2: Structure of the TNX KO and WT uterus.
H&E stained sections of the uterus of WT mice (a) and of TNX KO mice (b) are shown. No differences in structure of the uterus were noticeable between TNX KO and WT mice. The uterus of mice consists of a thin outer layer, the perimetrium (denoted as P). A muscle layer, the myometrium (denoted as M), consist of two oppositely orientated layers of muscle, although this is difficult to distinguish in H&E stained slides. The endometrium (denoted as E) consist of loose connective tissue. The endometrium is separated from the lumen (denoted as L) by an epithelium. Bars are 0.01 mm.

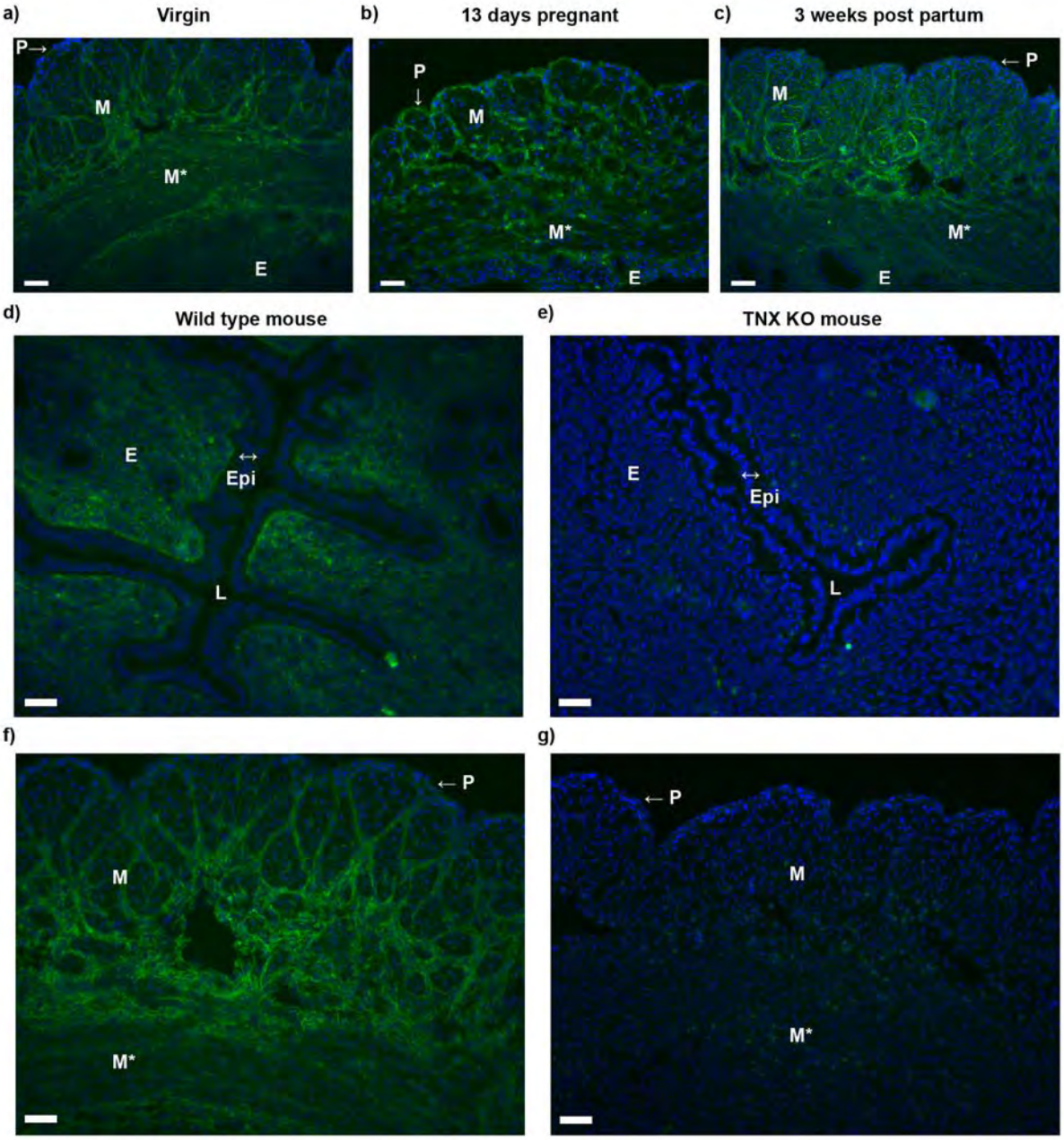

Figure 3: Immunostaining of TNX in the uterus.
TNX (green) is present throughout the uterus of virgin mice (a) and in the uterus during and after pregnancy (shown for 13 days pregnant (b) and 3 weeks postpartum (c) uteri). Cell nuclei are stained with DAPI (blue). TNX is present in the endometrium (d) and the layers of connective tissue ensheathing muscle bundles of the myometrium (f). The TNX staining of the perimetrium can be relatively weak (a-c and f). The epithelium of the lumen is negative for TNX (d). Specificity of our TNX antibody is demonstrated in figures (e) and (g). Panels (d-g) are from uteri 3 weeks postpartum. Bars are 50 µm (P = perimetrium, M = myometrium; longtidunal muscle bundles, M* = myometrium; transverse muscle bundles, E = endometrium, Epi = epithelium of the lumen, L = lumen).

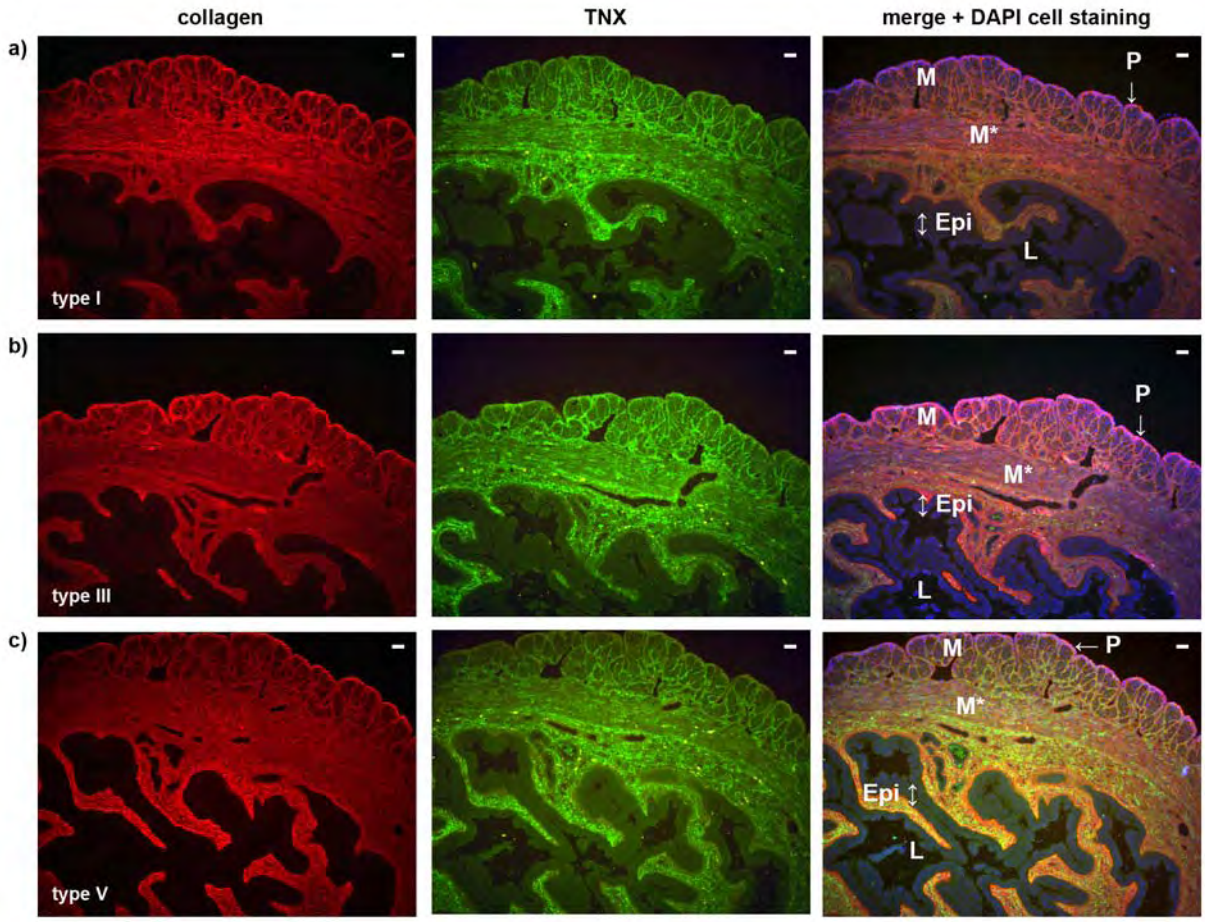

Figure 4: TNX colocalizes with major fibrillar collagens type I, III and V.
TNX (green) and collagen types I (a), III (b) and V (c) (red) colocalize (yellow to orange) as is shown for uteri 3 weeks postpartum. Similar results were obtained for uteri from virgin, 13 days pregnant and 1-day postpartum mice. No difference in collagen type I, III and V immunostaining was found between WT and TNX KO mice (data not shown). Bars are 50 µm (P = perimetrium, M = myometrium; longtidunal muscle bundles, M* = myometrium; transverse muscle bundles, E = endometrium, Epi = epithelium of the lumen, L = lumen).

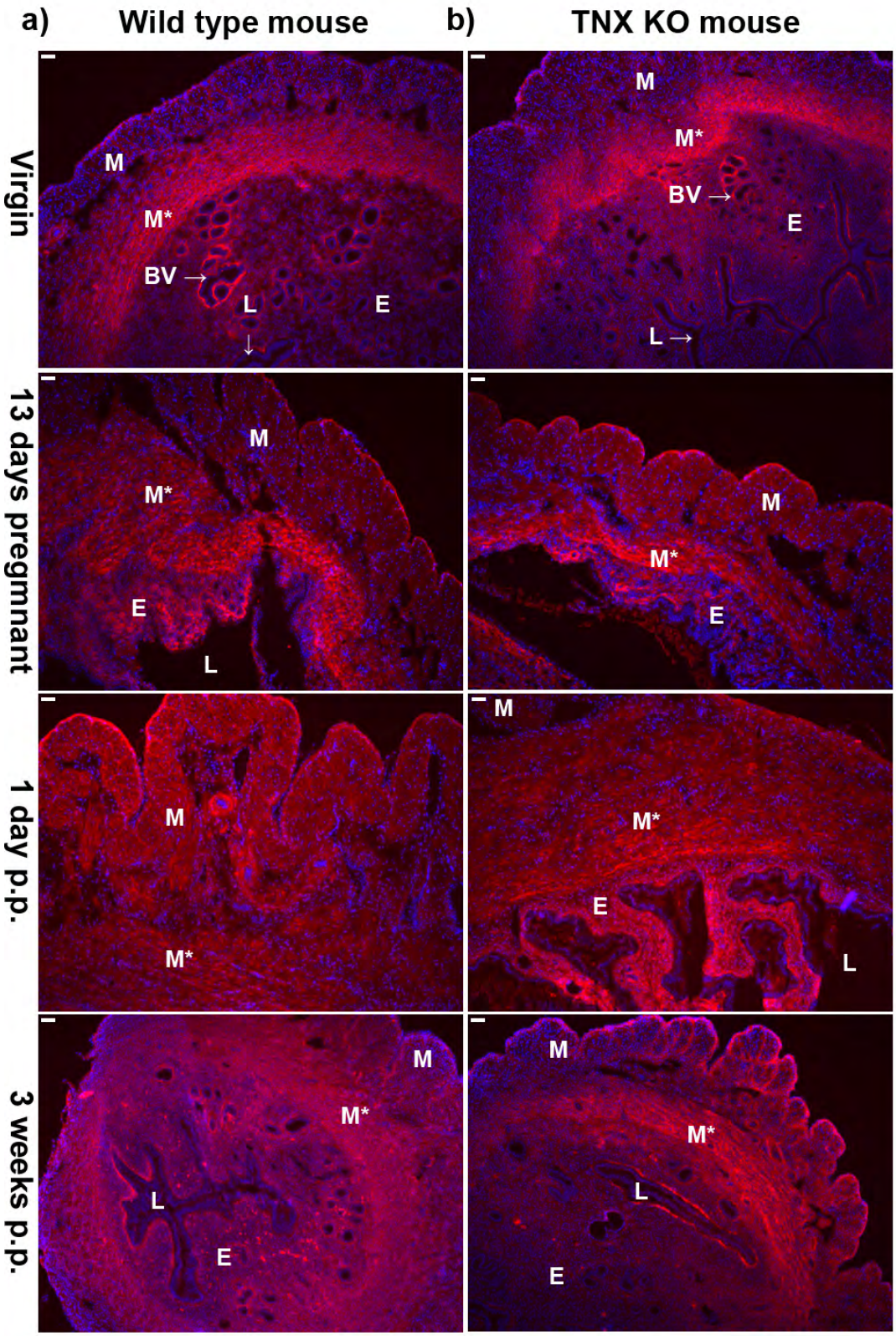

Figure 5: Immunostaining of collagen type XII in uterus.
Collagen XII (red) is present throughout the uterus. The immunostaining appears the strongest in the transverse muscle bundles of the myometrium (M*), around blood vessels (BV) and around the lumen (L), although the signal intensity is not always completely continuous. No differences in the collagen type XII localization in the uterus between WT (a) and TNX KO (b) mice were observed. Bars are 50 µm (P = perimetrium, M = myometrium; longtidunal muscle bundles, M* = myometrium; transverse muscle bundles, BV = blood vessel, E = endometrium, L = lumen).

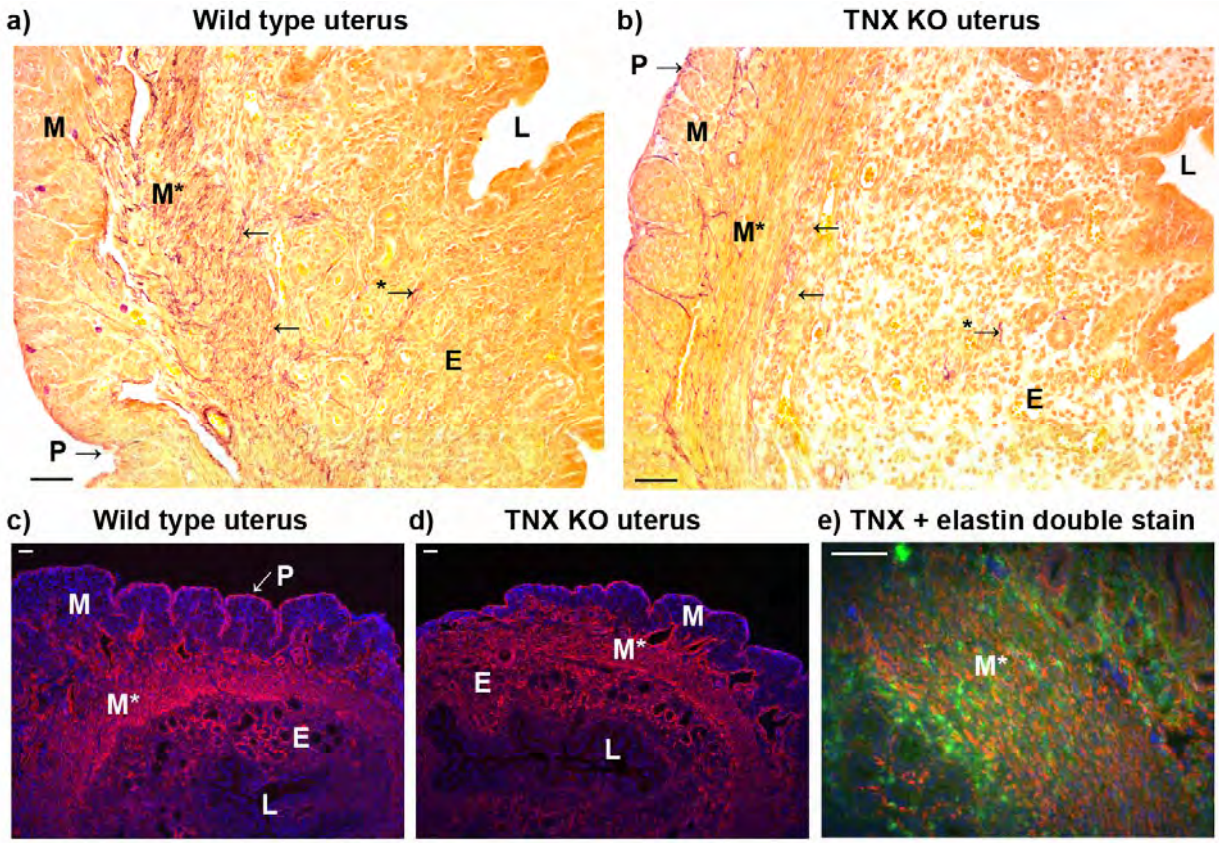

Figure 6: Elastin and elastic fibers in the uterus.
Elastic fibers (purple, modified Hart's staining) are mostly located in the myometrium (M, M*) and perimetrium (P), whereas the endometrium (E) appears to contain fewer elastic fibers as shown for WT (a) and TNX KO mice (b). No elastic fiber abnormalities were found in the TNX KO mice. Elastin (red) immunostaining is observed in the myometrium, predominantly in the transverse bundles (M*) as shown in panels (c) and (d). The layers of connective tissue ensheathing muscle bundles of the myometrium (M) and perimetrium (P) are stained positive for elastin (red). Strong elastin staining is also seen in the endometrium (E). Elastin immunoreactivity was similar for WT (c) and TNX KO mice (d). Elastin (red) colocalizes (orange) with TNX (green) as shown in the myometrium (M*) (e). Not all TNX colocalizes with elastin as TNX also colocalizes with different collagen types (fig. 4). Bars are 50 µm (P = perimetrium, M = myometrium; longtidunal muscle bundles, M* = myometrium; transverse muscle bundles, BV = blood vessel, E = endometrium, L = lumen).